ROLE OF SYNDECAN-1 IN PERITONEAL DIALYSIS AND PERITONITIS

INTRAVITAL MICROSCOPY OF THE PARIETAL PERITONEUM MICROCIRCULATION AND THE ROLE OF SYNDECAN-1 IN *STAPHYLOCOCCUS AUREUS* INFECTION IN PERITONEAL DIALYSIS

By

PAULINA M. KOWALEWSKA, BHSc

A Thesis

Submitted to the School of Graduate Studies

in Partial Fulfillment of the Requirements for the Degree

Doctor of Philosophy

McMaster University

DOCTOR OF PHILOSOPHY (2014) McMaster University

(Medical Sciences) Hamilton, Ontario

TITLE: Intravital Microscopy of the Parietal Peritoneum Microcirculation and the Role of Syndecan-1 in *Staphylococcus aureus* Infection in Peritoneal Dialysis

AUTHOR: Paulina M. Kowalewska, BHSc (McMaster University)

SUPERVISOR: Alison E. Fox-Robichaud, BSc, MSc, MD, FRCPC (Internal Medicine, Critical Care)

NUMBER OF PAGES: xvii, 191

ABSTRACT

Chronic peritonitis contributes to technique failure in peritoneal dialysis (PD), an effective replacement therapy for chronic kidney failure. *Staphylococcus aureus* infection is one of the most common causes of peritonitis in PD. Interestingly, mice deficient in the cell surface heparan sulfate proteoglycan, syndecan-1, were reported to clear *S. aureus* corneal infection more effectively than wild-type mice. The objectives of this study were to examine the protein expression and role of syndecan-1 in leukocyte recruitment, chemokine presentation and *S. aureus* infection in the microcirculation underlying the parietal peritoneum in wild-type and syndecan-$1^{-/-}$ mice.

Immunofluorescence intravital microscopy (IVM) of the parietal peritoneum microcirculation revealed that syndecan-1 was localized to the subendothelial region of venules and the mesothelial layer but does not regulate leukocyte recruitment and is not necessary for presentation of the chemokine MIP-2 in peritoneal venules. IVM was also used to study the effects of a conventional PD solution injected through a peritoneal catheter in a mouse PD model. After 6 weeks of dialysis, the peritoneal catheter implant increased leukocyte rolling and extravasation, fibrosis and angiogenesis in the parietal peritoneum independently from the dialysis solution treatment. Furthermore, the role of syndecan-1 was examined using a 4 week PD model. Four hours after infection with *S. aureus* through the dialysis catheter or intraperitoneal injection, the dialyzed syndecan-$1^{-/-}$ mice were more susceptible to *S. aureus* infection than undialyzed syndecan-$1^{-/-}$ controls and wild-type animals. IVM showed that in *S. aureus* infection, syndecan-1

was removed from the subendothelial surface of peritoneal venules but syndecan-1 deficiency did not affect leukocyte recruitment during *S. aureus* infection.

This study indicates that syndecan-1 in the peritoneum and microcirculation is not a regulator of inflammatory responses but is crucial for providing a barrier to *S. aureus* infection, which may have important implications for susceptibility to *S. aureus* infections in PD.

ACKNOWLEDGMENTS

First and foremost I would like to extend my sincerest gratitude to my PhD supervisor, Dr. Alison E. Fox-Robichaud, for providing me with many opportunities, for believing in me and giving me a chance to explore my project from many different angles. The experience I gained with various rodent surgical techniques and live animal microscopy will definitely shape my future research aspirations. I would also like to thank our wonderful technician, Amanda L. Patrick. Mandy, your help, friendship and constant support and encouragement made my PhD experience so much less stressful. I have been truly blessed to work with many brilliant and inspiring students in the Fox-Robichaud laboratory, past and present, who provided a friendly and supportive environment to work in.

I also have my PhD supervisory committee members to thank. Dr. Peter Margetts, thank you for the invaluable suggestions you provided on how to approach the peritoneal dialysis project. Hearing your expert opinion was very reassuring for me. Dr. Kim Jones, I appreciate the input you provided on biomaterial responses and thank you for giving me feedback on the work regarding urinary catheters and peritoneal dialysis catheters, as well as allowing me to make use of your flow cytometer. Last but not least, thank you Dr. Lori Burrows, for providing expertise on the microbiology aspect of my work and providing me with the *Staphylococcus aureus* as well as welcoming me into your lab to complete parts of my experiments. I also have Burrows laboratory members to thank for their help with the *S. aureus* work. Specifically, I would like to thank Uyen Nguyen, for streaking out bacterial samples for me and providing me with Microbiology

101 training and accommodating me in every way possible. I also thank Dr. Ryan Lamers for providing very helpful suggestions with the protocol on preparing bacterial samples for inoculation in mice.

I am also thankful to Marcia Reid at the Electron Microscopy Facility, McMaster University, for training and help with the scanning electron microscopy. Also, I would like to thank Dr. Pyong Woo Park (Children's Hospital, Harvard Medical School) for providing the syndecan-1 deficient mice.

I also thank my wonderful parents, Barbara and Edward Kowalewski, and my beloved sisters, Marta, Małgosia and Sandra, for their constant support, encouragement and patience with me on my journey to complete my PhD studies.

DECLARATION OF ACADEMIC ACHIEVEMENT

The design of the experiments was conceived by the author of the thesis with the help of Dr. Fox-Robichaud. All of the experimental work was carried out by the author with a few exceptions. Help with the syndecan-1 ELISA was provided by Amanda L. Patrick. The peritoneal catheters were prepared for scanning electron microscopy by Marcia Reid (McMaster Electron Microscopy Facility). Samples of *S. aureus* were streaked out by Uyen Nguyen (L.L. Burrows Laboratory). All of the writing and figure preparations were performed by the author of this thesis.

Overall, the PhD work of the author resulted in the following publications or manuscripts:

Kowalewska, P.M., Patrick, A.L. and Fox-Robichaud, A.E. (2011). Innate Immunity of the Liver Microcirculation. *Cells and Tissue Research.* 343(1): 85-96.

Kowalewska, P.M., Burrows, L.L. and Fox-Robichaud, A.E. (2011). Intravital Microscopy of the Murine Urinary Bladder Microcirculation. *Microcirculation.* 18(8): 613-622.

Grin, P.M., **Kowalewska, P.M.,** Alhazzani, W., Fox-Robichaud, A.E. (2013). *Lactobacillus* for preventing recurrent urinary tract infections in women: meta-analysis. *Can J Urol*. 20(1):6607-14.

Kowalewska, P.M., Patrick, A.L. and Fox-Robichaud, A.E. (2014). Syndecan-1 in the mouse parietal peritoneum microcirculation in inflammation. *PLOS ONE*. 9(9): e104537.

Kowalewska, P.M., Margetts, P.J. and Fox-Robichaud, A.E. Peritoneal dialysis catheter increases leukocyte recruitment in the mouse parietal peritoneum microcirculation. *Peritoneal Dialysis International, SUBMITTED.*

The remaining data in this thesis will be published as:

Kowalewska, P.M., Nguyen, U., Burrows, L.L. and Fox-Robichaud, A.E. Syndecan-1 in *Staphylococcus aureus* infection in a mouse model of peritoneal dialysis.

TABLE OF CONTENTS

LIST OF FIGURES AND TABLES

LIST OF ABBREVIATIONS AND SYMBOLS

Please note that while both the common name and the approved nomenclature are provided for cytokines, chemokines, adhesion molecules, receptors and other clusters of differentiation (CD) antigens, the common name is used throughout the body of this thesis for simplicity.

αSMA	α smooth muscle actin
bFGF	Basic fibroblast growth factor
CLP	Cecal ligation and puncture
CX_3CR1	CX_3C chemokine receptor-1
ELISA	Enzyme-linked immunosorbent assay
EMT	Epithelial-mesenchymal transition
ESAM	Endothelial cell-selective adhesion molecule
ESRD	End-stage renal disease
fMLP	*N*-formylmethionyl-leucyl-phenylalanine
GAG	Glycosaminoglycan
GDP	Glucose degradation products
GFP	Green fluorescent protein
ICAM-1; CD54	Intercellular adhesion molecule-1
ICAM-2; CD102	Intercellular adhesion molecule-2
IL-6	Interleukin-6
IL-8; CXCL8	Interleukin-8
IP	Intraperitoneal
IV	Intravascular
IVM	Intravital microscopy
JAM-A	Junctional adhesion molecule-A

JNK	Jun N-terminal kinases
KC; CXCL1	Keratinocyte chemoattractant
LFA-1; CD11a/CD18	Lymphocyte function-associated antigen-1 ($\alpha_L\beta_2$)
LPS	Lipopolysaccharide
LTA	Lipoteichoic acid
Mac-1; CD11b/CD18	Macrophage-1 antigen ($\alpha_M\beta_2$)
MAPK	Mitogen activated protein kinase
MCP-1; CCL2	Monocyte chemotactic protein-1
MIP-1α; CCL3	Macrophage inflammatory protein-1α
MIP-1β; CCL4	Macrophage inflammatory protein-1β
MIP-2; CXCL2	Macrophage inflammatory protein-2
MMP	Matrix metalloproteinase
OCT	Optimal cutting temperature
PBS	Phosphate buffered saline
PD	Peritoneal dialysis
PDZ	PSD-95, Discs-large and zonula occludens-1
PECAM-1; CD31	Platelet endothelial cell adhesion molecule-1
PI	Propidium iodide
PSGL-1	P-selectin glycoprotein ligand-1
RANTES; CCL5	Regulated on activation, normal T cell expressed and secreted
Sdc1; CD138	Syndecan-1
SDF-1; CXCL12	Stromal cell-derived factor-1
SEM	Scanning electron microscopy
TGF-*β*	Transforming growth factor-*β*
TLR	Toll-like receptor

TNFα	Tumour necrosis factor-α
VCAM-1; CD106	Vascular cell adhesion molecule-1
VE-cadherin; CD144	Vascular endothelial-cadherin
VEGF	Vascular endothelial growth factor
VEGFR-2	Vascular endothelial growth factor receptor-2
VLA-4; CD49d/CD29	Very late antigen-4 ($\alpha_4\beta_1$)

CHAPTER 1: INTRODUCTION AND BACKGROUND

1.1 INTRODUCTION

Peritoneal dialysis (PD) is a life-saving replacement therapy for chronic kidney failure. It is estimated that approximately 11% of the worldwide dialysis population of 1.7 million uses PD (Fresenius Medical Care, 2008). In PD, the peritoneal membrane and the underlying microcirculation are used as a dialysis membrane for exchange of solutes and waste products between blood and the dialysis solution. Although PD is an effective renal replacement therapy, mortality or technique failure is typically experienced within 5-6 years of commencement of the therapy (Davies *et al.*, 1998; Williams *et al.*, 2002). The exposure to dialysis solutions is believed to drive deleterious functional alterations of the peritoneal lining and the microcirculation, making it no longer an effective dialysis membrane (Chaudhary & Khanna, 2010). Animal studies indicate that the peritoneal catheter may contribute to this pathology as well (Flessner *et al.*, 2007; Flessner *et al.*, 2010a). In addition, infections, many of which are caused by *Staphylococcus aureus* (Kavanagh *et al.*, 2004), and the resulting acute or chronic peritonitis exacerbate the peritoneal damage in PD (Mactier, 2009). Thus, the understanding of the molecular mechanisms that drive the histopathologic changes, inflammation and responses to infection of the peritoneal layer can lead to improvements in the therapy to preserve the peritoneum as an effective dialysis membrane.

1.2 MICROCIRCULATION, INNATE IMMUNITY AND INFLAMMATION

1.2.1 Microcirculation and microcirculatory responses during inflammation

The flow of blood through the smallest components of the vascular network is referred to as the microcirculation. At the arterial side of the microcirculatory network, arterioles, 10 μm to 100 μm in diameter, regulate blood flow into the capillary bed by contraction and relaxation of their muscular walls. The capillaries, generally 4 μm to 10 μm in diameter, are composed of an endothelial layer with a basement membrane and function primarily in exchange of nutrients and wastes between blood and the rest of the tissue cells. The capillaries converge to form venules, with diameters ranging from 10 μm to 100 μm, which also contribute to exchange of materials at their ends proximal to the converging capillaries. The venular wall is composed of an inner endothelial layer covered by scattered pericytes within a basement membrane. The pericytes are similar to the smooth muscle cells of larger vessels (Tortora & Derrickson, 2006). Because walls of the smallest venules are much thinner than arteriolar walls, lack a continuous smooth muscle layer and are more porous like the capillaries, they form the primary site of leukocyte migration from blood to the inflamed tissues (Ley & Gaehtgens, 1991). This process is referred to as leukocyte recruitment and is a major part of the inflammatory response.

The inflammatory response is a nonspecific host response to tissue damage or breach by pathogens and their products. The basic stages of the inflammatory response are vasodilation and increased vascular permeability, leukocyte trafficking to the

inflamed tissue and ultimately, tissue repair. These stages are manifested as redness, heat, pain and swelling or edema.

The microvascular inflammatory response in the venules involves coordinated activation of the endothelium and mobilization of leukocytes from the blood. Neutrophils are the predominant cell in the leukocyte infiltrate in early acute inflammation (Kolaczkowska & Kubes, 2013). The multi-step paradigm of leukocyte recruitment starts with 1) leukocyte margination (deflection towards the vessel wall) (Schmid-Schonbein *et al.*, 1980) and tethering to the endothelium, 2) leukocyte rolling, 3) firm adhesion, 4) extravasation and migration in the interstitial space (**Figure 1**).

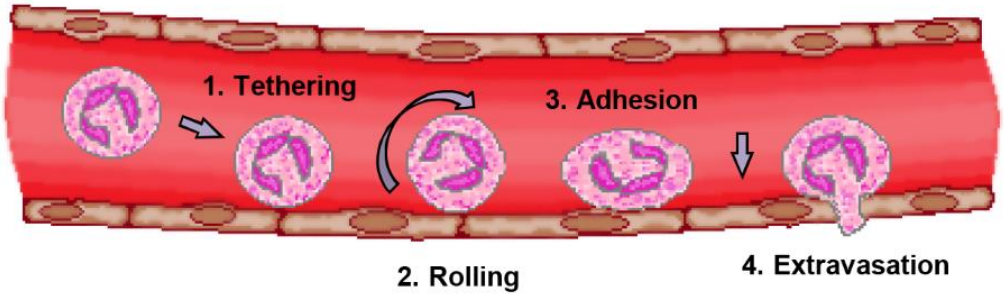

Figure 1. The classic paradigm of leukocyte recruitment. Leukocyte recruitment is a multistep process initiated by 1) leukocyte tethering and 2) rolling on the venular endothelium, 3) firm adhesion of the leukocyte to endothelial cells and 4) leukocyte extravasation/transendothelial migration.

1.2.2 Molecular mechanisms of leukocyte recruitment in different tissues

Intravital imaging has been an invaluable technique in the study of the mechanisms of inflammatory responses in many different tissues. Inflammatory reactions are characterized by leukocyte trafficking to and accumulation in inflamed tissues, a process that ensues by 4 hours after administration of a pro-inflammatory stimulus such as TNFα (Fox-Robichaud & Kubes, 2000) and immediately in models of ischemia-reperfusion injury (Arndt *et al.*, 1991; Oliver *et al.*, 1991). The multistep process of leukocyte recruitment to sites of inflammation is defined by the interactions of endothelial cells with leukocytes and is carefully regulated by the expression of adhesion molecules and cytokines with chemoattractant properties, termed chemokines. Intravascular leukocytes are initially tethered to the endothelium by the interaction of the endothelial P-selectin (CD62P) and E-selectin (CD62E) with glycoprotein ligands on leukocytes, such as proteins containing the sialylated tetrasaccharide, sialyl Lewis^X. An important selectin ligand is P-selectin glycoprotein ligand (PSGL)-1. PSGL-1 is concentrated at the tip of microvilli on leukocytes and binds both P- and E-selectin (Abbal *et al.*, 2006). These interactions are transient and reversible so the leukocyte is seen as rolling along the endothelium (Kelly *et al.*, 2007). P-selectin mediates leukocyte rolling at high velocities, approximately 40 μm/s (Jung *et al.*, 1996), while E-selectin mediates slow leukocyte rolling at approximately 3-7 μm/s (Kunkel & Ley, 1996; Zarbock *et al.*, 2007).

P-selectin is preformed and stored in platelet α-granules and in secretory granules of endothelial cells called Weibel-Palade bodies (Burns *et al.*, 1999). Inflammatory

stimulation causes rapid mobilization of P-selectin to the cell surface within minutes. E-selectin, on the other hand, is usually *de novo* synthesized and appears on the endothelium as early as 30 minutes after inflammatory stimulation (Kansas, 1996). The exception to this is skin endothelium which constitutively expresses E-selectin, allowing for leukocyte rolling in the absence of inflammation (Hwang *et al.*, 2004). Although the selectins are the major mediators of leukocyte tethering and rolling and elimination of selectins diminishes leukocyte recruitment (Collins *et al.*, 2001), roles for α_4 integrins (Fox-Robichaud & Kubes, 2000) and β_2 integrins (Jung *et al.*, 1998) in leukocyte rolling were also identified in the liver and cremaster muscle, respectively.

As the inflammatory response advances, the number of rolling leukocytes increases and the rolling velocities decrease (Kunkel & Ley, 1996). The slow-rolling leukocyte comes to a halt upon firm adhesion to the endothelium which is achieved by the interaction of integrins on leukocytes and intercellular adhesion molecules (ICAM's) on the endothelium (Garrood *et al.*, 2006). Levels of chemokines are increased in inflamed tissues and binding of chemokines to G-protein coupled receptors on leukocytes triggers complex intracellular signalling pathways that induce conformational changes in leukocyte integrins, increasing the affinity and avidity of the integrins for their ligands (Laudanna *et al.*, 2002). Firm adhesion of the leukocyte occurs via binding of endothelial ICAM-1 and ICAM-2 to the β_2 integrins lymphocyte function-associated antigen-1 (LFA-1; CD11a/CD18) and macrophage-1 antigen (Mac-1; CD11b/CD18) (Petri & Bixel, 2006) on leukocytes. Interactions of the vascular cell

adhesion molecule-1 (VCAM-1) with the $\alpha_4\beta_1$ integrin very late antigen-4 (VLA-4; CD49d/CD29) on leukocytes also mediate leukocyte adhesion (Norman *et al.*, 2003).

After firm adhesion, the leukocyte extravasates (Schubert *et al.*, 1989). This process is also referred to as leukocyte transmigration or diapedesis. However, before extravasation occurs, a leukocyte may crawl along the endothelial layer in a process dependent on Mac-1 and ICAM-1 interactions (Phillipson *et al.*, 2006). This process is believed to be important for a leukocyte to find a site for extravasation. A leukocyte may move across the endothelium through either the intercellular route or the transcellular route. With the intercellular route, for a leukocyte to cross the endothelial barrier, the connections between endothelial cells need to be loosened. Neutrophil adhesion to endothelial cells causes disorganization of vascular endothelial (VE)-cadherin/catenin, causing increased vascular permeability and accelerating neutrophil extravasation (Del Maschio *et al.*, 1996; Gotsch *et al.*, 1997). Intercellular transmigration is mediated by the adhesion molecules platelet-endothelial cell adhesion molecule-1 (PECAM-1), junctional adhesion molecule-A (JAM-A), ICAM-2 and endothelial cell-selective adhesion molecule (ESAM), that are all expressed on endothelial cells (Huang *et al.*, 2006; Nourshargh *et al.*, 2006; Wegmann *et al.*, 2006).

Most neutrophils migrate via the intercellular route (Phillipson *et al.*, 2006). However, in some tissues, such as the skin, most neutrophils extravasate through the transcellular route (Feng *et al.*, 1998). The transcellular route of leukocyte extravasation occurs directly through the endothelial cell, as the name implies. This process is dependent on β_2 integrin-ICAM-1 interactions (Yang *et al.*, 2005). The extravasated

leukocyte then migrates through the tissue under the direction of a chemokine gradient (Middleton *et al.*, 2002).

1.2.3 Intravital microscopy (IVM)

IVM is a useful technique for direct visualization of the events of leukocyte trafficking and microvascular inflammatory responses since it allows for the *in vivo* observation of tissues. Interactions of leukocytes with endothelium of venules was described as early as the 19th century by IVM (Cohnheim, 1889). Over the last 30 years, this technique contributed an immense amount of knowledge on the paradigm of leukocyte trafficking (Zarbock & Ley, 2009).

In IVM, the transillumination technique involves the transmission of light through a sample and the bright field images generated are used to count the number of rolling and adherent leukocytes in venules as well as extravascular leukocytes in the perivenular region. IVM is commonly used to observe microcirculatory events in anesthetized animals, which requires surgical manipulation and exteriorization of the organ of interest without the removal of its neurovascular supply. To bypass the surgical preparation and its inevitable pro-inflammatory effects, the dermal microcirculation of the ear has been a popular model (Kamler *et al.*, 1993; Kilarski *et al.*, 2013; Milstone *et al.*, 1998). The more surgically invasive, but also very useful and common rodent models for visualizing leukocyte trafficking are IVM of the liver (Fox-Robichaud & Kubes, 2000), the mesentery (Ley & Gaehtgens, 1991) and the cremaster muscle microcirculation (Baez, 1973). These models have been indispensable for identifying

the molecular mechanisms of leukocyte recruitment and demonstrating the tissue specific differences in these mechanisms (Patrick *et al.*, 2007). For example, unlike the hepatic central and portal venules, leukocyte rolling has not been shown to precede leukocyte adhesion in the hepatic sinusoids and selectin depletion does not inhibit adhesion in these capillaries (Fox-Robichaud & Kubes, 2000; Wong *et al.*, 1997). IVM was also used to study microvascular responses in the brain (Cabrales & Carvalho, 2010), lung (Kuebler *et al.*, 2000) and bladder (Bajory *et al.*, 2002; Kowalewska *et al.*, 2011).

1.2.4 Fluorescence confocal microscopy

When coupled with fluorescence techniques, IVM is a powerful method for visualizing molecular expression, pathogen dissemination and identifying infiltrating cell types *in vivo* (Kowalewska *et al.*, 2011; Lee *et al.*, 2010). In fluorescence microscopy with epi-illumination technique, the image quality is degraded by the superimposition of out-of-focus images on the in-focus image, resulting in a low contrast image with a bright but blurred background. Furthermore, the increasing thickness of the sample increases light scattering and distorts the image. One way to circumvent these issues is to use thinner sections of the fluorescent sample. However, this is not easily controlled when imaging living cells or performing IVM on whole organs. Thus optical sectioning (a microscope design that excludes out-of-focus light) is widely used to image living tissues (Murray, 2005).

By excluding out-of-focus light and using pinpoint illumination via pinhole apertures, confocal microscopy increases contrast of images. A spinning disc confocal microscope uses a series of pinholes on a spinning disc for multiple point illumination, making acquisition of the entire image more rapid compared with single point illumination of laser scanning confocal microscopes. The light is captured by a charge-coupled device (CCD) camera with high quantum efficiency (Murray, 2005). Spinning disc confocal microscopy is a preferred technique for imaging live cells and tissues because this configuration decreases photobleaching of the fluorochromes and phototoxicity of the living sample and at the same time allows for rapid spatial and temporal detection of samples.

1.2.5 Proteoglycans and the endothelial glycocalyx in inflammation

The surface of the endothelial cells lining the blood vessels is covered by a structurally complex layer of a wide variety of membrane bound macromolecules known as the glycocalyx. These macromolecules include proteins, glycolipids, proteoglycans with their glycosaminoglycan (GAG) side chains, as well as glycoproteins with their acidic oligosaccharides and terminal sialic acids (Pries *et al.*, 2000). The constituents of these macromolecules impart a net negative charge onto the glycocalyx (Pahakis *et al.*, 2007). This negative charge contributes to the anti-adhesive nature of the endothelial surface (Silvestro *et al.*, 1994; Simionescu & Simionescu, 1986).

GAGs are linear heteropolysaccharides with distinctive disaccharide repeats, such as a disaccharide of a hexosamine (*N*-acetyl-D-glucosamine/D-GlcNAc or *N*-acetyl-D-galactosamine/D-GalNAc) bound to a hexuronic acid (D-glucuroic/D-GlcA or L-iduroic/L-IdoA acid) (Jackson *et al.*, 1991). Different GAG families arise from combinations of these monosaccharides in the disaccharide unit, such as hyaluronan, heparan sulfate and chondroitin sulfate. Variable numbers of these GAG chains are attached to a core protein via the *O*-glycosyl linkage and the glycoconjugate is termed a proteoglycan. The major protein core families associated with heparan sulfate proteoglycans are the syndecans, glypicans and perlecans (Rosenberg *et al.*, 1997). Chondroitin sulfate and heparan sulfate are the glycans commonly associated with the vascular glycocalyx along with hyaluronan, a unique GAG that it is not associated with a core protein. Of these, heparan sulfate proteoglycans are the most abundant in the body (Ihrcke *et al.*, 1993; Oohira *et al.*, 1983). Heparan sulfate proteoglycans exhibit a cleavage site at the extracellular domain, where upon protease action the proteoglycan may be freed from the endothelial surface (Park *et al.*, 2000b). The main suppliers of heparan sulfate at the cell surface are the syndecans (Bernfield *et al.*, 1999).

The glycoproteins, which have short and branched polysaccharide chains, as opposed to the long unbranched GAG chains of the proteoglycans, confer a variety of saccharide moieties onto the glycocalyx, such as *N*-acetylgalactosamine and *N*-acetylglucosamine, as well as mannosyl, fucosyl, galactosyl and sialyl residues (Haldenby *et al.*, 1994; Leabu *et al.*, 1987). Action of sialidases on sialic acid residues influences leukocyte-endothelium interactions (Champigny *et al.*, 2009). Desialylation

results in increased adhesiveness of neutrophils (Cross *et al.*, 2003). Neutrophil-associated sialidase also desialylates the endothelial cell surface and the action of sialidase influences neutrophil adhesion and migration across the endothelium. This increased adhesion of neutrophils to the endothelial cells after sialidase treatment is time- and dose-dependent and treatment of both cell types results in a higher degree of adhesiveness than treatment of either cell type alone (Sakarya *et al.*, 2004).

Mulivor and Lipowsky (2002) studied the role of the glycocalyx in leukocyte-endothelial cell adhesion in the rat mesentery. Using fluorescently labeled microspheres coated with antibodies to ICAM-1, they demonstrated that removal of the glycocalyx with heparinase increases microsphere-endothelial cell adhesion at levels similar to that obtained by treating the rat mesentery post-capillary venules with the chemoattractant *N*-formylmethionyl-leucyl-phenylalanine (fMLP). The authors concluded that the glycocalyx blocks adhesion to the endothelium and that during the inflammatory response, the glycocalyx is shed (Mulivor & Lipowsky, 2002). Decreased binding of lectins specific for the glucose and galactose residues showed that the components of the glycocalyx being shed during fMLP treatment were GAGs (Mulivor & Lipowsky, 2004).

1.2.6 Chemokine presentation

Chemokines regulate leukocyte recruitment to sites of inflammation. Chemokine immobilization and presentation on the surface of endothelial cells is mediated by the endothelial glycocalyx (Middleton *et al.*, 2002). The acidic and thus negatively charged

GAGs, due to the presence of sulfate and carbonyl groups, interact with positively charged domains of chemokines, which are largely basic, immobilizing and concentrating them on the endothelial surface for presentation to their respective G protein-coupled receptors (Kuschert *et al.*, 1999). Four subfamilies of chemokines are distinguished based on the structure of a conserved cysteine-containing motif in the amino-terminal region. Based on the position of the cysteines, chemokines are classified as C, CC (adjacent cysteines), CXC (cysteines separated by an amino acid) or CX_3C (cysteines separated by 3 amino acids) (Zlotnik & Yoshie, 2000). The corresponding receptors are named based on the chemokine class that they recognize, for example CCR1 and CXCR1.

Neutrophils are recruited in response to the CXC chemokine interleukin-8 (IL-8) in humans or the mouse homologs macrophage inflammatory protein-2 (MIP-2) and keratinocyte chemoattractant (KC). The CC chemokine monocyte chemotactic protein-1 (MCP-1) (Rollins *et al.*, 1991) and CC chemokine referred to as "regulated on activation, normal T cell expressed and secreted (RANTES)" (Schall *et al.*, 1990), on the other hand, recruit monocytes.

The molecular basis of chemokine-heparan sulfate interactions and the functional implications were examined *in vitro*. For some chemokines, including IL-8, it was reported that the C-terminal α-helix is the binding site for GAGs (Chakravarty *et al.*, 1998; Kuschert *et al.*, 1998; Luo *et al.*, 1999; Webb *et al.*, 1993). IL-8 exists as a homodimer, each subunit consisting of a flat bundle of β-pleated sheets with an α-helix that exposes the heparin binding positively charged residues. The two α-helices in the

dimer are antiparallel (Baldwin *et al.*, 1991; Clore *et al.*, 1990; Clore & Gronenborn, 1991). Spillmann and colleagues elucidated the IL-8 binding domain of heparan sulfate. Heparan sulfate contains sulfated and acetylated sequences of variable length. The study indicated that the region of the heparan sulfate chain that binds IL-8 consists of 6-7 *N*-acetylated disaccharide units that separate two 4-6 *N*-sulfated monosaccharide units. Each of the two *N*-sulfated regions bound an α-helix of the IL-8 dimer (Spillmann *et al.*, 1998). The three-dimensional structures of chemokine complexes with heparin-derived disaccharides were resolved for RANTES (Shaw *et al.*, 2004) and stromal cell-derived factor-1 (SDF-1) (Murphy *et al.*, 2007). Furthermore, Proudfoot and colleagues demonstrated that binding to GAGs is essential for the activity of MCP-1, macrophage inflammatory protein-1β (MIP-1β) and RANTES as mutations in the GAG binding regions of these chemokines abrogated their ability to recruit cells *in vivo* (Proudfoot *et al.*, 2003). Specific heparan sulfate proteoglycans that bind chemokines were also identified. For example, IL-8 was shown to bind syndecan-2 on human endothelial cells (Halden *et al.*, 2004). Here, IL-8 was co-immunoprecipitated with syndecan-2 from TNFα-treated as well as unstimulated human umbilical vein endothelial cells. However, IL-8 was not co-immunoprecipitated with syndecan-1, syndecan-3 nor syndecan-4 (Halden *et al.*, 2004). In mice, the co-immunoprecipitation approached showed that syndecan-1 binds the IL-8 homolog KC (Li *et al.*, 2002). Although much research focused on deciphering how chemokines bind heparan sulfate and the structure of chemokine-heparan sulfate complexes (Lortat-Jacob, 2009), very little work focused on visualizing chemokine-heparan sulfate interactions *in vivo* (Massena *et al.*, 2010). As

well, despite the vast amounts of knowledge on the molecular mechanisms of chemokine-mediated leukocyte recruitment in various tissues, the inflammatory responses of the peritoneum during infection and PD are poorly understood.

1.3 PERITONEAL DIALYSIS

1.3.1 Peritoneum and the peritoneal microcirculation

The peritoneum is a serous membrane composed of a layer of simple squamous epithelium of mesodermal origin, known as the mesothelium, with an underlying basement membrane. Underneath this layer, is a thin layer of areolar connective tissue with collagen and scattered elastin fibres known as the compact zone which is followed by looser connective tissue with fibroblast-like cells, leukocytes and adipocytes. The loose connective tissue zone contains small blood vessels and lymphatic vessels. In healthy individuals, the submesothelial compact zone is 50 μm in thickness. The peritoneum is a continuous sheath divided into two regions, the visceral peritoneum and the parietal peritoneum. The visceral peritoneum lines the abdominal organs and their neurovascular supplies. The part of the visceral peritoneum that covers the arcade of blood vessels, nerves and lymphatic vessel that supply and drain the small intestine is referred to as the mesentery. The parietal peritoneum lines the wall of the abdominopelvic cavity. The potential space between the visceral and parietal peritoneal layers is the peritoneal cavity. The peritoneal cavity is filled with a slippery serous fluid, allowing the two layers of the peritoneum to slide over each other as the visceral organs move (Tortora & Derrickson, 2006). Approximately 85% of the peritoneal surface is the visceral peritoneum and the remaining 15% is the parietal peritoneum (Rubin *et al.*, 1988a).

The parietal peritoneum is perfused by the microcirculation arising from the vessels that also supply the abdominal muscles. The paired superior and inferior

epigastric arteries, deep circumflex iliac arteries, lumbar arteries as well as intercostal and subcostal arteries contribute to the microcirculation underlying the parietal peritoneum (Schuenke *et al.,* 2006). The contribution of peritoneal arterioles to solute and fluid transport in PD is negligible since they are less permeable and have a smaller surface area than peritoneal capillaries and venules. The peritoneal capillaries are the primary sites of peritoneal transport in PD. The postcapillary venules also have some contribution to solute and fluid exchange. The permeability of venules increases in inflammation as these vessels are the primary sites of leukocyte recruitment (Vriese *et al.*, 2009).

1.3.2 Renal failure and types of dialysis

End-stage renal disease (ESRD) is a debilitating chronic condition with high-cost treatment options (Zelmer, 2007). The lifetime risk of ESRD in Canada for a man is 1 in 40 and for a woman 1 in 60 (Turin *et al.*, 2012). With severe impairment of kidney function, blood cleansing artificially with dialysis solutions is an alternative to kidney transplantation. The dialysis solutions are specially formulated to maintain diffusion gradients to promote waste removal from the blood such as creatinine, urea, uric acid, phosphate, potassium and sulfate ions along with excess water.

The most common form of dialysis in Canadian patients is hemodialysis (Yeates *et al.*, 2012). In hemodialysis, the patient's blood is removed and passed through a hemodialysis machine that serves as an artificial kidney where wastes and solutes are filtered through a selectively permeable membrane against the dialysate, and then the

blood is returned into the patient through the venous access. Hemodialysis typically entails three medical facility visits per week and the amount of treatment is based on the patient's body mass and residual kidney function (Tortora & Derrickson, 2006).

The other and less costly dialysis option is PD, where the dialysis solution is administered into the peritoneal cavity through a surgically implanted catheter. There is an exchange of water and solutes between the patient's blood and the indwelling solution across the peritoneal layer, allowing for removal of excess water and wastes from the blood. The mesothelial layer, submesothelial connective tissue (compact zone) and the vascular endothelium with its basement membrane constitute the dialysis membrane. Diffusion, convective transport and osmosis are the physiologic basis of dialysis. The solution is drained after every night with automated peritoneal dialysis or through daily exchanges with continuous ambulatory peritoneal dialysis (CAPD). In CAPD, the solution remains in the abdomen until it is drained and replaced with fresh dialysate 4-6 times per day. In Canada about 19% of patients use PD as renal replacement therapy for chronic kidney failure (Mendelssohn & Wish, 2009). Without the need to visit a medical facility, PD is the preferred modality for patients living in remote and rural areas and for patients in whom mobility is important (Tonelli *et al.*, 2007). Furthermore, PD allows a less restricted diet and avoids the biochemical and fluid fluctuations of intermittent hemodialysis. It is also more suitable for patients with diabetes and cardiovascular problems (Gokal & Mallick, 1999). As well, the incidence of bacteremia (presence of bacteria in the blood) is higher in hemodialysis patients compared with PD (Wang *et al.*, 2012). Nevertheless, due to technique complications,

there is a high drop-out rate in long-term PD (Maiorca *et al.*, 1996) with a switch to hemodialysis. Thus, the recommended approach is use of PD until kidney transplantation is possible or until technique failure occurs and a switch to hemodialysis is necessary (Gokal & Mallick, 1999). Despite the eventual switch to hemodialysis, evidence suggests that kidney failure patients who started with PD survive up to three years longer compared to those who start on hemodialysis (Fenton *et al.*, 1997).

1.3.3 PD failure and pathology of the peritoneal membrane

PD failure typically occurs due to infection or loss of ultrafiltration (Barone *et al.*, 2009; Davies *et al.*, 1998; Kolesnyk *et al.*, 2010). This functional abnormality is accompanied by high dialysate to plasma ratios or high mass transfer area coefficients of low molecular weight solutes such as urea and creatinine. Underlying this failure is a change in the phenotype of the mesothelial cells of the peritoneal membrane (Yung & Chan, 2007a), where there is initial inflammation and neovascularization, and eventually transition of the mesothelial cell to a fibroblast-like state, a process referred to as epithelial-mesenchymal transition (EMT). The initial angiogenesis results in increased permeability to glucose and loss of osmotic capability, eventually leading to ultrafiltration failure (Davies *et al.*, 1998; Williams *et al.*, 2002). The mechanism for this failure is likely multifactoral and involves a complex interaction between the uremic host, the bioincompatible dialysis fluid with glucose degradation products (GDPs), the presence of the foreign body dialysis catheter and recurrent infections (Kendrick & Teitelbaum, 2010; Lai *et al.*, 2007).

The phenotypic appearance of the peritoneal membrane is altered at 8 to 12 months of PD in patients where there is no evidence of peritonitis (Yanez-Mo *et al.*, 2003). A comprehensive study of the parietal peritoneum changes that occur in PD showed that after 6 years of PD treatment, severe fibrosis, manifested by 16-fold thickening of the submesothelial compact zone, is observed along with vasculopathy of the peritoneal layer in 89% of patients (Williams *et al.*, 2002). Increased submesothelial fibrosis was also found in uremic pre-dialysis patients, indicating that uremia also contributes to peritoneal changes before commencement of treatment. In this study of 130 patients, increased duration of peritoneal dialysis was associated with increased submesothelial fibrosis and increased severity and prevalence of vasculopathy with subendothelial hyalinization in the peritoneal biopsies (Williams *et al.*, 2002). Loss of surface mesothelium was apparent in half of the PD samples. Vessel density was also significantly increased in PD patients with membrane failure. There was a strong correlation between vasculopathy and fibrosis with vasculopathy contributing to fibrosis by promoting ischemia. Not only was the mesothelial layer disrupted in long-term dialysis, but the mesothelial cells also took on an altered appearance with an increased apical-basolateral diameter (cuboid shape), decreased surface microvilli, discohesion and increased intracytoplasmic vacuolation (Williams *et al.*, 2003). These morphologic mesothelial changes are the most common phenotype observed in PD but a fibroblastic/mesenchymal phenotype with migratory behaviour has also been observed with mesothelial cells collected form the effluent in long-term PD (Yanez-Mo *et al.*, 2003). However, it is not clear whether effluent mesothelial cells are representative of

the remaining surface mesothelial cells. Overall, the study indicated that there is much variation in the morphologic changes in the PD patients but the changes are more profound in patients that experienced technique failure (Williams *et al.*, 2002). Also, the degree of the pathological peritoneal changes that occur is greater in the parietal peritoneum compared with the visceral peritoneum in the same patients (Williams *et al.*, 2003).

The dialysis solution is an important factor that contributes to technique failure. Conventional peritoneal dialysis solutions have high glucose concentrations, and thus high osmolarity, and many contain lactate as the buffer system. The pH is low (approximately 5.2 to 5.5) so that caramelization of glucose is minimized during heat sterilization and formation of toxic GDPs is reduced. However, these solutions are unphysiologic because the acidic pH, high lactate and glucose concentrations, hypertonicity and GDPs ultimately contribute to functional impairment of the peritoneal membrane and peritoneal advanced glycosylation end-products accumulate in the vascular walls of the PD patients and positively correlate with dialysate/plasma ratios of various solutes (Nakayama *et al.*, 1997). To decrease the GDP content of a solution at a more neutral pH, the two-chambered bag system was developed, where the glucose is sterilized separately at a pH of 3 while the buffer and electrolytes are kept separately at a pH of 8. Immediately before intraperitoneal use, the contents of the two bags are mixed and the result is a neutral pH fluid. This double chamber design also allows for the use of the bicarbonate-based buffer system (Passlick-Deetjen *et al.*, 2001).

Effects of different constituents of dialysis solutions were examined in animal models of PD. Superfusion of the rat mesentery with a conventional PD solution caused a reversible dilation of the arteries by 20% but not of small arterioles (Mortier *et al.*, 2002). However, the flow through these arterioles increased and this resulted in a 20% increase of the number of perfused capillaries. While PD fluid with high lactate and low GDP-content transiently induced increased vasodilation and capillary perfusion, the low-GDP and bicarbonate buffered solution did not affect these hemodynamic parameters. However, resterilization of this solution to increase GDP-content yielded the same type of effects as the conventional PD solution. This indicates that the GDP-content, rather than glucose and the lactate buffer system, had major hemodynamic effects (Mortier *et al.*, 2002).

Peritonitis due to bacterial infection is another major contributor to complications in PD. Turbidity of the effluent is a sign of a potential peritoneal infection. The main site of infection in PD is the lumen of the catheter from touch-contamination as well as the outside of the catheter at the exit site. *S. aureus*, *Staphylococcus epidermidis* and *Escherichia coli* are amongst the most common microorganisms causing peritonitis in PD (Betjes *et al.*, 1993; Davies *et al.*, 1996; Kavanagh *et al.*, 2004). *Pseudomonas* species and fungal organisms are also involved in PD-associated infections (Davies *et al.*, 1996). Chronic peritonitis drives peritoneal damage, with permeability changes and poor outcomes for patients. Chronic peritonitis may require catheter removal and is the leading cause of technique failure in PD (Kavanagh *et al.*, 2004). During peritonitis, inflammatory reactions contribute to peritoneal damage and eventual technique failure.

In particular, recurrent peritonitis was associated with increased small solute transport and decreased ultrafiltration (Davies *et al.*, 1996). It is important to note that some studies saw no link between peritonitis and peritoneal function (Lo *et al.*, 1994). It appears that occurrences of peritonitis in close proximity had greater effects on peritoneal function rather than the total number of infections over time in PD (Davies *et al.*, 1996).

1.3.4 Animal models of peritoneal dialysis

Histopathologic changes in the peritoneal tissue and the process of PD were studied with animal models, with the rat and rabbit being the most popular, allowing for the testing of biocompatibility of peritoneal dialysis solutions and the development of new solutions (Stojimirovic *et al.*, 2001). This work was essential to the understanding of the mechanisms of PD-associated angiogenesis and fibrosis. The rat model was instrumental in the investigation of the role of PD fluids (Mortier *et al.*, 2003) and catheters (Flessner *et al.*, 2007). However, despite the difficulties with manipulation due to its size, the mouse is a useful model of PD due to the wide availability of transgenic animals (Gonzalez-Mateo *et al.*, 2009; Ni *et al.*, 2003).

1.3.5 Effects of dialysis solutions on leukocyte recruitment to the peritoneal microcirculation

Currently, it is unclear whether PD solutions, or specific components of PD solutions, have pro-inflammatory or anti-inflammatory effects on the parietal peritoneal

microcirculation and how leukocyte recruitment is affected by one-time exposure versus long-term exposure to PD. Even less is known about the effects of the peritoneal catheter on the peritoneal microcirculation. IVM was applied to examine the effects of PD solutions on leukocyte-endothelial cell interactions in the visceral peritoneum in order to determine whether dialysis solutions are pro-inflammatory or whether PD fluids dampen inflammatory responses.

To delineate which components of dialysis solutions have effects on leukocyte recruitment in response to lipopolysaccharide (LPS), Mortier and colleagues examined the response to several conventional, new and homemade dialysis solutions in mesenteric venules of the small bowel (Mortier *et al.*, 2003). *E. coli* LPS was added to the dialysis fluids at 0.01 μg/mL and the rat mesenteric peritoneal membrane was superfused with the solutions. In general, the solutions had negative effects on leukocyte recruitment in response to LPS, with a conventional 4.25% dextrose lactate-buffered solution of pH 5.2 having the greatest inhibitory effects on leukocyte rolling (Mortier *et al.*, 2003). These inhibitory effects were more profound with higher lactate concentrations and hyperosmolarity. pH adjustment to 7.4 and increased GDP content of a solution, on the other hand, did not seem to further alter leukocyte recruitment. In general, the pH-neutral, bicarbonate-buffered solutions with low GDP content had milder depressive effects on LPS-induced leukocyte recruitment. Superfusion with spent dialysate (1.5% dextrose, L-lactate buffered) had similar depressive effects on leukocyte recruitment as fresh dialysate, indicating that the solutions retain their sufficiently elevated osmolarity and lactate concentrations to reduce leukocyte-endothelial cell

interactions. Finally, the authors reported no significant differences in systemic leukocyte counts and hematocrit between the treatment groups. These findings highlight important implications of the dampening effects of the presence of conventional PD fluids on inflammatory responses in peritonitis.

In a subacute (5 week) PD model, somewhat contradictory effects of dialysis on leukocyte recruitment were found by Schilte and colleagues. Compared with buffer controls, significantly increased numbers of spontaneously rolling leukocytes were noted in rat mesenteric venules after exposure to Dianeal with 3.86% glucose but not the more physiologic Physioneal solutions administered through a tunneled peritoneal catheter daily for 5 weeks (Schilte *et al.*, 2010). Interestingly, the increased baseline rolling could not be attributed to the presence of the peritoneal catheter since there were no significant differences between the catheterized and buffer-injected group when compared to the naïve animals. After superfusion with the bacterial product fMLP to induce inflammatory conditions, the presence of dialysis solutions and buffered control solution increased leukocyte-endothelial cell interactions in response to fMLP compared with naïve mice. Since this effect was more rapid in the Dianeal-treated animals compared to the Physioneal group, it is plausible that the more physiologic pH and lower GDP content of Physioneal solution caused less endothelial activation.

In another study of rat mesenteric venules, 5 week exposure to Dianeal 3.86% glucose, lactate-buffered PD fluid through a peritoneal catheter induced a significantly higher number of rolling leukocytes but not adherent leukocytes compared to catheterized and naive controls (Zareie *et al.*, 2002). There was no difference in

leukocyte rolling between the catheterized control rats and the naïve group, however. Furthermore, no significant differences were seen in leukocyte rolling velocities, blood flow velocities and vascular permeability between the three groups. Importantly, no differences in systemic leukocyte counts and differential leukocyte counts were noted. Compared with naïve rats, the catheterized controls exhibited mild neovascularisation, whereas the dialyzed animals had severe neovascularization. The authors of the study attributed the increased leukocyte rolling to the formation of new blood vessels.

To examine the early peritoneal response to PD solutions, rats were injected IP with several different PD solutions with a dwell time of 5 hours. IVM of the mesenteric venules was performed. The number of rolling and adherent leukocytes was significantly increased after single exposure to PD solutions containing high concentrations of glucose (4.25%) and high GDP-content as well as polyglucose (Icodextrin 7.5%, low GDP content), indicating an acute inflammatory response of the peritoneal venules. However, the more physiologic solutions, with low glucose and more neutral pH, did not induce acute inflammation (Frajewicki *et al.*, 2009). Taken together, these studies indicate that in general, exposure to PD fluids increases baseline rolling in mesenteric venules and during inflammation, PD fluids can lead to an increase or a decrease in leukocyte-endothelial cell interactions depending on the pro-inflammatory stimulus. Also, it appears that characteristics of PD fluids that contribute to suppression of leukocyte recruitment in the peritoneal inflammatory response are low pH, high lactate and glucose concentrations and high GDP content.

While most studies focused on the mesenteric portion of the visceral peritoneum microcirculation, there is a report on the effects of a PD fluid on the microcirculation of the intestinal mucosa. This study sought to determine the effects of a conventional PD solution on the jejunal microcirculation in rats during hemorrhagic shock with resuscitation. Venules on the luminal side of the jejunum were observed after topical application of a conventional glucose based PD solution and compared to physiologic Kreb's solution (Campbell *et al.*, 2006). The PD fluid significantly attenuated leukocyte rolling in the intestinal venules in sham-operated animals but not in rats that underwent hemorrhagic shock.

Although the visceral peritoneum accounts for 70% of the peritoneal surface with the liver accounting for 15% and the parietal peritoneum for 15%, studies showed that the contribution of visceral peritoneum does not dominate the total peritoneal membrane exchange of solutes as there was a reduction by only 10% to 30% of the mass transport of solutes in animal evisceration studies (Rubin *et al.*, 1991; Rubin *et al.*, 1989; Rubin *et al.*, 1988b; Rubin *et al.*, 1986; Rubin *et al.*, 1987). It is important to note that with evisceration the contact between the parietal peritoneum and the PD solution may be increased, which may explain these findings. Although the parietal peritoneal surface and underlying microcirculation appear to be major contributors to the dialysis membrane, reports on the effects of PD fluids and peritoneal catheter on leukocyte recruitment and the inflammatory microcirculatory response are lacking in the current literature.

Previous work in our lab indicated that acute exposure to 4.25% glucose PD fluid alters baseline leukocyte-endothelial cell interactions in the parietal peritoneum microcirculation (Patrick & Fox-Robichaud, 2010; Quinn & Fox-Robichaud, 2009). C57BL/6 mice were injected IP with sterile saline or TNFα and 3 hours after, the animals received an IP injection of 2 mL of conventional or new PD fluids with a 1 hour dwell. The mice were then prepared for IVM of the parietal peritoneum microcirculation and the effects of acute exposure to PD fluids on leukocyte-endothelial cell interactions were examined under baseline (saline) and inflammatory (TNFα) conditions. The control solution in the study was Ringer's Lactate.

Baseline leukocyte rolling was significantly increased after exposure to Dianeal (4.25% glucose, lactate buffered) solution compared with Ringer's Lactate (Quinn & Fox-Robichaud, 2009). Baseline rolling was not altered by exposure to Dianeal solutions with lower glucose concentrations (1.50% and 2.50%) or solutions that used a different buffer system (Physioneal, 3.85% glucose, bicarbonate-buffered) or polyglucose instead of glucose (Extraneal, 7.5% icodextrin, lactate-buffered). There were no significant differences in the number of adherent leukocytes in the peritoneal venules between any of the solutions tested. These findings indicate that a combination of high glucose and lactate concentrations contributed to increased baseline rolling. Treatment with TNFα significantly increased the number of adherent leukocytes compared with saline controls in the group treated with Ringer's Lactate but there were no significant differences between saline and TNFα-injected mice after treatment with the PD solutions. TNFα depressed leukocyte rolling in all groups. None of the PD

solutions altered leukocyte-endothelial cell interactions during the inflammatory response induced by TNFα.

We also examined the effects of the same PD solutions on the liver microcirculation in a separate set of animals (Patrick & Fox-Robichaud, 2010). In the hepatic post-sinusoidal venules, TNFα-treatment significantly elevated the number of rolling and adherent leukocytes compared with saline controls in each treatment group. However, leukocyte rolling and adhesion were not altered by any of the solutions under baseline conditions with saline nor inflamed conditions with TNFα. Similarly, the number of adherent leukocytes in the hepatic sinusoids was significantly increased with TNFα injection compared with saline, but none of the PD fluids had effects on baseline adhesion or TNFα-induced adhesion of leukocytes. Taken together, these results indicate that acute IP exposure to high glucose and lactate fluids can stimulate increased baseline leukocyte rolling in venules of the parietal peritoneum but leukocyte recruitment is not altered by PD fluids during inflammation. Furthermore, leukocyte recruitment under baseline and inflamed conditions is not altered in the hepatic microcirculation with acute PD fluid treatment.

Overall, the current literature indicates that dialysis solutions may impair host defense mechanisms in the visceral peritoneum which may impact infections and peritonitis in PD. However, the leukocyte-endothelial cell interactions in the parietal peritoneum venules in PD are not well described.

1.3.6 Effects of the peritoneal catheter on the peritoneal layer, biofilm formation and peritonitis

Bacteria and fungi attach to a surface, form communities and secrete gelatinous exopolymers, forming a cell-polymer matrix referred to as a biofilm. Biofilm formation on medical devices is a common problem in hospital settings. This mode of bacterial growth is also found on PD catheters (Finelli *et al.*, 2002). Biofilm formation is particularly problematic as it enables bacteria to resist high levels of antibiotics and disinfectants and it confers protection from the host immune responses, the result being a chronic or recurrent infection for as long as the medical device is employed (Bryers, 2008). Interestingly, there is biofilm formation on peritoneal catheters even without detectable infection in PD patients (Swartz *et al.*, 1991).

Peritonitis is the most common reason patients switch from PD to hemodialysis (Gokal, 2002). PD catheters provide a surface for the attachment of bacterial cells and the PD effluent fluid rich in glucose provides nutritional support for the bacterial colonies (Dasgupta *et al.*, 1992; Dasgupta *et al.*, 1993; Dasgupta *et al.*, 1991; Donlan, 2001). Clinical studies showed that chronic peritonitis and catheter-related infections are associated with biofilm formed on PD catheters (Dasgupta *et al.*, 1991). In PD, biofilm-related infections were found to be caused by gram-positive and gram-negative bacteria, which commonly involved *S. aureus, S. epidermidis, P. aeruginosa* and *E. coli* (Dasgupta, 2002). These pathogens were also found to form biofilm on silastic material in an experimental PD environment (Dasgupta *et al.*, 1994). *S. aureus* peritonitis cases have a particularly poor prognosis (Kavanagh *et al.*, 2004). Interestingly, *S. aureus*

biofilms reduced host inflammatory responses by evading recognition by TLR2 and TLR9 and attenuating macrophage phagocytosis in a mouse model of biofilm infection (Thurlow *et al.*, 2011).

The difficulties associated with eradicating biofilms with traditional antibacterial therapies inspired the development of catheter materials that resist bacterial colonization. Using a rabbit model of PD, it was shown that bacterial colonization in a biofilm starts at the catheter exit site and progresses along the catheter surface into the peritoneal cavity. Bacterial biofilms covered the PD catheters within three weeks of implantation and dialysis resulted in an increased rate of biofilm development, bacterial invasion of peritoneal tissues and peritonitis (Read *et al.*, 1989). Silver-coated materials have already been tested as PD catheters. However, although the silver coating appeared promising as an anti-bacterial surface (Dasgupta, 1994), there are concerns over toxicity resulting from the release of silver into surrounding tissue (Dasgupta, 1997).

Silicone PD catheter implants act as foreign bodies. The host response to a foreign body is described by several phases, starting with blood-material interactions, acute and chronic inflammation, followed by foreign body reaction and fibrous encapsulation. A study by Flessner and colleagues (Flessner *et al.*, 2007) demonstrated that part of the damage to the peritoneal membrane observed in chronic animal models of PD is caused by the presence of the PD catheter. A careful comparison of the injection of a sterile 4% glucose solution through a needle versus implanted catheter revealed that the effects of PD on the peritoneum differ based on the injection route (Flessner *et al.*, 2007). The presence of the catheter resulted in increased submesothelial compact zone thickness in

the parietal peritoneum, increased vascular density in the submesothelial compact zone and more intense immunohistochemical staining of the growth factors vascular endothelial growth factor (VEGF), basic fibroblast growth factor (bFGF) and transforming growth factor-β1 (TGF-β1). These changes were noted at 2, 4, 6 and 8 weeks after the commencement of fluid injections. Solute transport, measured as mass transport coefficients for mannitol and albumin, was significantly greater for the catheter-injected group compared with the needle injected group through the duration of the study. However, measurements of fluid flow across the peritoneum were not significantly different between the two groups. The authors concluded that the PD catheter as a foreign body is an important factor in the peritoneal responses during PD and further investigation into the interaction of local peritoneal immune defense mechanisms and the catheter are required.

In a follow-up study by Flessner and colleagues, animals with subcutaneous silicone catheters tunnelled into the peritoneal cavity that were not exposed to dialysis solutions exhibited changes in the peritoneum at 4 weeks of catheter acclimatization after surgical implantation. At this time point, the catheter contained a sterile cell layer that included red blood cells, leukocytes, mesothelial cells and fibroblasts. Thus, the catheter acts as an inflammatory source in the peritoneum. Interestingly, these animals had more striking histopathologic alterations of the peritoneum than animals treated with a 4% glucose solution through a catheter for 20 weeks. Animals that did not have a catheter implanted but received daily intraperitoneal injections of dialysis solution, on the other hand, exhibited comparatively less alterations in the peritoneum (Flessner *et*

al., 2010a). This study found that the catheter did not affect the transport function of the peritoneum, however.

The degree of catheter-induced inflammatory changes in the peritoneal abdominal wall vary over time and appear to be the greatest with subacute exposure and gradually decline with chronic exposure (Flessner *et al.*, 2010b). Intraperitoneal silicone catheter ring implants induced maximal submesothelial thickening and angiogenesis in the parietal abdominal wall at 4 weeks of exposure, which decreased by 20 weeks of exposure in rats. No infection was detected in the animals with the implants which were covered by macrophages, fibroblasts and mesothelial cells. A similar experiment in mice indicated that the adherent cell layer on the catheter declined in total white blood cell density from the first week following catheter implantation to 5 weeks later (Peters *et al.*, 2011). Throughout this subacute experiment, the thickness and angiogenesis of the submesothelial layer increased with exposure time. The authors also found evidence of changes in transport function of the peritoneum in mice with catheter implants compared with naïve controls. These studies emphasize that the effects of dialysis solution on peritoneal pathology, function and inflammatory responses cannot be examined without careful differentiation of the effects of the peritoneal catheter versus the PD fluid. At the same time, these studies suggest that animal models of PD may not be entirely accurate in replicating the catheter contributions to the peritoneal pathology in humans.

1.3.7 Mechanisms of fibrosis, angiogenesis and inflammation in peritoneal dialysis

Evidence suggests that inflammation is a major contributor to the histopathologic changes in PD. Inflammation of the peritoneal membrane was linked to progressive development of fibrotic changes that lead to technique failure in PD (Margetts & Bonniaud, 2003). During infection, the neutrophils dominate the influx of cells in the peritoneal cavity and the release of reactive metabolites and enzymes contributes to the peritoneal damage (Donovan *et al.*, 1993; Mariano *et al.*, 1992). Acute exposure of the parietal peritoneum to the pro-inflammatory cytokines TNFα and IL-1β induced elevated IL-6, TGF-β and VEGF levels along with increased neutrophil counts in the peritoneal fluid and increased cytokine levels in peritoneal tissues (Margetts *et al.*, 2002b). This was accompanied by histological changes in the visceral and parietal peritoneum, including hypertrophy of the mesothelial cells, submesothelial thickening with increased collagen content and leukocyte infiltration. There was also increased angiogenesis and increased dilation of blood vessels. These changes led to decreased net ultrafiltration and increased glucose transport. In general, the histopathologic alterations and decreased function of the peritoneal layer resolved faster with TNFα-treated animals compared with IL-1β. These findings are significant because they showed that inflammatory cytokines can initiate peritoneal angiogenesis, resulting in acute ultrafiltration failure. Because the observed histologic and functional changes resemble the consequences of peritonitis in PD patients, this study suggests a link between peritonitis, inflammatory cytokines and functional deterioration of the peritoneum.

Acute exposure to TGF-β1 resulted in fibrosis and angiogenesis with reduction in ultrafiltration of the rat peritoneum (Margetts *et al.*, 2001). EMT was induced by transient overexpression of TGF-β1, which involved increased expression of genes involved in EMT in peritoneal tissues and disruption of the basement membrane (Margetts *et al.*, 2005). A rat model of peritoneal fibrosis showed that the mesothelial cells undergoing EMT express genes involved in angiogenesis and fibrosis. Acute exposure of the parietal peritoneum to TGF-β1-expressing adenovirus resulted in changes resembling histopathologic alterations in PD. Immunohistochemical analysis and quantitative polymerase chain reaction showed that with TGF-β1 exposure, mesothelial cells expressed VEGF and VEGF-expression increased in vascular cells while the EMT-marker, α smooth muscle actin (αSMA), was expressed in the mesothelial cells and submesothelium (Zhang *et al.*, 2008). The mesothelial cells of the TGF-β1-treated rats also had increased gene expression of angiopoietin-2 and connective tissue growth factor (Zhang *et al.*, 2008). These findings are significant because dialysate VEGF (Zweers *et al.*, 1999) and TGF-β (Lai *et al.*, 1999) concentrations were correlated with measures of peritoneal membrane solute transport in dialysis patients.

Since the histologic and functional changes in PD implicate angiogenic and fibrogenic processes, antiangiogenic and antifibrotic treatments were examined in a 4-week dialysis and catheter exposure rat model (Margetts *et al.*, 2002a). Gene transfer of angiostatin with an adenovirus vector decreased vascularization of the peritoneum and improved dysfunction with ultrafiltration and solute transport. Decreased fibrosis was

noted in animals given adenoviral gene transfer of decorin, but this did not improve peritoneal membrane function. These findings highlight the importance of angiogenesis over fibrosis as a cause of peritoneal membrane dysfunction.

1.3.8 Effects of peritoneal exposure to PD fluids on the innate immune system

There is evidence that the innate immune responses of the peritoneum and leukocytes become impaired with acute and chronic exposure to PD fluids. While inflammation and leukocyte recruitment in peritonitis are essential for clearance of infection, they are associated with loss of peritoneal function (Betjes *et al.*, 1994). *In vitro* work and study of peritonitis cases in PD patients have identified the molecular mechanisms of inflammatory responses in peritonitis. Roles for IL-8, IL-6 and MCP-1 were identified in leukocyte recruitment in peritonitis and steady-state PD (Betjes *et al.*, 1996; Brauner *et al.*, 1993; Tekstra *et al.*, 1996; Zemel *et al.*, 1994). The leukocyte infiltrate in peritonitis is initially dominated by neutrophils and is gradually replaced by monocytes and eventually lymphocytes. This temporal switch in leukocyte subtype recruitment was shown to be mediated by IL-6 and its soluble IL-6 receptor and this process involved a shift from CXC chemokine production (MIP-2 and KC) to attract neutrophils to CC chemokine production (MCP-1 and RANTES) to attract monocytes (Hurst *et al.*, 2001). ICAM-1 and VCAM-1 are expressed on the peritoneal mesothelial layer and mediate the attachment of several different leukocytes subtypes (Andreoli *et al.*, 1994; Cannistra *et al.*, 1994; Liberek *et al.*, 1996). Human peritoneal mesothelial cells secrete IL-8, MCP-1 and RANTES with cytokine stimulation as well as

constitutively, and the chemokine levels are higher on the apical surface of the mesothelium (Li *et al.*, 1998). Apical addition of IL-8 induced polymorphonuclear cell migration across the mesothelial layer while apical addition of MCP-1 and RANTES induced mononuclear cell transmigration (Li *et al.*, 1998). Mesothelial cells stimulated with IL-1β also promoted transmigration of leukocytes from the basolateral compartment to the apical compartment of mesothelial cells and this process appeared to be mediated by ICAM-1. For this transmigration to occur, neutrophils required IL-8 and monocytes required MCP-1 (Li *et al.*, 1998).

In CAPD with peritonitis, the percentage of macrophages in the effluent is decreased while the proportion of neutrophils and lymphocytes is increased compared with healthy controls. The macrophages of PD patients had a less mature phenotype and the percentage of phagocytosing macrophages was also reduced (Betjes *et al.*, 1993). Immunophenotypic analysis of T cells revealed more immune activation in the PD patients. The peritoneal cells of CAPD patients also had reduced chemotaxis to fMLP and PD effluent compared with controls (Betjes *et al.*, 1993). This study suggests that in PD, the peritoneal immune system exhibits immaturity and increased activation, a possible consequence of chronic stimulation by PD fluids.

Liberek and colleagues attempted to determine the effects of increasing osmolarity and glucose content on human polymorphonuclear and mononuclear cells (Liberek *et al.*, 1993). Although the pH and lactate concentration of a solution normalize within the first hour of dwell time, the osmolarity and glucose concentration do not normalize even after a standard 4 hour dwell time in CAPD. *In vitro* work

indicates that exposure of leukocytes to solutions of high osmolarity and glucose concentrations inhibits cell function. Specifically, increasing glucose concentrations increased polymorphonuclear cell toxicity but did not affect respiratory burst activation. High osmolarity decreased phagocytosis and leukotriene B_4 generation from polymorphonuclear cells. Increased osmolarity and elevated glucose concentration also diminished TNFα and IL-6 release from mononuclear cells (Liberek *et al.*, 1993). Furthermore, *ex vivo* testing of peritoneal macrophages that were isolated from peritoneal effluents showed impaired cytokine production, phagocytosis, respiratory burst activity and bacterial killing capacity (Posthuma *et al.*, 1999). Bicarbonate/lactate-buffered solutions appeared to preserve peritoneal macrophage activity in response to LPS compared to standard Dianeal solution (Rogachev *et al.*, 1997). However, no difference in macrophage inflammatory activation was found in spent dialysate from bicarbonate/lactate-buffered Physioneal solution-treated patients compared with the lactate-buffered Dianeal (Pajek *et al.*, 2008).

Animal models also indicate that PD exposure interferes with innate immune responses. With acute (2-week) exposure to PD solution delivered through a peritoneal catheter in rats, there was decreased neutrophil recruitment and reduced *S. aureus* clearance from the peritoneal cavity in an IP infection rat model (Hekking *et al.*, 2001a). After subacute (10-week) exposure to dialysis solutions through a peritoneal catheter, the *ex vivo* bacterial killing capacity of cells from the peritoneal lavage was diminished (Hekking *et al.*, 2001b). In this chronic rat model, the bicarbonate/lactate-buffered PD fluids had less negative effects on bacterial killing capacity compared with lactate-

buffered fluids. However, the molecular mechanisms through which PD interferes with innate immune responses and the role of molecular regulators, such as syndecans, in these pathological processes are not clearly defined.

1.4 SYNDECAN-1

1.4.1 Structure and function

Syndecan-1 belongs to a family of 4 heparan sulfate proteoglycans that act as co-receptors for various heparan sulfate-binding ligands. The 4 syndecan family members are encoded from paralogous genomic regions (Chakravarti & Adams, 2006). Syndecan-1 is a single-pass type I transmembrane heparan sulfate proteoglycan composed of a cytoplasmic domain, a transmembrane domain and an extracellular *N*-terminal domain containing a proteolytic cleavage site (**Figure 2**). The major functional domain of syndecan-1 is composed of several heparan sulfate GAG chains covalently attached to the distal portion of the extracellular domain of the protein core. The repeating unit of these heparan sulfate chains is a disaccharide of hexuronic acid (either glucuronic or iduronic acid) linked to *N*-acetylglucosamine. The glucosamine can also be unsubstituted or sulfated at the *N*-position, 2-, 3-, and/or 6-*O*-position (Esko & Selleck, 2002). The proximal portion of the extracellular domain contains a chondroitin sulfate chain composed of alternating *N*-acetylgalactosamine and glucuronic acid. Both, heparan sulfate and chondroitin sulfate are linear polysaccharides (Varki *et al.*, 1999).

Syndecan-1 is found on cell surfaces as a homodimer. The human syndecan-1 monomer is expected to be a 32 kDa protein. However, with the addition of the heterogeneous heparan sulfate chains, the molecular weight of syndecan-1 tends to be higher and variable as determined by Western blotting (Gattei *et al.*, 1999). Specifically, the differences arise from variability in the number of GAG chains attached, their

lengths and arrangement of sulfated residues. On epithelia of different tissues, for example, differential glycosylation of syndecans results in the existence of polymorphic forms (Sanderson & Bernfield, 1988). As a highly glycosylated and sulfated molecule, heparan sulfate is negatively charged. Heparin is a more heavily sulfated pharmaceutical analogue of heparan sulfate. While heparin is confined to intracellular vesicles of mast cells in connective tissues, heparan sulfate is ubiquitously expressed in extracellular matrices and on cell surfaces.

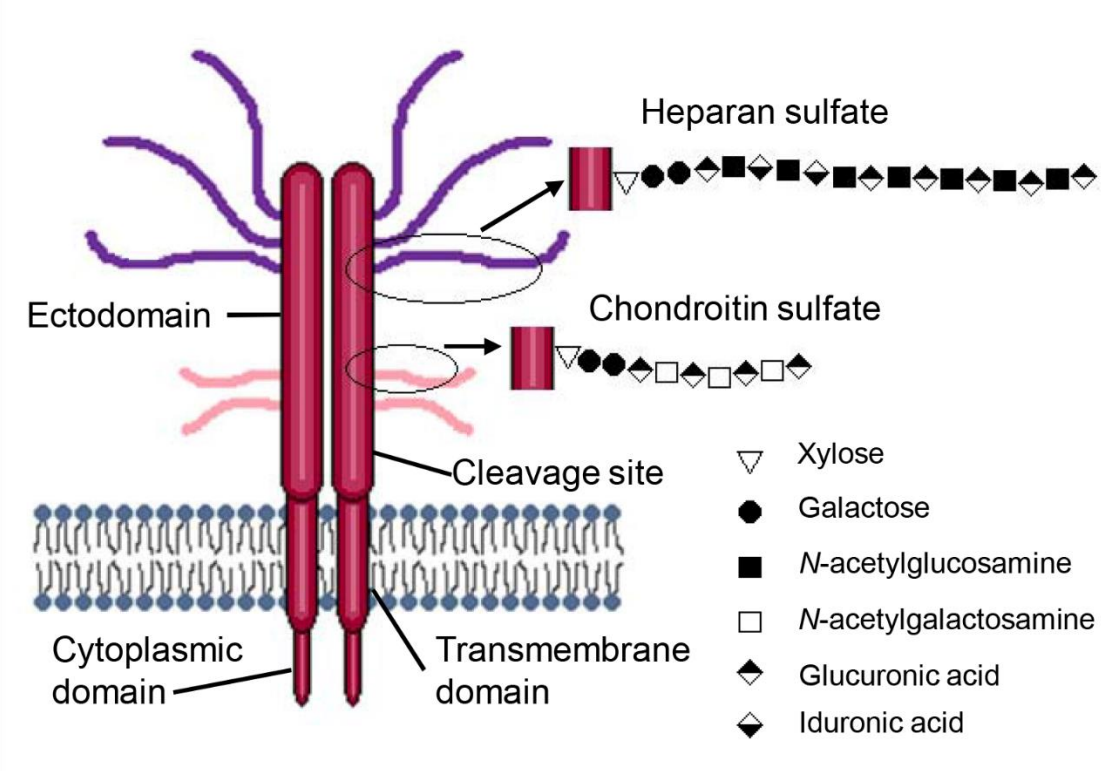

Figure 2. Structure of syndecan-1. Syndecan-1 is a type I transmembrane proteoglycan that is found on cell surfaces as a dimer. The extracellular portion of the protein core can bear up to three heparan sulfate chains and two chondroitin chains of heterogeneous length. The symbol nomenclature described in reference (Varki *et al.*, 1999) was used to render the GAGs.

Compared to the human ortholog, mouse syndecan-1 exhibits sequence identity of 70% for the extracellular domain, 96% for the transmembrane domain and 100% for the cytoplasmic domain (Purushothaman & Sanderson, 2009). Syndecan-1 is used as a cell marker for B cells and is highly expressed in epithelial cells and fibroblastic cells, with very low expression in neural and endothelial cells (Kim *et al.,* 1994). Syndecan-1 is also expressed in mouse vascular smooth muscle cells where syndecan-1 deficiency led to increased gene expression of syndecan-2 and syndecan-4 (Chaterji *et al.,* 2014). Syndecan-1 is also commonly expressed as a soluble factor as its extracellular domain is cleaved by matrix metalloproteinases (MMPs). The endogenous proteinases that shed syndecan-1 include MMP-7 (Li *et al.*, 2002), MMP-9 (Brule *et al.*, 2006) and MMP-14 (Endo *et al.*, 2003).

The cytoplasmic tail of syndecan-1 contains a PDZ domain binding motif. The protein families with PDZ domains organize protein complexes that interact with the actin cytoskeleton at the cytoplasmic side of the cell membrane (Grootjans *et al.*, 2000). Through these interactions, syndecan-1 is involved in cell migration (Chakravarti *et al.*, 2005). Also, syndecan-1 modulates signaling pathways that involve the kinase cascade (extracellular signal-regulated kinases/mitogen activated protein kinase (MAPK), c-Jun N-terminal kinases (JNK) and p38/MAPK) and downstream transcription factors Myc, Fos, JNK and Jun (Szatmari *et al.,* 2012). As well, given the ability of syndecan-1 heparan sulfate chains to bind various extracellular matrix components and soluble ligands, syndecan-1 participates in processes as diverse as wound healing, inflammation, angiogenesis, fibrosis and EMT (Alexopoulou *et al.,* 2007; Gotte, 2003).

Although no mutations in the syndecan-1 gene have been reported in humans, syndecan-1 is highly expressed on multiple myeloma cells and in its shed form is associated with poor prognosis (Aref *et al.,* 2003).

1.4.2 Syndecan-1 in wound healing

Wound healing is a highly regulated sequence of events that repairs damaged tissues and may result in fibrosis with loss of function. The initial phase of tissue repair is inflammatory and involves blood clot formation as well as recruitment of neutrophils and monocytes, which develop into macrophages, to phagocytize microbes and dying cells as well as to release proteases that digest extracellular proteins (Tortora & Derrickson, 2006). The next phase involves granulation tissue formation and tissue remodelling with stem cell migration and proliferation, fibroblast-mediated deposition of connective tissue and revascularization (Tortora & Derrickson, 2006).

During repair of skin wounds, syndecan-1 expression is increased in the epidermis and dermis and shed syndecan-1 ectodomain accumulates in granulation tissue and wound fluid (Bernfield *et al.*, 1999). Specifically, syndecan-1 expression in keratinocytes changes during differentiation and stratification (Sanderson *et al.*, 1992). Histochemical staining revealed syndecan-1 is also induced in the endothelial cells of the skin wound bed (Elenius *et al.,* 1991). In periodontal wounds in rats, immunohistochemistry techniques showed that syndcan-1 was expressed in the newly formed vessels and the recovering epithelium (Worapamorn *et al.*, 2002). The pattern of syndecan-1 expression in wounded tissue changes depending on the stage of the healing

process (Worapamorn *et al.*, 2002). A number of growth factors that regulate wound repair bind heparan sulfate to signal through their receptors, including VEGF (Gitay-Goren *et al.*, 1992), platelet-derived growth factor (Feyzi *et al.*, 1997) and fibroblast growth factors (Allen *et al.*, 2001). Consequently, syndecan-1 was implicated in mediating responses to growth factors at sites of wound repair (Worapamorn *et al.*, 2002).

In animal wound models, syndecan-1 deficiency and syndecan-1 overexpression both appear to show dysregulated and delayed wound healing. After skin wounding with a punch biopsy, transgenic mice that overexpressed syndecan-1 as well as syndecan-$1^{-/-}$ (*Sdc1*$^{-/-}$) mice exhibited reduced keratinocyte proliferation at the wound edge and disorganized granulation tissue (Ojeh *et al.*, 2008). The reduced re-epithelialization was more pronounced in the transgenic mice in this study compared to the deficient mice. In corneal wounds in mice, syndecan-1 deficiency inhibited keratinocyte migration and proliferation (Stepp *et al.*, 2002). Corneal re-epithelialization was delayed and there were increased numbers of inflammatory cells at the wound edge of *Sdc1*$^{-/-}$ corneas. This was associated with decreased α_9 integrin expression at the leading edge of the wound and failure of the tight junction protein zonula occludens-1 to repolarize to the apical layer of the cornea after wounding in the *Sdc1*$^{-/-}$ mice (Stepp *et al.*, 2002). In this study, similar defects were observed with epithelial cell proliferation and α_9 integrin localization in the cutaneous wounds of *Sdc1*$^{-/-}$ mice (Stepp *et al.*, 2002). In another model of cutaneous injury with a dorsal skin punch biopsy and incisional wounds, mice overexpressing syndecan-1 had a 5 day delay in re-epithelialization,

granulation tissue formation and remodelling with a prolonged and higher levels of syndecan-1 ectodomain shedding into wound fluid (Elenius *et al.*, 2004). The syndecan-1 overexpressing mice also appeared to have increased microvessel dilation. Syndecan-1 immunodepletion, heparan sulfate degradation and skin-graft experiments implicated the soluble syndecan-1 ectodomain in the delayed healing which increased proteolytic activity in the wounds (Elenius *et al.*, 2004). In fact, syndecan-1 appeared to maintain proteolytic balance in acute wound fluids (Kainulainen *et al.*, 1998) which is important as prolonged or excessive proteolysis destroys tissues and hampers repair. This may explain the delayed wound healing with syndecan-1 overexpression in animal models (Elenius *et al.*, 2004). The syndecan-1 ectodomain was found to bind neutrophil derived serine proteases elastase and cathepsin G and protect them from their inhibitors and degradation of heparan sulfate or removal of syndecan-1 from human dermal wound fluids reduced the proteolytic activity in the fluid (Kainulainen *et al.*, 1998). Thus, soluble syndecan-1 has an important physiologic role in maintaining proteolytic balance during wound healing. The fact that syndecan-1 deficiency as well as overexpression result in dysregulated and delayed wound healing indicate that the expression and shedding of this heparan sulfate proteoglycan is tightly regulated for optimal level of syndecan-1 expression in tissues to promote adequate and timely wound repair.

1.4.3 Syndecan-1 in leukocyte recruitment and inflammation

Syndecan-1 was shown to modulate leukocyte recruitment in several different tissues. In the retinal microcirculation, syndecan-1 decreased leukocyte adhesion to the

venular wall (Gotte *et al.*, 2002). In this study, fluorescent lectin staining of leukocytes and endothelial cells of retinas that were imaged *ex vivo* showed that retinas of *Sdc1*$^{-/-}$ mice contained increased numbers of adherent leukocytes in arterioles, venules and capillaries under uninflamed conditions, compared with wild-type animals, even though the animals had similar levels of systemic leukocyte counts. Bone marrow transplants indicated that syndecan-1 deficiency in leukocytes promoted the increased adhesion rather than the endothelial component. This suggests that there is leukocyte priming in the absence of syndecan-1 even though, aside from B cells at certain stages of development, syndecan-1 expression on leukocytes is not easily detected *in vivo* (Sanderson *et al.*, 1989; Zhang *et al.*, 2013). In the same study, absence of syndecan-1 resulted in decreased leukocyte rolling, increased leukocyte adhesion and increased leukocyte extravasation in mesenteric venules in response to TNFα-stimulation for 3 hours (Gotte *et al.*, 2002). The extravascular cells were not subset-specific and included neutrophils, monocytes and lymphocytes. *In vitro* evidence corroborated these findings, with increased numbers of *Sdc1*$^{-/-}$ polymorphonuclear cells and monocytes adhering to human umbilical vein endothelial cells compared to wild-type (Gotte *et al.*, 2005). The increase was more pronounced with monocytes. Addition of heparin, which is structurally very similar to heparan sulfate, abrogated the increased adhesiveness of *Sdc1*$^{-/-}$ leukocytes only in unstimulated conditions. With TNFα-stimulation, heparin did not revert the increased adhesion of *Sdc1*$^{-/-}$ leukocytes (Gotte *et al.*, 2005). Increased leukocyte adhesion was also noted in the cremasteric microcirculation of *Sdc1*$^{-/-}$ mice

observed by IVM (Savery *et al.*, 2013). This was associated with a thinner but hydrodynamically relevant glycocalyx.

The enhanced immune cell infiltration in syndecan-1 deficient mice has important implications for disease severity and recovery in pathologies involving leukocyte infiltration. In experimental autoimmune encephalomyelitis, *Sdc1*$^{-/-}$ mice exhibited increased disease severity and prolonged recovery. This was associated with increased numbers of the pro-inflammatory Th1 and Th17 cells that infiltrated the central nervous system and decreased numbers of the suppressive Tregs (Zhang *et al.*, 2013). The areas that were infiltrated by these cells showed more extensive demyelination. Interestingly, syndecan-1 expression was not detected on the vessels, perivascular region or immune cells in the brain. However, syndecan-1 was detected on the basolateral surface of the choroid plexus epithelium which is lost during experimental autoimmune encephalomyelitis. This correlated with loss of CCL20 and elevation of IL-6 on the choroid plexus epithelium which was more exaggerated in *Sdc1*$^{-/-}$ mice (Zhang *et al.*, 2013). This suggests that syndecan-1 controls chemokine gradients in encephalomyelitis and has suppressive effects on leukocyte infiltration in the brain, both processes that are dysregulated in syndecan-1 deficiency. Another pathology that becomes exacerbated in syndecan-1 deficiency is nephritis (Rops *et al.*, 2007). The influx of polymorphonuclear cells, macrophages and T cells to the glomeruli of *Sdc1*$^{-/-}$ mice was significantly higher compared with wild-type mice during experimental anti-glomerular basement membrane nephritis. This increased infiltrate was explained by enhanced ICAM-1 expression and increased expression of the inflammatory heparan sulfate domains with

N- and 6-*O*-sulfated patterns in syndecan-1 deficiency in this study. This resulted in decreased renal function and more glomerular injury in *Sdc1*$^{-/-}$ mice, along with increased pro-inflammatory cytokine expression and a shift from a Th1 to a Th2 response (Rops *et al.*, 2007). Thus, syndecan-1 appears to have anti-inflammatory properties in nephritis.

In dermal tissue, syndecan-1 attenuated delayed-type hypersensitivity by decreasing leukocyte recruitment (Masouleh *et al.*, 2009). Here, syndecan-1 deficiency resulted in increased and prolonged edema, leukocyte infiltration and microabscesses in the mouse pinna. There was also significantly increased expression of TNFα, RANTES, MIP-1α, MCP-1, IL-6 and ICAM-1 in the *Sdc1*$^{-/-}$ ear skin. In this study, *in vitro* evidence showed that polymorphonuclear cells from *Sdc1*$^{-/-}$ mice had increased adhesiveness to ICAM-1 which was efficiently blocked by antibodies to CD18 (Masouleh *et al.*, 2009). This suggests that syndecan-1 attenuated allergic inflammation in the skin by negatively modulating ICAM-1-CD18 interactions that mediate leukocyte recruitment.

Together, these studies indicate that syndecan-1 deficiency results in increased leukocyte recruitment with increased adhesive interactions between white blood cells and the endothelium. Thus, syndecan-1 appears to function as a negative regulator of leukocyte adhesion and heparan sulfate is the major functional domain in this process. In fact, used as a heparan sulfate analog, heparin was shown to inhibit the molecules that mediate interactions of leukocytes with endothelial cells (Diamond *et al.*, 1995; Nelson *et al.*, 1993). For example, E-selectin binding to endothelial cells was inhibited

by heparin, chondroitin sulfate and syndecan-1 ectodomain *in vitro* (Luo *et al.,* 2001). P-selectin and L-selectin were also inhibited by heparin which interfered with leukocyte recruitment (Wang *et al.,* 2002). However, *in vivo* evidence suggests that syndecan-1 deficiency has little effect on leukocyte rolling (Gotte *et al.*, 2002).

1.4.4 Modulation of chemokine gradients by syndecan-1

Evidence indicates that syndecan-1 binds chemokines with its heparan sulfate chains and generates chemokine gradients across epithelial and endothelial cell layers, and thereby regulates the magnitude of inflammatory responses as well as the resolution of inflammation. Syndecan-1 was shown to mediate the resolution of neutrophilic inflammation in multiple organs during endotoxemia by clearing chemokines (Hayashida *et al.*, 2009b). In a mouse model of endotoxemia induced by an IP injection of *E. coli* LPS, *Sdc1*$^{-/-}$ mice had increased multiorgan injury and dysfunction with increased mortality. This involved delayed removal of MIP-2 and KC from lungs and livers of endotoxemic *Sdc1*$^{-/-}$ mice with prolonged neutrophilic inflammation. Similar observations were made in wild-type mice after inhibition of syndecan-1 shedding with a metalloproteinase inhibitor (Hayashida *et al.,* 2009b). This study showed that syndecan-1 deficiency is detrimental in endotoxemia because syndecan-1 shedding is important for removal of MIP-2 and KC which are tethered to cell surfaces by syndecan-1, resulting in dissipation of the chemokine gradient and diminishing neutrophil infiltration of the lung and liver.

In the lung, syndecan-1 attenuated allergic lung inflammation by suppressing T cell recruitment (Xu *et al.*, 2005). *Sdc1*$^{-/-}$ mice that were challenged intranasally with allergens showed increased airway hyperresponsiveness, eosinophilia and glycoprotein secretion in bronchoalveolar lavage fluid compared with wild-type. This involved increased CCL7, CCL11 and CCL17 in bronchoalveolar lavage and enhanced Th2 cell activity in syndecan-1 deficient mice. In wild-type mice, syndecan-1 was shed into bronchoalveolar lavage fluid after allergen challenge. The shed syndecan-1 ectodomains attenuated lung inflammation by binding and inhibiting the Th2 chemokines CCL7, CCL11 and CCL17 which mediate the accumulation of Th2 cells in the lung (Xu *et al.*, 2005). This study showed that syndecan-1 is a beneficial host factor with protective effects in allergic lung inflammation.

However, syndecan-1 can also have negative effects in certain lung pathologies. In an experimental model of lung fibrosis, syndecan-1 bound KC and generated transepithelial chemokine gradients that mediated neutrophil migration into the alveolar space (Li *et al.*, 2002). In the absence of syndecan-1 shedding by MMP-7, there was an impairment of neutrophil transepithelial migration, which protected mice from the lethal effects of lung injury with bleomycin (Li *et al.*, 2002). Thus, despite the importance of syndecan-1 shedding in the confinement of inflammation to specific epithelial sites and the alveolar space, syndecan-1 deficiency was beneficial in this study. *In vitro* work also suggested that syndecan-1 regulates chemokine gradients in humans. Syndecan-1 was shown to bind IL-8 and form a chemotactic gradient on the human umbilical vein endothelial cell surface in an *in vitro* model of transendothelial migration. Shedding of

these syndecan-1/IL-8 complexes inhibited transendothelial neutrophil migration (Marshall *et al.*, 2003). These studies highlight that syndecan-1 is an important host factor in the balance between health and disease through its involvement in co-ordination and resolution of inflammation.

1.4.5 Pathogen subversion of syndecan-1

The involvement of syndecan-1 in binding, concentrating and confining various ligands in a tissue-specific and temporal manner highlights its importance in the body. At the same time, many pathogens have evolved a way to subvert this protein and use it to increase virulence, dissemination and for host defense evasion during infection. In fact, many bacterial organisms possess virulence factors that promote syndecan-1 shedding. For example, challenge of mice with *Bacillus anthracis* spores induced syndecan-1 shedding and *in vitro* syndecan-1 shedding from epithelial surfaces in response to *B. anthracis* hemolysins compromised tissue integrity (Popova *et al.*, 2006). The occlusive thrombi that occur in the hepatic microcirculation during *B. anthracis* infection in mice consist of aggregated bacteria with shed syndecan-1 (Popova *et al.*, 2012). *Streptococcus pneumoniae* also induced syndecan-1 shedding from epithelial cells *in vitro* (Chen *et al.*, 2007) but the significance of this is not clear. The more well characterized pathogens that manipulate syndecan-1 shedding in infection are *S. aureus* (Hayashida *et al.*, 2011) and *Pseudomonas aeruginosa* (Haynes *et al.*, 2005). In addition, there is evidence that *S. aureus* directly interacts with syndecan-1. *S. aureus* bound heparan sulfate (Liang *et al.*, 1992) and *S. aureus* internalization by intestinal

epithelial cells was mediated by heparan sulfate binding (Hess *et al.*, 2006). Syndecan-1 promoted *S. aureus* interactions with epithelial cells and participated in *S. aureus* translocation across the intestinal epithelial barrier (Henry-Stanley *et al.*, 2005).

Using *Sdc1*$^{-/-}$ mice, *S. aureus* was shown to use syndecan-1 to promote its pathogenesis in the cornea (Hayashida *et al.*, 2011). In this study, *S. aureus* infection induced syndecan-1 shedding from the corneal epithelium in a corneal scratch injury model with topical application of a suspension of *S. aureus* cells. Although the bacterial burden was similar in corneas of *Sdc1*$^{-/-}$ and wild-type mice at 1 hour post infection, the syndecan-1 deficient mice had significantly reduced bacterial counts 7 and 24 hours after inoculation, suggesting that the *Sdc1*$^{-/-}$ mice cleared the infection more rapidly (Hayashida *et al.*, 2011). Topical application of syndecan-1 ectodomains or heparan sulfate to *Sdc1*$^{-/-}$ corneas increased their susceptibility to *S. aureus* infection. At the same time, inhibition of syndecan-1 shedding from wild-type corneas with a metalloproteinase sheddase inhibitor significantly decreased the bacterial load of the corneas. Syndecan-1 ectodomains and heparan sulfate did not appear to have effects on *S. aureus* growth rate or adhesion to corneal epithelium, however. Furthermore, syndecan-1 did not directly bind *S. aureus* cells, but instead the shed syndecan-1 ectodomains with heparan sulfate inhibited *S. aureus* killing by interfering with neutrophil microbicidal abilities even though syndecan-1 did not affect leukocyte influx to the infected corneas. This suggests that syndecan-1 is a host factor that promotes corneal *S. aureus* infection which involves syndecan-1 shedding from cell surfaces. In experimental *S. aureus* pneumonia, syndecan-1 shedding from mouse alveolar

epithelium resulted in increased neutrophil influx and lung injury and was dependent on expression of *β*-toxin by *S. aureus* (Hayashida *et al.*, 2009a). The *Sdc1*$^{-/-}$ mice were largely protected from lung injury in this infectious model. Another study showed that in addition to *β*-toxin, the *S. aureus α*-toxin also induced syndecan-1 shedding *in vitro* (Park *et al.*, 2004). These toxins induced syndecan-1 shedding by activating the host cell's protein-tyrosine kinase-dependent shedding mechanisms (Park *et al.*, 2004).

P. aeruginosa also possesses a virulence factor, protease LasA, that caused syndecan-1 shedding from mouse epithelial cells *in vitro* by activating the host cell's shedding machinery and not by direct interactions with syndecan-1 ectodomain (Park *et al.*, 2000a). Twenty hours after intranasal infection with *P. aeruginosa*, *Sdc1*$^{-/-}$ mice had decreased pneumonia, bacteremia and mortality (Park *et al.*, 2001). The decreased susceptibility of *Sdc1*$^{-/-}$ mice to the infection was reversed by addition of heparin or heparan sulfate-containing syndecan-1 to the inoculum but not with syndecan-1 core protein alone. *P. aeruginosa* did not use syndecan-1 as an attachment site but induced LasA-dependent syndecan-1 shedding in the lungs (Park *et al.*, 2001). Similarly, *P. aeruginosa* subcutaneous injection caused syndecan-1 shedding in full thickness burn wounds in mice (Haynes *et al.*, 2005). In this burn model, *Sdc1*$^{-/-}$ mice had reduced mortality, decreased dissemination of *P. aeruginosa* into the blood stream and colonization of internal organs and decreased accumulation of *P. aeruginosa* in the perivascular regions of infected skin with reduced systemic inflammation. Surprisingly, compared to wild-type, the *Sdc1*$^{-/-}$ mice did not have altered leukocyte recruitment to the infected skin. These results strongly implicated syndecan-1 as a host factor

contributing to *P. aeruginosa* pathogenesis in burn wounds (Haynes *et al.*, 2005). Together, these studies indicate that shed syndecan-1 modulates the extent and outcome of inflammatory responses in infection and is also commonly manipulated by pathogens to dysregulate inflammation and increase virulence.

1.4.6 Syndecan-1 in angiogenesis

Angiogenesis is a highly regulated process involving basement membrane degradation, endothelial cell proliferation, extension of pseudopodia and migration as well as connective tissue cell and vascular smooth muscle cell recruitment leading to vessel wall maturation. Angiogenesis occurs in normal processes such as embryogenesis and wound healing to satisfy the high metabolic requirements of the repair process. However, angiogenesis also supports pathological processes such as tumour growth (Chiorean *et al.*, 2014). A role for syndecan-1 in angiogenesis was suggested as syndecan-1 deficient mice exhibited increased corneal neovascularization in an angiogenesis assay (Gotte *et al.*, 2002). However, overexpression of syndecan-1 also increased the angiogenic phenotype of endothelial cells from multiple myeloma patients (Lamorte *et al.*, 2012). In fact, syndecan-1 expression has pro-angiogenic effects on tumours such as myeloma (Purushothaman *et al.*, 2010) and medulloblastoma (Asuthkar *et al.*, 2014). Syndecan-1 also exhibited pro-angiogenic effects on epithelium-derived tumours, including breast cancer (Gotte *et al.*, 2007) and endometrial cancer (Oh *et al.*, 2010).

The observations that both, syndecan-1 deficiency and overexpression promoted angiogenesis indicates that syndecan-1 is a regulator of this process. Syndecan-1 appears to modulate angiogenesis by increasing local concentration of growth factors (Ruhrberg *et al.*, 2002), by mediating the binding of these growth factors to their receptors (Cohen *et al.*, 1995; Gitay-Goren *et al.*, 1992) and by interacting directly with the growth factor receptors (Schlessinger *et al.*, 1995). Syndecan-1 binds the pro-angiogenic factors VEGF and bFGF (Iozzo & San Antonio, 2001). Syndecan-1 also binds the vascular endothelial growth factor receptor-2 (VEGFR-2). In syndecan-1-knockdown cells, there was absence of VEGFR-2 nuclear translocation which prevented VEGF signalling and angiogenesis (Lamorte *et al.*, 2012). Syndecan-1 also activated the integrins $\alpha_V\beta_3$ and $\alpha_V\beta_5$ (Beauvais *et al.*, 2009), which are critical in driving angiogenesis. Disruption of the interactions of syndecan-1 with $\alpha_V\beta_3$ and $\alpha_V\beta_5$ on endothelial cells blocked angiogenesis *in vitro* with human aortic explants and *in vivo* in mouse tumours (Beauvais *et al.*, 2009). Furthermore, syndecan-1 coupling to the insulin-like growth factor-1 receptor and activation of $\alpha_V\beta_3$ was critical for VEGF signalling and endothelial cell dissemination during angiogenesis (Rapraeger *et al.*, 2013). Thus, syndecan-1 interacts with and modulates the activity of various angiogenic mediators.

1.4.7 Syndecan-1 in fibrosis

Fibrosis is a normal part of the wound healing process, which involves fibrous connective tissue deposition, and supports re-epithelialization. However, excess

formation of fibrous tissue is pathological in conditions such a pulmonary fibrosis (Kolb & Collard, 2014), liver cirrhosis (Iwakiri *et al.*, 2014), endomyocardial fibrosis (Mueller *et al.*, 2013), encapsulating peritoneal fibrosis (Augustine *et al.*, 2009) and PD histopathology (Williams *et al.*, 2002). In a mouse model of myocardial infarction, increased syndecan-1 adenoviral expression in the infarcts protected against exaggerated inflammation, injury and dysfunction (Vanhoutte *et al.*, 2007). In syndecan-1 deficient mice, there was elevated leukocyte recruitment, increased chemokine expression, increased matrix metalloproteinase activity with increased collagen fragmentation and disorganization (Vanhoutte *et al.*, 2007). This also involved increased cardiac dilation and dysfunction. Thus, syndecan-1 had protective effects in cardiac myocardial infarction. However, in an angiotensin II-induced cardiac fibrosis mouse model, wild-type mice showed extensive cardiac fibrosis with increased expression of collagen type I and III while the *Sdc1*$^{-/-}$ mice exhibited less fibrotic changes. In this study, loss of syndecan-1 reduced cardiac dysfunction during angiotensin II-induced hypertension (Schellings *et al.*, 2010). The protective effects of syndecan-1 deficiency were associated with decreased expression of TGF-β-inducible gene connective tissue growth factor and decreased activation of the Smad2 pathway (Schellings *et al.*, 2010). Also, in another study, oxidant-induced syndecan-1 shedding and its effects on neutrophil chemotaxis contributed to pulmonary fibrosis (Kliment *et al.*, 2009). Overall, these studies indicate that syndecan-1 is a mediator of fibrosis and the effects of syndecan-1 deficiency differ based on the model of fibrosis examined.

1.4.8 Modulation of EMT by syndecan-1

The transition of epithelial cells to mesenchymal-like cells occurs during wound healing (Kalluri, 2009) and is vital in embryogenesis (Acloque *et al.*, 2009). However, a pathologic role for EMT was defined in fibrosis (Kalluri & Weinberg, 2009) and cancer (Wang *et al.*, 2014). Loss of syndecan-1 is associated with EMT. In cultured cells, EMT with changes in cell polarity, intercellular adhesion and epithelial gene expression were induced by disruption of syndecan-1 expression (Dobra *et al.*, 2000; Rapraeger, 2001). Syndecan-1 deficient epithelial cells showed mesenchymal cell behaviour and anchorage-independent growth, with rearrangement of β_1 integrins, reduced E-cadherin expression along with disorganized F-actin filaments (Kato *et al.*, 1995). These *in vitro* studies show that syndecan-1 is important for normal phenotype and structure of epithelial cells.

1.5 PURPOSE OF INVESTIGATION

1.5.1 Rationale

The damaging effects of conventional dialysis solutions are manifested as fibrosis, angiogenesis and EMT (Williams *et al.*, 2002) in the peritoneal lining. These deleterious alterations are further complicated by bacterial peritonitis, commonly caused by *S. aureus* (van Diepen *et al.*, 2014), and ultimately lead to PD failure. An understanding of the molecular mechanisms of the histopathologic changes that occur in PD and the basis of the injury caused by dialysis solutions and catheter can lead to advancements in the therapy.

Syndecan-1 is a multifunctional protein that interacts with various inflammatory mediators through its heparan sulfate chains but its role in peritoneal injury, infection and inflammation is not known. Heparan sulfate was demonstrated to bind several different chemokines (Li *et al.*, 2002; Slimani *et al.*, 2003), growth factors (Salmivirta *et al.*, 1992), coagulation factors (Cizmeci-Smith & Carey, 1997) and extracellular matrix components (Carulli *et al.*, 2012). As a result, syndecan-1 was implicated in many vital processes, including wound repair (Stepp *et al.*, 2002), angiogenesis (Oh *et al.*, 2010), fibrosis (Schellings *et al.*, 2010), EMT (Kato *et al.*, 1995; Masola *et al.*, 2012) as well as inflammation (Li *et al.*, 2002). Furthermore, *S. aureus* was shown to manipulate syndecan-1 to promote its pathogenesis (Hayashida *et al.*, 2011). Given that syndecan-1 modulates inflammation, fibrosis, angiogenesis and EMT and syndecan-1-microbial

interactions are important in the pathogenesis of *S. aureus*, we chose to examine the function of this proteoglycan in *S. aureus* infection during PD.

1.5.2 Hypotheses

1. Syndecan-1 is expressed on the venules and presents chemokines to leukocytes interacting with the vessel wall.

2. Given that the peritoneal catheter is tunneled through the abdominal wall, the implant promotes chronic inflammation in the musculoperitoneal tissue, resulting in increased baseline leukocyte-endothelial cell interactions in the microcirculation underlying the parietal peritoneum.

3. Syndecan-1 deficient mice have altered responses to *S. aureus* infection and greater peritoneal pathology in subacute peritoneal dialysis compared with wild-type animals.

1.5.3 Objectives

1. To characterize the protein expression of syndecan-1 in the parietal peritoneum and the underlying microcirculation, as well as to examine the role of syndecan-1 in leukocyte recruitment and chemokine presentation.

2. To examine the subacute effects of peritoneal catheter implants and dialysis solutions on leukocyte recruitment in the parietal peritoneum microcirculation in a mouse model of PD with a surgically implanted catheter.

3. To study the effects of syndecan-1 deficiency on peritoneal pathology and *S. aureus* infection during peritoneal dialysis.

To address these objectives, we developed a mouse model of the parietal peritoneum microcirculation using IVM. With this *in vivo* technique, we directly visualized syndecan-1 and chemokine expression, as well as leukocyte-endothelial cell interactions in the parietal peritoneum microcirculation. We also used a subacute PD mouse model with a catheter implant to assess the effects of syndecan-1 deficiency in *S. aureus* infection in PD.

CHAPTER 2: MATERIALS AND METHODS

2.1 Animals

The animal protocols met the regulations set by the Canadian Council of Animal Care and were approved by the McMaster University Animal Research Ethics Board (Animal Utilization Protocol #11-01-03). Six to eight week old male BALB/c mice were obtained from Taconic (Germantown, NY, USA). The mice were given at least one week to acclimatize. Age-matched syndecan-1 null (*Sdc1*$^{-/-}$) male mice on a BALB/c background were used in the study. The *Sdc1*$^{-/-}$ breeders were a kind gift from Dr. Pyong W. Park (Children's Hospital, Boston, MA) and the *Sdc1*$^{-/-}$ mouse colony was interbred and maintained at McMaster University Central Animal Facility. Under specific pathogen-free housing conditions, the *Sdc1*$^{-/-}$ mice are healthy and fertile with normal growth and tissue morphology (Alexander *et al.*, 2000; Hayashida *et al.*, 2008; Stepp *et al.*, 2002). The animals were kept in sterilized filter-top cages and housed in a specific pathogen-free facility with a 12-hour light/dark cycle. The mice had free access to water and low-fat rodent chow (Harlan, Teklad, Inc., Madison, WI, USA). The health status of each animal was assessed before experimental procedures.

2.2 Generation of syndecan-1 knockout mice

Sdc1$^{-/-}$ mice were generated as described by Alexander and colleagues (Alexander *et al.*, 2000) in the laboratory of Dr. Park (Children's Hospital, Boston, MA) by mutation of the mouse *Sdc1* locus using embryonic stem cells. A genomic clone was

derived from a mouse genomic DNA library containing the 5' flanking sequence, first exon and part of the first intron of syndecan-1. The sequence was mutated by the insertion of a PGKneo cassette in exon 1 signal sequence and a negative *tk* selection marker was added at the 3' end of this signal sequence. This DNA was electroporated into embryonic stem cells and clones with a mutated *Sdc1* locus were selected by Southern-blot analysis. The embryonic cells with the mutation were injected into blastocysts and the chimeric mice were crossed with wild-type until the mutation was homozygous.

2.3 Study design for IVM experiments

Mice were injected intraperitoneally (IP) with 125 μg of LTA from *S. aureus* (Sigma-Aldrich, St. Louis, MO, USA) in 50 μL of sterile saline. Lipopolysaccharide (LPS) from *Escherichia coli* serotype 0127:B8 (Sigma-Aldrich, St. Louis, MO, USA) was injected IP at 125 μg in 50 μL of sterile saline per mouse. Murine recombinant tumor necrosis factor-α (TNFα) was injected IP at 500 ng in 50 μL of sterile phosphate buffered saline per mouse (R&D Systems®, Inc., Minneapolis, MN, USA). Control animals were injected IP with 50 μL clinical grade saline (0.9% NaCl). All IP injections were done on the right side. Four hours after IP injections of LPS, LTA, TNFα or saline, animals were prepared for IVM and the microcirculation underlying the parietal peritoneum was observed.

2.4 Preparation for IVM

The surgical preparation of mice for IVM is illustrated in **Figure 3**. The animals were anaesthetized with a subcutaneous injection of a mixture of ketamine (200 mg/kg) and xylazine (10 mg/kg). The subcutaneous route was chosen over IP injection for anaesthetic administration to minimize the disruption of the parietal peritoneum. The fur was clipped over the right ventral neck and the abdomen. The animals were placed on a heat pad and the right internal jugular vein was cannulated with a polyethylene catheter (PE 10, ID 0.28 mm, OD 0.61 mm, Intramedic™, Becton, Dickinson and Company, Mississauga, ON, Canada) for maintenance of anaesthesia, administration of fluids or fluorescent antibodies. The skin overlying the abdomen was bluntly dissected away. A midline incision, along the linea alba, was made in the abdominal wall extending inferiorly from the xiphoid process towards the left inguinal region and a flap was created on the left side. Gauze soaked in normal saline was placed over the abdominal contents for constant perfusion of the peritoneum and to keep the abdominal organs intact. The animals were placed in the right lateral position and the flap of peritoneum on the left side of the abdominal wall was laid out on a Plexiglas® microscope stage (Altuglas International, Arkema Inc., Philadelphia, PA, USA). The exposed tissue was immediately covered with plastic wrap (Saran Wrap®; S.C. Johnson and Sons, Inc., Racine, WI, USA) to prevent evaporative loss.

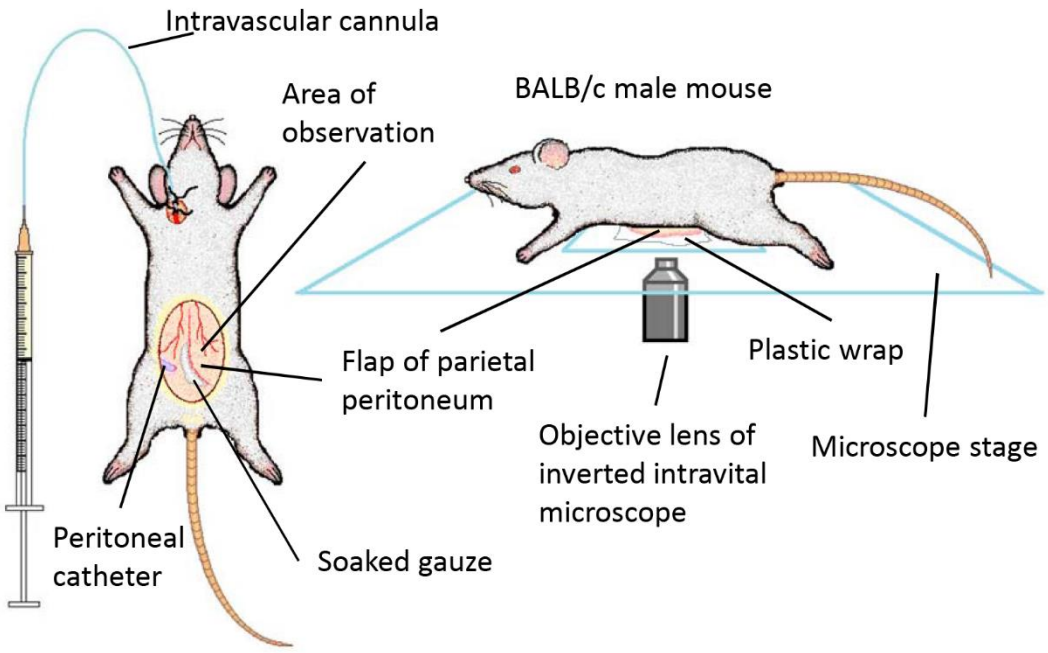

Figure 3. Mouse preparation for intravital microscopy of the parietal peritoneum microcirculation.

2.5 IVM: fluorescence confocal microscopy

Mice were injected with *S. aureus* LTA (125 μg) or saline IP with a dwell time of 4 hours and after preparation for IVM, the left side of the parietal peritoneum was visualized *in vivo*. Fluorescent antibodies were injected via the intravascular cannula and the peritoneal microcirculation was visualized with a spinning disc confocal system (Leica DMI 6000 B; Leica Microsystems, Mannheim, Germany) based on a Yokogawa spinning disc confocal unit, spectral laser merge module LMM5, and Hamamatsu back-thinned electron multiplying charge-coupled device (EMCCD) C9100-12 camera (Hamamatsu, Hamamatsu City, Japan). During the IVM observations, the animals were

placed in a chamber (LiveCell2 temperature and CO_2 environment control system; Quorum Technologies Inc., Guelph, Ontario, Canada) mounted on the confocal microscope and the temperature in the chamber was set to 37°C. The peritoneal microcirculation was observed with a 40X objective lens and images were acquired using the Volocity® 4 acquisition software (Improvision, Waltham, MA, USA), (n = 7).

2.6 Reagents for immunofluorescence confocal microscopy

All fluorescent antibodies were injected intravenously (IV) following preparation for IVM 4 hours after IP injection of saline or LTA. Syndecan-1 was detected with fluorescent monoclonal rat anti-mouse syndecan-1 antibody specific for the extracellular portion of the protein core (40 μg, clone 300506; R&D Systems®, Inc.). The anti-syndecan-1 antibody was labeled with Alexa Fluor® 488 and Alexa Fluor® 568 Monoclonal Antibody Labeling Kits (Molecular Probes®, Burlington, ON, Canada). Alexa Fluor® 647-conjugated monoclonal rat IgG1 was used as the isotype control for anti-syndecan-1 (40 μg, clone 43414; R&D Systems®, Inc.). Platelet endothelial cell adhesion molecule-1 (PECAM-1; CD31) was detected with Alexa Fluor® 647 monoclonal rat anti-mouse PECAM-1 (20 μg, clone 390; BioLegend, San Diego, CA, USA).

To examine the protein expression of adhesion molecules in the parietal peritoneum microcirculation, Alexa Fluor® 488-labeled anti-mouse vascular cell adhesion molecule-1 (VCAM-1; CD106) monoclonal rat antibodies (40 μg, clone 429 (MVCAM.A); BD Pharminogen™, Mississauga, ON, Canada) or anti-mouse

intercellular adhesion molecule-1 (ICAM-1; CD54) monoclonal Armenian Hamster antibodies (40 μg, clone 3E2; BD Pharminogen™) were injected IV 4 hours after LTA challenge. Alexa Fluor® 568-labeled rat IgG2a (40 μg, clone 54447; R&D Systems®, Inc.) was used as the isotype control antibody for anti-VCAM-1 and Alexa Fluor® 568-labeled IgG1 (40 μg, clone 43414; R&D Systems®, Inc.) was used as the isotype control for anti-ICAM-1.

To determine which leukocyte subtypes are recruited in the peritoneal microcirculation 4 hours after injection of saline, LTA or TNFα, Alexa Fluor® 488-labeled anti-mouse Ly6G/Gr1 monoclonal rat antibody (40 μg, clone RB6-8C5; R&D Systems®, Inc.) and Alexa Fluor® 568-labeled anti-mouse CX_3C chemokine receptor-1 (CX_3CR1) polyclonal goat antibodies (40 μg; R&D Systems®, Inc.) were co-injected IV.

To examine whether syndecan-1 co-localizes with chemokines *in vivo*, Alexa Fluor® 568-labeled anti-syndecan-1 and Alexa Fluor® 488-labeled anti-mouse macrophage inflammatory protein-2 (MIP-2; CXCL2) monoclonal rat antibody (40 μg, clone 40605; R&D Systems®, Inc.), anti-mouse keratinocyte chemoattractant (KC; CXCL1) monoclonal rat antibody (40 μg, clone 59526; Creative Diagnostics, Shirley, NY, USA) or anti-mouse monocyte chemoattractant protein-1 (MCP-1; CCL2) monoclonal rat antibody (40 μg, clone 123616; R&D Systems®, Inc.) were co-injected IV 4 hours after LTA challenge. Alexa Fluor® 568-labeled rat IgG2b (40 μg, clone 141945; R&D Systems®, Inc.) was used as isotype control for anti-MIP-2. In this study,

co-localization refers to spatial overlap between two fluorescent antibodies and reflects the location of two molecules of interest either in the same area or in close proximity.

To image other members of the syndecan family, Alexa Fluor® 488-labeled anti-mouse syndecan-2 monoclonal mouse antibody (40 μg, clone F-5; Santa Cruz Biotechnology, Inc., Dallas, TX, USA), anti-mouse syndecan-3 monoclonal rat antibody (40 μg, clone 312607; R&D Systems®, Inc.) or anti-mouse syndecan-4 monoclonal rat antibody (40 μg, clone KY/8.2; BD Pharminogen™) were injected IV 4 hours after wild-type mice were injected IP with LTA. Alexa Fluor® 568-labeled mouse IgG1 (40 μg, clone 11711; R&D Systems®, Inc.) or Alexa Fluor® 568-labeled rat IgG2a (40 μg, clone 54447; R&D Systems®, Inc.) were co-injected as isotype control antibodies. To image the Duffy Antigen/receptor for chemokines (DARC), Alexa Fluor® 488-labeled anti-mouse/rat DARC polyclonal sheep antibody was injected IV (40 μg; R&D Systems®, Inc.).

2.7 *Ex vivo* immunofluorescence imaging of the parietal peritoneum

Four hours after LTA treatment, animals (n = 3) were anaesthetized and an intrajugular cannula was inserted. Alexa Fluor® 488-labeled anti-syndecan-1 (40 μg) and Alexa Fluor® 647-labeled isotype control antibodies (40 μg) were injected IV. Tissue samples of the abdominal wall were collected after 15 min and the animal was euthanized. The tissue samples were embedded in optimal cutting temperature (OCT) compound and snap frozen. The samples were sectioned, counterstained with propidium iodide (PI)-containing mounting medium (Fluoroshield™ with PI; GeneTex Inc., Irvine,

CA, USA) and imaged with a spinning disc confocal system (Leica DMI 6000 B; Leica Microsystems).

2.8 Quantification of fluorescence intensity

The fluorescence intensity of the labeled antibodies was quantified from the captured *in vivo* images of peritoneal venules using ImageJ (NIH, W. Rasband, Bethesda, Maryland, USA). The fluorescence intensity of the Alexa Fluor® 488-conjugated anti-syndecan-1 was measured along the length of the basolateral side of the venular endothelium and the value for the corresponding intravascular fluorescence intensity was subtracted. This relative difference in intensity was calculated for 3 - 4 venules per mouse (n = 7) and the values were recorded as the difference in mean fluorescence intensity (gray levels). For each venule, the difference in mean fluorescence intensity between the extravascular and intravascular region was also quantified from the Alexa Fluor® 647-labeled isotype control antibodies.

2.9 Syndecan-1 levels measured by enzyme-linked immunosorbent assay

Animals were injected IP with 50 μL saline, 125 μg *S. aureus* LTA or 500 ng TNFα, n = 5. Four hours after, the mice were anaesthetized with a subcutaneous injection of a mixture of ketamine and xylazine. Peritoneal lavage was done with 2 mL of clinical grade saline. Blood was collected via cardiac puncture in a heparinized syringe. Peritoneal effluent and blood were centrifuged at 1188 x g. Samples of the abdominal wall were collected and immediately frozen in liquid nitrogen. The tissues

were homogenized in cell lysis buffer (BioVision, Milpitas, CA, USA). Blood plasma and the supernatant from the tissue homogenate were analyzed at a 50-fold dilution. Peritoneal effluent was analyzed at a 10-fold dilution in PBS. Syndecan-1 levels in the tissue homogenate, peritoneal effluent and blood plasma were measured with a commercially available ELISA kit for mouse syndecan-1 (E91966Mu; USCNK Life Sciences Inc., Wuhan, China). To account for differences in tissue sample sizes, a Bradford assay was performed to measure total protein concentration in tissue homogenates and results were normalized to the total protein recovered.

2.10 Transillumination IVM

The microcirculation underlying the left side of parietal peritoneum was observed by an inverted intravital microscope (transillumination technique) (Zeiss Inverted Axiovert 100; Carl Zeiss, Jena, Germany) under 40X objective lens. The tissue was transilluminated with a light source via fiberoptic (The ACE® Series; Schott-Fostec, LLC, Auburn, NY, USA) equipped with a 150 Watt tungsten halogen lamp. Images were captured with an attached camera (Newvicon; DAGE-MTI, Michigan City, IN, USA), projected onto a monitor (Panasonic, CT-2086YD; Panasonic Canada Inc., Mississauga, ON, Canada) and recorded with a DVD recorder (Panasonic, DMR-EH55) for offline analysis. During the intravital observations, the animals were warmed with an infrared heat lamp positioned over the intravital microscope. To minimize the effects of the surgery and exposure of the peritoneal layer, IVM observations were made within 10 min after completion of the surgical preparation. After completion of *in vivo*

imaging, blood was collected into a heparinized syringe via cardiac puncture. Euthanasia was ensured by cervical dislocation.

2.11 Offline analysis

Leukocyte-endothelial interactions were quantified in 4-6 venules per mouse (n = 4-5) and the number of extravascular leukocytes was determined. Rolling leukocytes were counted per minute and were considered as cells tethering to a venule with torsional motion. Cells that remained stationary for at least 30 seconds were identified as adherent leukocytes. Extravascular leukocytes were counted as perivenular leukocytes on a field of view measuring 180 μm x 135 μm.

2.12 Leukocyte and differential white blood cell counts

Leukocyte counts were done using a hemocytometer in 0.01 μL of blood collected with cardiac puncture immediately following the completion of IVM observations. The blood was mixed with 3% acetic acid and 1% crystal violet in a 5:44:1 ratio. Counts were averaged from 6 separate samples. Differential white blood cell counts were performed on 3 μL smears of blood fixed in methanol and stained with eosin and thiazine (Harleco Hemocolor stain set; EM Science, Gibbstown, NJ, USA).

2.13 Antibody blockade of adhesion molecules

Wild-type animals were injected IP with anti-mouse β_2 integrin/CD18 monoclonal rat antibody (40 μg, M18/2; BioLegend, San Diego, CA, USA), anti-ICAM-1/CD54 (40

μg, clone 3E2; BD Pharminogen™) and/or anti-VCAM-1/CD106 (40 μg, clone 429; BD Pharminogen™). The mice were then stimulated with *S. aureus* LTA (125 μg) and after 4 hours, the microcirculation underlying the parietal peritoneum was observed by IVM. For P-selectin studies, animals were prepared for IVM 4 hours after injection of LTA. Baseline recordings were taken and anti-mouse P-selectin/CD62P monoclonal rat antibodies (20 μg, RB40.34; BD Biosciences, Mississauga, ON, Canada) were injected IV through the jugular cannula and the response was recorded after five minutes.

2.14 Nonuremic subacute PD model

Under gaseous anaesthesia (4% Isoflurane), sterile silicone catheters (ID 0.635 mm, OD 1.1938 mm) that were attached to silicone injection ports with an internal stainless steel needle guard (Penny MousePort™; Access Technologies, Skokie, IL) were implanted following aseptic techniques. Similar silicone tubing is used in dialysis and intravenous catheters for human application. The animals were approximately 25 g at the time of surgery. Fur was clipped over the right posterior dorsum along with the area over the right lower quadrant of the abdomen. Buprenorphine hydrochloride (Temgesic®; Schering-Plough Ltd., Welwyn Garden City, UK) was injected subcutaneously at a dose of 0.1 mg/kg and skin was cleaned with Povidone-iodine solution (USP 10%). An incision was made in the skin over the right lower back and a subcutaneous pocket was created in the midscapular region for the insertion of the injection port. Before insertion, the port and catheter were flushed with 100 μL of 10% heparin (1000 USP Units/mL; Sandoz Canada Inc.) in saline to maintain patency. The

final position of the port was over the right posterior costal region. Another incision was made in the skin over the right lower abdomen and the pre-attached catheter was tunnelled subcutaneously from the back to the lower abdomen. The musculoperitoneal wall was penetrated and 1 cm tip of the catheter was inserted into the right lower quadrant of the peritoneal cavity. The catheter was secured in the abdominal wall with a purse string stitch between the movable beads on the catheter. The skin incisions were closed with clips. Omentectomy was not performed given the role of the omentum and its milky spots in local defenses (Panasco *et al.*, 2010). The animals were warmed with heat-pads and monitored for 8 hours and additional Ringer's Lactate fluids and buprenorphine (0.05 mg/kg) were administered during the recovery period. Two mice were housed per cage.

The mice were given two weeks to heal before commencement of injection of the dialysis solution. To ensure catheter patency, 70 μL of 10% heparin solution was injected into the subcutaneous port one week after catheter implantation. The use of heparin in this study was minimized given the effects of heparin on the peritoneal membrane (Margetts, 2009). The animals were weighed daily and monitored for altered appearance, behaviour, wound dehiscence and infection, as well as reddening and scabbing of skin over the port and catheter. Subcutaneous injections of Ringer's Lactate solution and buprenorphine were performed as required away from the implant area. Daily 2 mL injections of a conventional lactate-buffered dialysis solution (Dianeal PD4 CAPD Solution with 2.5% dextrose and 2.5 mEq/L Calcium, approximate pH 5.2; Baxter, Mississauga, ON, Canada) from a single-chamber bag were administered into

the Penny MousePort^{TM} for 6 weeks after the catheter acclimatization period. This volume is scaled down to the mouse body weight and approximates a single exchange in PD patients. Before each injection, skin over the port was sterilized with 2% W/V chlorhexidine gluconate and 70% isopropyl alcohol. Injections were performed using sterile technique in a biological safety cabinet.

2.15 Study design for 6 week-dialysis model

After a two-week healing period following catheter implantation, one group of mice (n = 4) was dialyzed over a 6 week period. The other group of animals with catheters (n = 4) served as the catheter control and the mice received a mock injection where a needle was inserted into the port but no dialysis solution was injected. The catheter was in the animals for a total of 8 weeks. On the last day of the 6 week period, mice were given the last injection of dialysis solution and 4 hours later, were prepared for IVM of the parietal peritoneum microcirculation. The region of the anterior abdominal wall that was imaged was on the left side and was around the area where the intra-abdominal portion of the catheter was positioned. The number of rolling, adherent and extravascular leukocytes was compared to naïve mice with no catheter implant and no dialysis solution treatment. At the end of IVM observations, blood was collected via cardiac puncture. Systemic leukocyte counts and differential white blood cell counts were performed. Samples of the anterior abdominal wall were taken from the left upper quadrant and the left lower quadrant adjacent to the midline. The samples were fixed in 10% buffered formalin, sectioned and stained with hematoxylin and eosin (H&E).

The peritoneal microcirculation was imaged by IVM and leukocyte-endothelial cell interactions were quantified. The preparation of the parietal peritoneum for *in vivo* imaging required exposure of the tissue by removal of the overlying skin and a midline incision along the abdominal wall. This procedure can be expected to contribute to local inflammation, which is of particular significance when tissues are imaged over a longer period of time. We observed that baseline values for leukocyte-endothelial cell interactions in the mouse bladder were maintained for the first half hour after the initial microscopy observations (Kowalewska *et al.*, 2011). In order to minimize the effects of this surgical preparation involving an incision through the peritoneal wall, care was taken to complete the preparatory surgery in approximately 10 minutes and the peritoneal layer was imaged within a 10 minute timeframe. To obtain more representative values of leukocyte-endothelial cell interactions in the parietal peritoneum, 4-6 different venules were imaged within this 10 minute period and leukocyte rolling, adhesion and extravasation were averaged in each animal.

2.16 Study design for 4 week-dialysis model with *S. aureus* infection

After peritoneal catheter implantation and a two-week catheter-acclimatization period, wild-type and *Sdc1*$^{-/-}$ mice were dialyzed over a 4 week period with daily 2 mL fluid instillation. On the last day of the 4 week period, mice received an injection of *S. aureus* through the subcutaneous port, which was immediately followed by an injection of 2 mL of dialysis solution through the port. Wild-type and *Sdc1*$^{-/-}$ animals that did not have an implant and were not dialyzed served as controls and were injected with

equivalent amounts of *S. aureus*-containing suspensions IP. Four hours later, mice were anaesthetized and catheters and tissues were collected. Results were compared to baseline levels in wild-type and *Sdc1*$^{-/-}$ mice. In total, 6 groups were observed with n = 8-14.

2.17 Bacterial strain and growth conditions

S. aureus h1559 (a kind gift from Dr. Burrows, McMaster University) cultures were grown overnight in tryptic soy broth (TSB) (EMD, Darmstadt, Germany) infused with 15 μg/mL of erythromycin (Sigma-Aldrich, Co., St. Louis, MO, USA). This strain carries a green fluorescent protein-expressing (GFP) plasmid, constitutively transcribed from the prsA promoter. The plasmid is selected by erythromycin. The overnight cultures were diluted 100-fold in fresh TSB and grown for 2.5 hours on a slant with shaking at 37°C to an optical density of 0.500 at 600 nm. For subacute peritoneal dialysis experiments, *S. aureus* was subcultured in TSB without erythromycin while in preparation for fluorescence IVM experiments, *S. aureus* was subcultured in the presence of erythromycin.

The Staphylococci were sedimented, washed and suspended in 100 μL of sterile PBS. Colony forming units (CFU) from the innocula were enumerated following serial dilution and plating on tryptic soy agar (TSA) plates with 10 µg/mL erythromycin (Teknova, Hollister, CA, USA) and grown overnight at 37°C. The innocula were found to contain approximately 1.8 X 10^8 CFU.

2.18 Mouse *S. aureus* peritoneal infection model and tissue collection

A 100 μL suspension of *S. aureus* containing approximately 1.8 x 10^8 CFU was injected through the subcutaneous injection port into the abdominal cavity and was immediately flushed with 2 mL of dialysis solution 4 hours before the study endpoint. Skin over the port was sterilized with 2% W/V chlorhexidine gluconate and 70% isopropyl alcohol before the injection. At study endpoint, *Sdc1*$^{-/-}$ and wild-type mice were anaesthetized with a subcutaneous injection of a mixture of ketamine (200 mg/kg) and xylazine (10 mg/kg). Animals were appropriately shaved. Under sterile conditions, peritoneal lavage was performed with 2 mL of sterile PBS. The intra-abdominal portion of the peritoneal dialysis catheter was retrieved and fixed in 2% glutaraldehyde in sodium cacodylate. Samples of the anterior abdominal wall were collected from the left upper quadrant adjacent to the midline and fixed in 10% buffered formalin for H&E staining. Additional samples of the anterior abdominal wall, taken from the left lower quadrant, were weighed and homogenized in sterile PBS. Blood was collected via cardiac puncture. CFU from the peritoneal lavage fluid, blood and abdominal wall homogenate were enumerated after serial dilutions and plating on TSA plates with 10 μg/mL erythromycin, which was followed with overnight incubation at 37°C. The CFU were recorder per 1 mL of peritoneal lavage fluid or blood and per 1 g of tissue.

The peritoneal lavage fluid and blood were mixed with 3% acetic acid and 1% crystal violet in a 5:44:1 ratio. Blood cell counts were averaged from 6 separate samples of the mixture of blood or lavage fluid. Differential white blood cell counts were

performed on 3 μL smears of blood fixed in methanol and stained with eosin and thiazine (Harleco Hemocolor stain set; EM Science, Gibbstown, NJ, USA).

2.19 Histopathologic examination

Cross-sections of the abdominal wall were collected in a standardized manner from the left side of the abdomen, contralateral to the catheter insertion site. The tissue samples were fixed with 10% buffered formalin, embedded in paraffin and thin-sectioned. Tissue sections were stained with H&E. Microscopic examination was done using an Olympus BX41 microscope with an Olympus DP72® camera (Olympus America Inc., Center Valley, PA, USA) and acquired using SlideBook 5.0 custom-built microscopy software (Intelligent Imaging Innovations, Inc., Denver, Co, USA) to determine the level of fibrosis and mesothelial integrity. The sections were examined for submesothelial thickening, vascularization and leukocyte infiltration. The thickness of the submesothelial zone was measured at five random locations in each section and averaged. The number of peritoneum-associated blood vessels was counted along the entire length of the peritoneum in the sections and recorded as vessels/mm of peritoneum.

2.20 Scanning electron microscopy (SEM)

The intra-abdominal portion of the catheters was cut into three sections and fixed in 2% glutaraldehyde in sodium cacodylate. The catheter pieces were immersed for 2 hours in primary fixative solution (2% glutaraldehyde in 0.1 M sodium cacodylate

buffer at pH 7.4). The samples were rinsed twice in buffer solution and post-fixed for 1 hour in 1% osmium tetroxide in 0.1 M sodium cacodylate buffer. After the second fixation step, the samples were dehydrated through a graded ethanol series (50% 70%, 70%, 95%, 95%, 100%, 100% and 100 %) and then dried in a critical point dryer. After drying, the catheter pieces were cut open to expose the inner surface of the catheters and mounted onto SEM stubs. The stubs were sputter coated with gold and viewed with a Tescan Vega II LSU scanning electron microscope (Tescan USA, Cranberry TWP, PA, USA) operating at 20 kV. Image acquisition was done with Tescan VegaTC operating software (Tescan USA, Cranberry TWP, PA, USA).

2.21 Confocal fluorescence IVM of *S. aureus*-infected mice

To determine if *S. aureus* physically interacts with syndecan-1 *in vivo* along the subendothelial surface of the parietal peritoneum microcirculation and whether infection with *S. aureus* alters the expression of syndecan-1, spinning disc confocal fluorescence IVM was performed on infected mice. Wild-type mice were injected IP with a 100 μL suspension of GFP-expressing *S. aureus* cells containing approximately 1.8 x 10^8 CFU. Four hours later, the mice were prepared for IVM of the parietal peritoneum microcirculation and injected IV with Alexa Fluor® 568-labeled rat anti-mouse syndecan-1 ectodomain antibody (40 μg, clone 300506; R&D Systems®, Inc.). Images were acquired and overlapped to determine co-localization between GFP-expressing *S. aureus* and anti-syndecan-1 antibodies.

2.22 Statistical Analysis

Data are expressed as mean ± standard error of the mean (SEM). Statistical significance was set at $p < 0.05$ and calculated using Student's *t* test or ANOVA with Bonferroni correction for multiple comparisons using the computer software package KaleidaGraph 3.6 (Synergy Software, Reading, PA, USA). In general, groups consisted of 5 animals. This sample size is generally needed to provide statistical significance with 30% difference and 80% power.

CHAPTER 3: RESULTS

3.1 Syndecan-1 protein expression in the parietal peritoneum and the underlying microcirculation

3.1.1 Syndecan-1 is present in the subendothelial region of post-capillary venules and on the mesothelial layer: Syndecan-1 expression in the microcirculation that supplies the parietal peritoneum was imaged *in vivo* with fluorescent antibodies after IP injection of saline or *S. aureus* LTA in wild-type mice. The merged fluorescent images showed that while the isotype control antibodies were mostly restricted to the intravascular space, the anti-syndecan-1 antibodies bound to the post-capillary venules away from the lumen in mice injected with saline (**Figure 4A**) and LTA (**Figure 4B**).

The small gap between the anti-syndecan-1-labeled surface and the isotype control antibodies in the intravascular space suggests that syndecan-1 protein expression was localized to the subendothelial region and not the luminal surface. To confirm that syndecan-1 was not expressed on the luminal surface of the venules, wild-type mice were co-injected with fluorescent anti-VCAM-1 and anti-syndecan-1 antibodies. The fluorescence from anti-VCAM-1 appeared on the luminal surface of the endothelium and was mostly distinct from the anti-syndecan-1-bound surface with some small regions overlapping (**Figure 5A**). The venular wall consists of an endothelial layer with a surrounding basement membrane with pericytes. To determine whether syndecan-1 is associated with the endothelial layer, animals were co-injected with anti-syndecan-1 and

anti-PECAM-1 antibodies (**Figure 5B**). PECAM-1 is an endothelial cell marker and is concentrated at junctions between cells (Albelda *et al.*, 1991). Fluorescence from the anti-syndecan-1 antibodies closely followed the anti-PECAM-1-bound layer but only on the basolateral side of the endothelium. Syndecan-1 did not appear to be expressed on the peritoneal arterioles (**Figure 6A**). The specificity of the anti-syndecan-1 antibody was verified in *Sdc1*$^{-/-}$ mice and no anti-syndecan-1 binding was observed (**Figure 6B**). These findings suggest that syndecan-1 is expressed at the protein level along the basolateral surface of the venular endothelium.

Since the peritoneal surface could only be viewed in the frontal plane with IVM, it was not possible to determine whether syndecan-1 is present on the mesothelial cells that form the parietal peritoneum. Thus, to image the mesothelial layer, transverse sections of the anterior abdominal wall were collected after an IV injection of fluorescent anti-syndecan-1 and isotype control antibodies and imaged with fluorescence confocal microscopy. The *ex vivo* images of the parietal peritoneum revealed that syndecan-1 was expressed on the mesothelial layer (**Figure 7**).

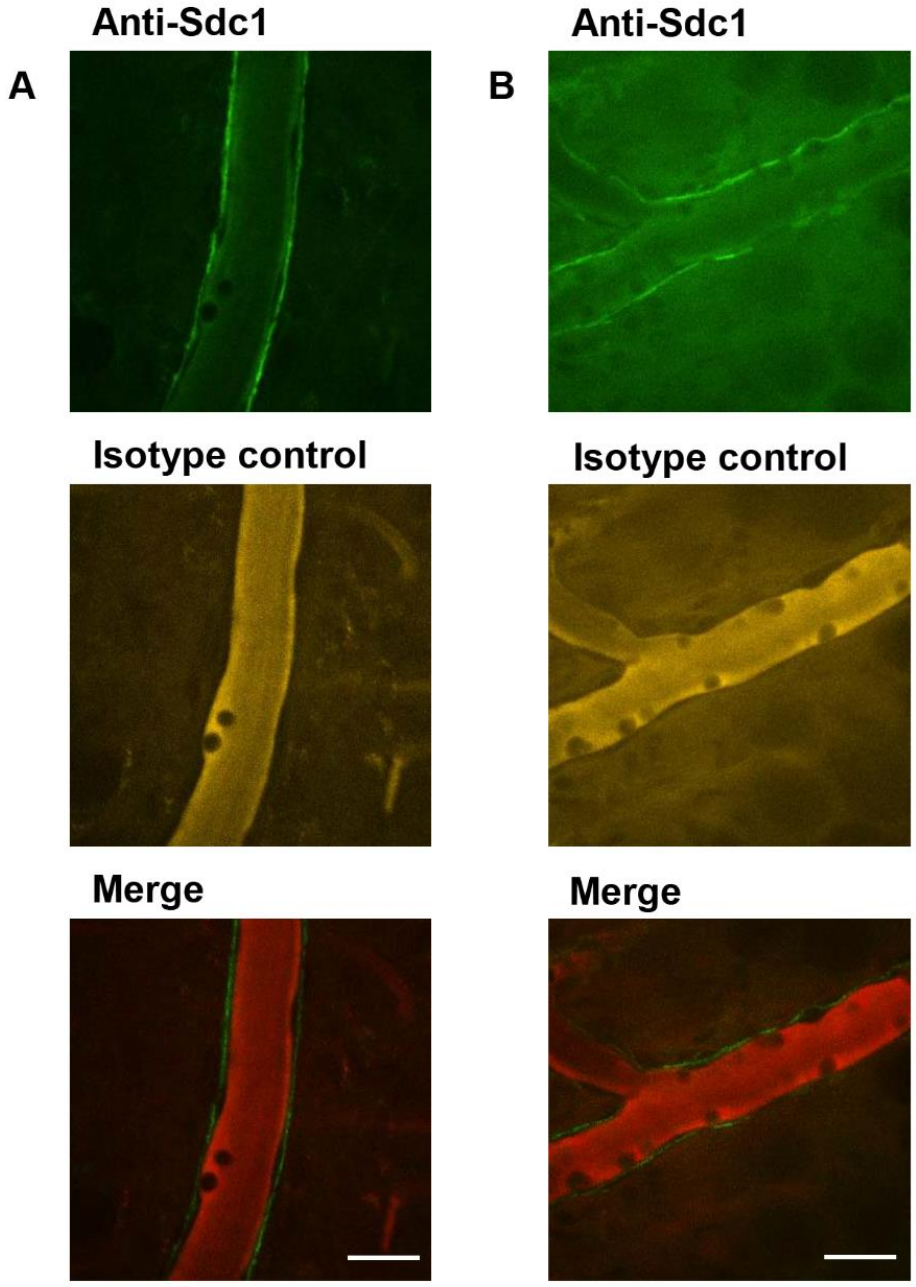

Figure 4. Syndecan-1 is expressed along the basolateral surface of the venular endothelium. ***In vivo*** **fluorescence confocal microscopy images of venules of the parietal peritoneum were acquired and merged after IV injection of Alexa Fluor® 488-conjugated anti-syndecan-1 and Alexa Fluor® 647-conjugated isotype control antibody 4 hours after IP injection of (A) sterile saline (50 *μ*L) or (B)** ***S. aureus*** **LTA (125 *μ*g) into wild-type mice, representative images, *n* = 7 mice. Scale bar = 20 *μ*m.**

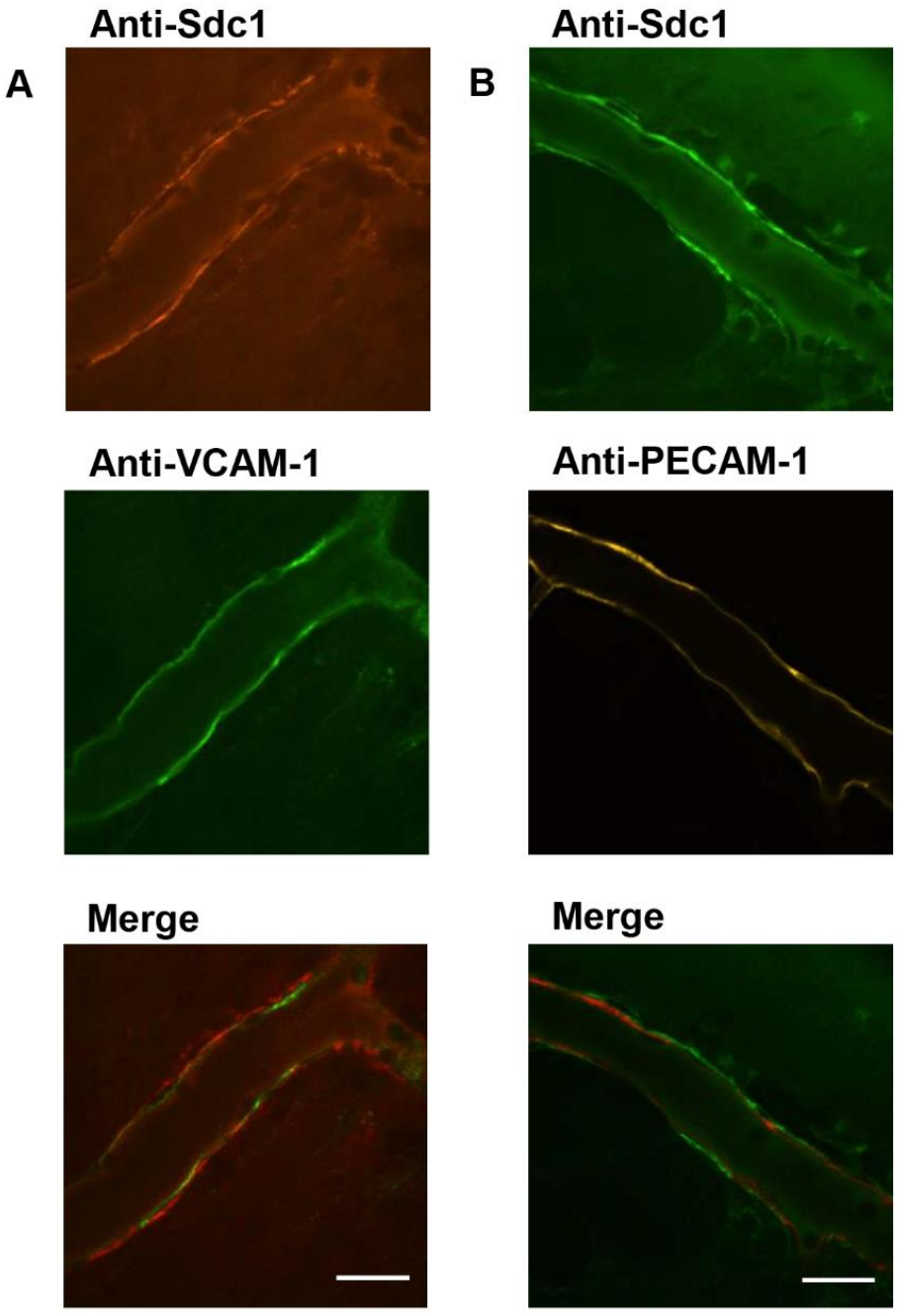

Figure 5. Syndecan-1 is present on the basolateral side and VCAM-1 is present on the luminal side of the venular endothelium. Peritoneal venules labeled with (A) Alexa Fluor® 568-conjugated anti-syndecan-1 and Alexa Fluor® 488-conjugated anti-VCAM-1 or (B) Alexa Fluor® 488-conjugated anti-syndecan-1 and Alexa Fluor® 647-conjugated anti-PECAM-1, visualized *in vivo* 4 hours after stimulation with LTA, representative images, *n* = 7 mice. Scale bar = 20 *μ*m.

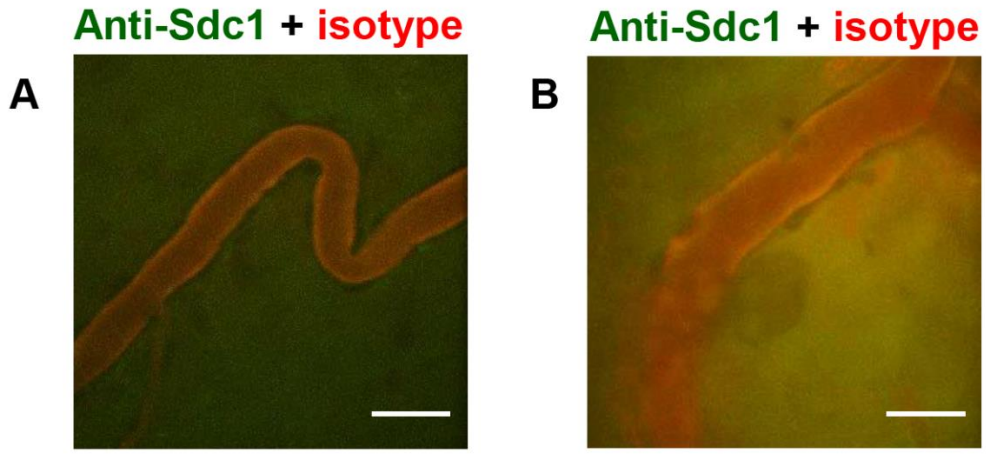

Figure 6. Syndecan-1 is not present on arterioles. Anti-syndecan-1-binding was not detected on (A) arterioles in wild-type animals and (B) venules of *Sdc1*$^{-/-}$ mice after injection of Alexa Fluor® 488-conjugated anti-syndecan-1 and Alexa Fluor® 647-conjugated isotype control antibody. Scale bar = 20 μm.

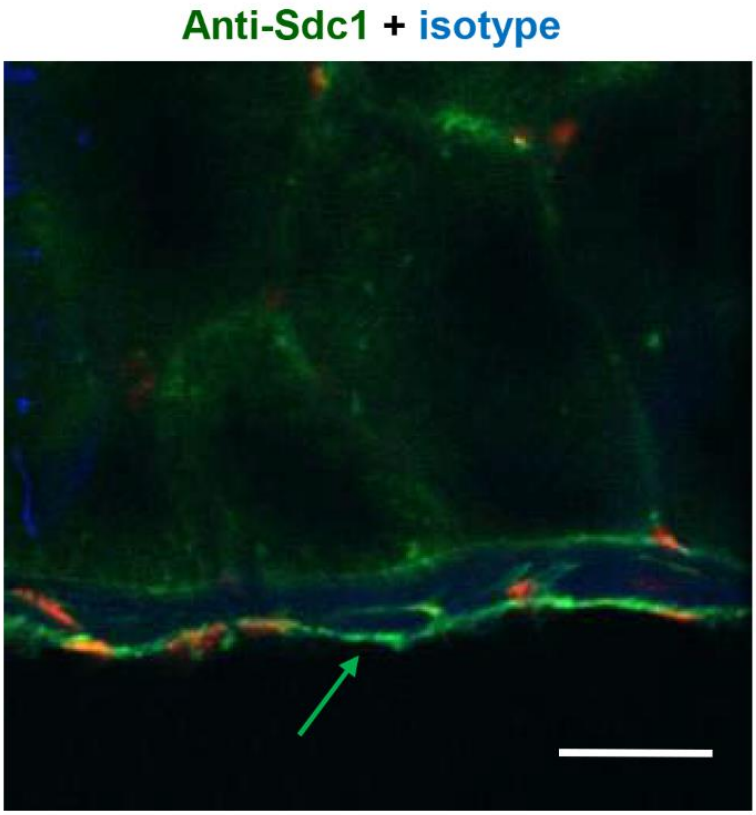

Figure 7. Syndecan-1 is present on the mesothelial layer of the parietal peritoneum. *Ex vivo* image of a cross section of the mouse abdominal wall after IV injection of Alexa Fluor® 488-labeled anti-syndecan-1 (green) and Alexa Fluor® 647-labeled isotype control (blue), counterstained with PI (red), representative image, *n* = 3 mice. Green arrow indicates binding of the fluorescent anti-syndecan-1 to the mesothelium. Scale bar = 20 *μ*m.

3.1.2 Syndecan-1 protein levels do not change during LTA-induced inflammation:

Because inflammation was shown to alter syndecan-1 levels in tissues (Day *et al.*, 2003), the level of syndecan-1 was measured in LTA-induced peritonitis and saline-injected controls. The fluorescence intensity from the syndecan-1 antibodies that bound along the basolateral side of endothelial layer and the isotype control antibodies was measured using image processing software from the images of venules collected with IVM. The florescence intensity was taken to represent molecular expression on the vascular endothelium. We showed that there is no significant difference in the level of syndecan-1 protein expression between LTA-treated animals and saline controls (**Figure 8**).

This finding was confirmed with an ELISA for syndecan-1. Because TNFα was shown to downregulate syndecan-1 expression at the protein and mRNA levels and to promote syndecan-1 shedding *in vitr*o from epithelial cells (Day *et al.*, 2003) and also suppressed syndecan-1 expression in endothelial cells (Kainulainen *et al.*, 1996), syndecan-1 levels were also measured in response to TNFα in addition to LTA. The ELISA showed that syndecan-1 levels in the abdominal wall homogenate (**Figure 9A**), peritoneal lavage and plasma (**Figure 9B**) did not significantly differ between mice that were given saline compared to the mice injected with the pro-inflammatory stimuli, LTA or TNFα.

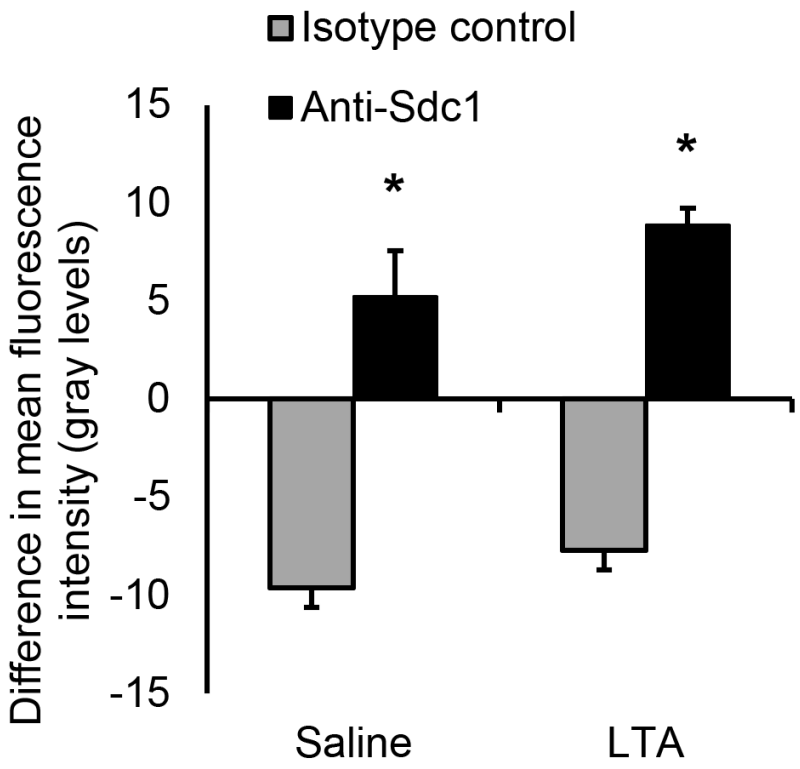

Figure 8. Syndecan-1 protein expression along the basolateral endothelial surface does not change in LTA-induced inflammation. Four hours after stimulation with *S. aureus* LTA (125 μg) or 50 μL of saline, wild-type mice were prepared for IVM and injected IV with Alexa Fluor® 488-labeled anti-syndecan-1 antibody and Alexa Fluor® 647-labeled isotype control antibody. Images of venules were captured and syndecan-1 expression, reflected as fluorescence intensity of the antibodies that labeled the venules, was measured with the image analysis software, ImageJ. The relative values were recorded as the difference in mean fluorescence intensity by subtracting intravascular fluorescence intensity from the fluorescence intensity at the basolateral endothelial surface of a given venule, *$p < 0.01$ compared with isotype control, $n = 7$ mice with 3 – 4 images analyzed per mouse. Data recorded as mean ± SEM and analyzed with ANOVA with Bonferroni correction. No significant difference in syndecan-1 expression was found between saline and LTA-treated animals.

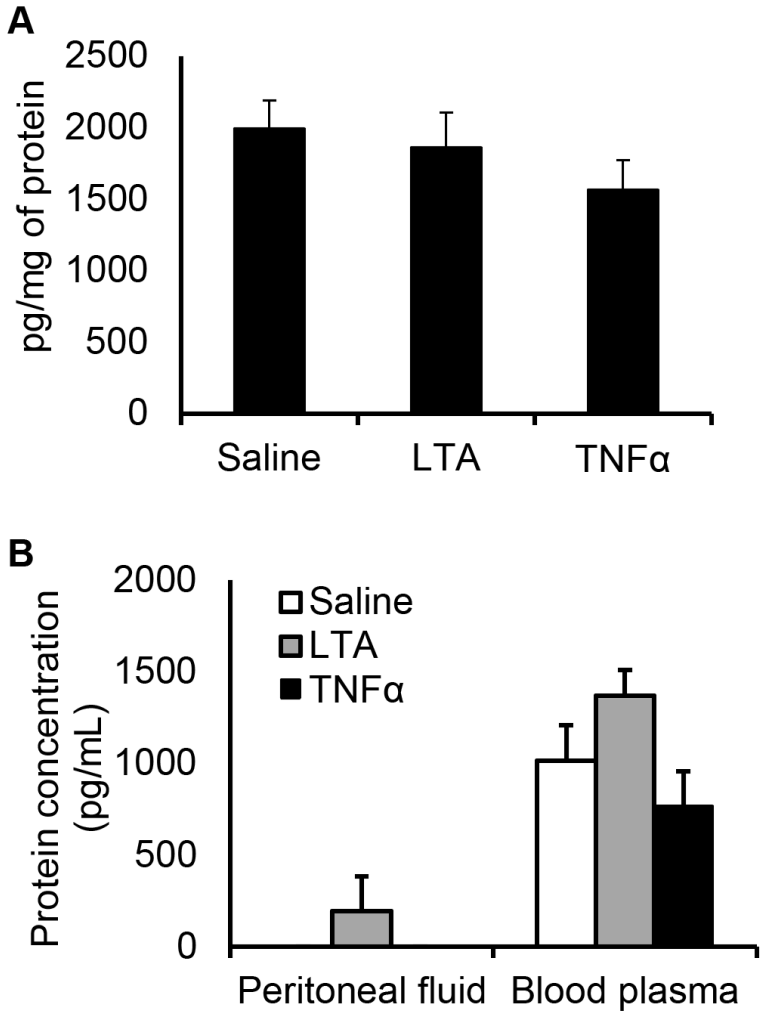

Figure 9. Syndecan-1 protein expression in the abdominal wall and plasma does not change after LTA or TNF*α* injection. ELISA measurements of syndecan-1 levels in (A) mouse abdominal wall samples and (B) peritoneal lavage and blood plasma were taken 4 hours after IP treatment with saline (50 *μ*L), LTA (125 *μ*g) or TNF*α* (500 ng), *n* = 5 mice. Data recorded as mean ± SEM and analyzed with ANOVA with Bonferroni correction. Syndecan-1 protein levels in the abdominal wall, peritoneal lavage and blood plasma did not significantly differ between saline and LTA or TNF*α*-injected animals.

3.2 *Sdc1*$^{-/-}$ mice have normal leukocyte recruitment to the microcirculation underlying the parietal peritoneum

Leukocyte-endothelial cell interactions were quantified in the peritoneal venules 4 hours after animals were injected IP with *S. aureus* LTA, *E. coli* LPS or TNF*α* using transillumination technique (**Figure 10A**) and the number of rolling, adherent and extravascular leukocytes was compared to saline-injected wild-type controls. Leukocyte rolling was significantly decreased with LPS treatment compared with saline controls and did not differ between wild-type and *Sdc1*$^{-/-}$ mice (**Figure 10B**). The number of adherent leukocytes was significantly increased with LTA and TNF*α* treatment compared with saline controls but did not differ between the wild-type animals and the *Sdc1*$^{-/-}$ mice (**Figure 10C**). *Sdc1*$^{-/-}$ mice had a significantly increased number of extravascular leukocytes compared with saline and wild-type controls with TNF*α* treatment (**Figure 10D**). After the completion of IVM observations, cardiac puncture was performed and blood was collected. Total systemic leukocytes were quantified along with differential white blood cell counts and did not show any significant differences between the different treatment groups (**Table 1**). These data suggest that syndecan-1 does not regulate leukocyte recruitment to the parietal peritoneum vasculature and *Sdc1*$^{-/-}$ mice have normal systemic leukocyte counts. To determine which leukocyte subtypes are recruited in response to saline, LTA and TNF*α* after 4 hours of exposure, fluorescence IVM was performed after IV injection of Alexa Fluor® 488-conjugated anti-Ly6G antibodies to label neutrophils and Alexa Fluor® 568-conjugated anti-CX_3CR1 antibodies to label monocytes. The confocal microscopic

images revealed that all of the intravascular cells were $Ly6G^+$ while no CX_3CR1^+ cells were observed at this time point (**Figure 11**).

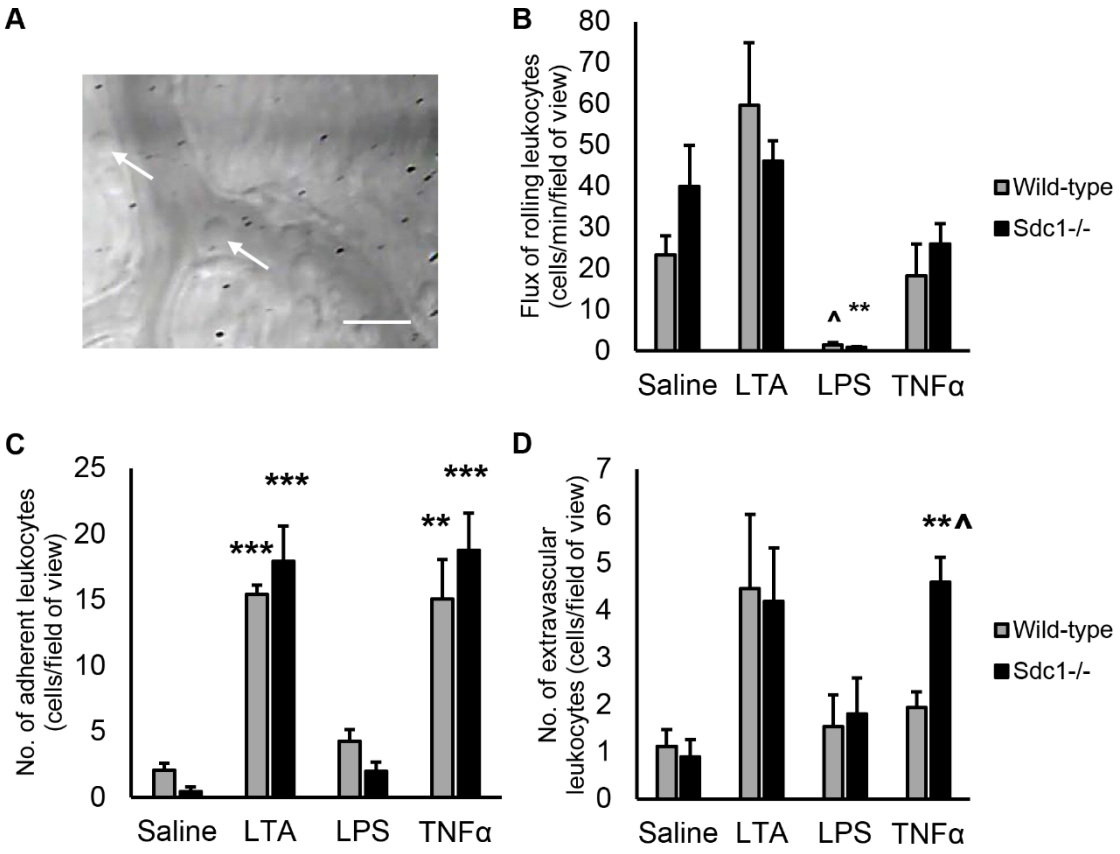

Figure 10. *Sdc1*$^{-/-}$ mice have normal leukocyte recruitment to the parietal peritoneum microcirculation. Wild-type and *Sdc1*$^{-/-}$ mice were injected IP with 50 *μ*L of saline, *S. aureus* LTA (125 *μ*g), *E. coli* LPS (125 *μ*g) or TNF*α* (500 ng). Four hours later, the mice were prepared for IVM and (A) the microcirculation of the parietal peritoneum was imaged, arrows indicate leukocytes, scale bar = 20 *μ*m. The number of (B) rolling and (C) adherent leukocytes in the peritoneal venules as well as the number of (D) extravascular leukocytes were quantified. These results show that LPS treatment significantly decreased leukocyte rolling while LTA and TNF*α* treatment significantly increased leukocyte adhesion but the *Sdc1*$^{-/-}$ mice did not have altered leukocyte recruitment compared to wild-type. Data recorded as mean ± SEM and analyzed with ANOVA with Bonferroni correction, 6 venules

averaged per count, *n* = 4 mice, ^*p* < 0.05 compared with wild-type, ***p* < 0.001 compared with saline, ****p* < 0.0001 compared with saline.

Table 1. Differential leukocyte counts in mice stimulated with LTA, LPS or TNF*α*.

Treatment/strain	Total cells x 10^9/L	Neutrophils	Lymphocytes	Monocytes
Saline/wild-type	4.96±1.06	1.12±0.43	3.70±0.81	0.12±0.03
Saline/*Sdc1*$^{-/-}$	6.91±0.89	1.58±0.14	5.25±0.78	0.08±0.01
LTA/wild-type	4.10±0.67	2.31±0.31	1.70±0.39	0.09±0.02
LTA/*Sdc1*$^{-/-}$	4.62±0.45	2.86±0.38	1.67±0.34	0.10±0.02
LPS/wild-type	1.49±0.25	0.40±0.06	1.03±0.27	0.05±0.02
LPS/*Sdc1*$^{-/-}$	3.29±1.57	0.84±0.29	2.36±1.29	0.08±0.03
TNF*α*/wild-type	3.74±0.59	2.14±0.46	1.55±0.43	0.05±0.03
TNF*α*/*Sdc1*$^{-/-}$	4.24±0.30	2.31±0.33	1.88±0.06	0.05±0.03

Wild-type and *Sdc1*$^{-/-}$ mice were injected with saline (50 *μ*L), *S. aureus* LTA (125 *μ*g), *E. coli* LPS (125 *μ*g) or TNF*α* (500 ng). After the completion of surgery and IVM observations, blood was collected via cardiac puncture and total systemic leukocyte counts and differential leukocyte counts were performed, *n* = 4 mice. Wild-type and *Sdc1*$^{-/-}$ mice did not have any significant differences in leukocyte counts in response to the pro-inflammatory agents after IVM.

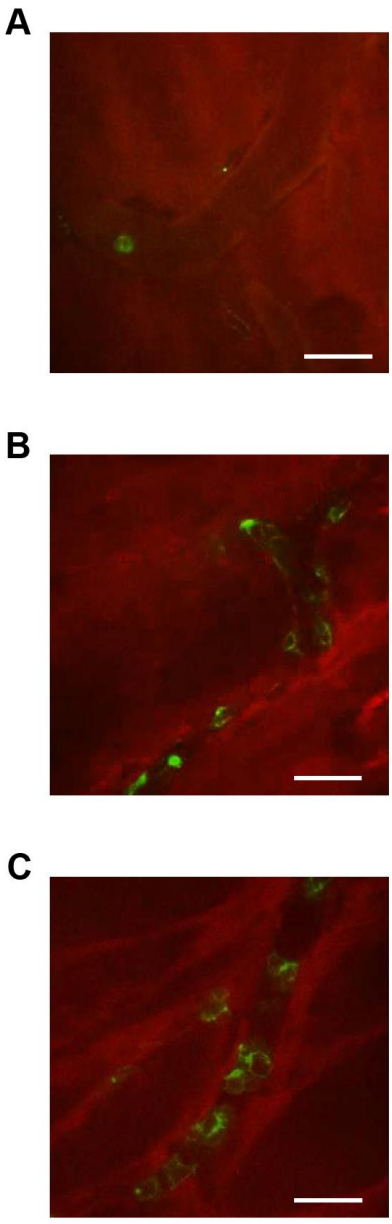

Figure 11. The leukocyte infiltrate in peritoneal venules in response to IP saline, LTA or TNF*α* injection consists of neutrophils. *In vivo* fluorescence microscopy image of a venule taken 4 hours after administration of (A) saline (50 *μ*L), (B) *S. aureus* LTA (125 *μ*g) or (C) TNF*α* (500 ng) in mice that were injected IV with Alexa Fluor® 488-labeled anti-Ly6G (green) and Alexa Fluor® 568-labeled anti-CX_3CR1 (red), scale bar = 20 *μ*m, *n* = 3 mice. Only $Ly6G^+$ cells (neutrophils) were observed in the venules and no intravascular CX_3CR1^+ cells (monocytes) were observed at this time.

3.3 Molecular mechanisms of leukocyte recruitment in the parietal peritoneum microcirculation

To determine whether P-selectin mediates leukocyte rolling in the parietal peritoneum microcirculation, wild-type animals were prepared for IVM 4 hours after injection of LTA. IVM recordings of venules taken before and after intravenous injection of anti-P-selectin showed that rolling in the peritoneal microcirculation is dependent on P-selectin (**Figure 12**). To identify the molecules that mediate firm adhesion in this tissue, anti-β_2 integrin/CD18, anti-ICAM-1 and/or anti-VCAM-1 antibodies were injected IP into wild-type mice immediately before LTA IP injection and IVM was performed after 4 hours. The number of rolling leukocytes was significantly reduced after injection of anti-β_2 integrin antibody due to slower rolling of leukocytes (**Figure 13A**). Treatment with these blocking antibodies did not change the number of adherent leukocytes (**Figure 13B**) or the number of extravascular leukocytes (**Figure 13C**) compared to the isotype control antibody. The finding that blockade of VCAM-1 and ICAM-1 did not decrease the number of adherent cells in the peritoneal microcirculation is surprising as both molecules are expressed on the venular endothelium in this tissue (**Figure 14**). Also, we previously validated the intraperitoneal injection route for delivery of antibodies by comparison of IV versus IP injection of fluorescent anti-syndecan-1, followed by IVM (**Figure 15**). The images indicated that IP route results in effective delivery of the fluorescent antibodies to the tissue which is comparable to the IV route. These results indicate that leukocyte rolling in the parietal peritoneum microcirculation is mediated by P-selectin and anti-β_2 integrin while

immunoblockade of ICAM-1 and VCAM-1 does not decrease leukocyte adhesion despite the expression of these molecules on the endothelium of the peritoneal venules.

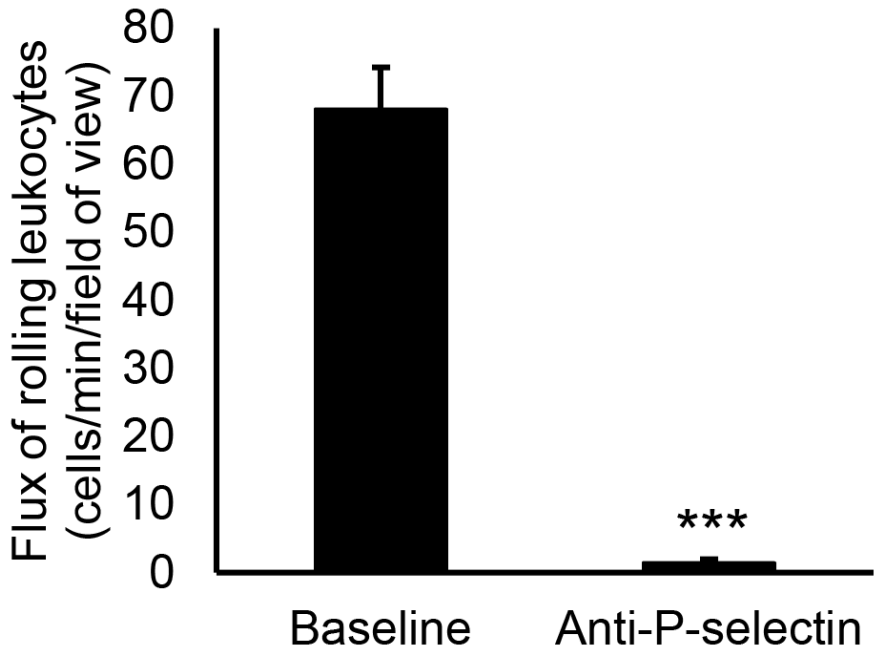

Figure 12. P-selectin mediates leukocyte rolling in the parietal peritoneum microcirculation. Wild-type animals were prepared for IVM 4 hours after injection of *S. aureus* LTA (125 μg). Baseline recordings were taken and then anti-P-selectin antibodies were injected IV through the jugular vein cannula and the response was recorded after five minutes. The number of rolling leukocytes in the peritoneal venules was quantified from the recordings. Values for 4 venules were averaged for each mouse with $n = 4$ mice and analyzed with a *t* test, $^{***}p < 0.0001$. P-selectin blockade inhibited leukocyte rolling in the peritoneal venules in response to LTA.

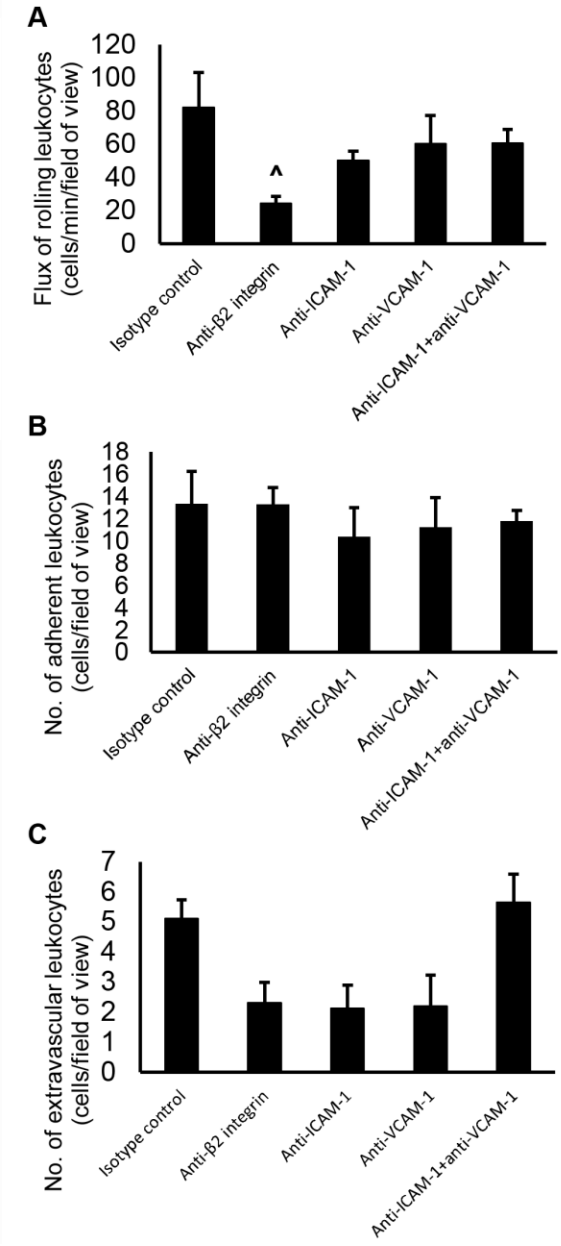

Figure 13. Mechanisms of leukocyte recruitment in the parietal peritoneum microcirculation. Wild-type mice were treated IP with 40 *μ*g of anti-β_2 integrin, anti-ICAM-1 and/or anti-VCAM-1 and then challenged with *S. aureus* LTA (125 *μ*g). Four hours later, the animals were prepared for IVM (transillumination technique) and the number of (A) rolling and (B) adherent leukocytes in the peritoneal venules as well as the number of (C) extravascular leukocytes were quantified. Data recorded as mean ± SEM and analyzed with ANOVA with Bonferroni correction, 4 venules averaged per mouse, n = 4-5 mice, ^$p < 0.05$ compared with isotype control.

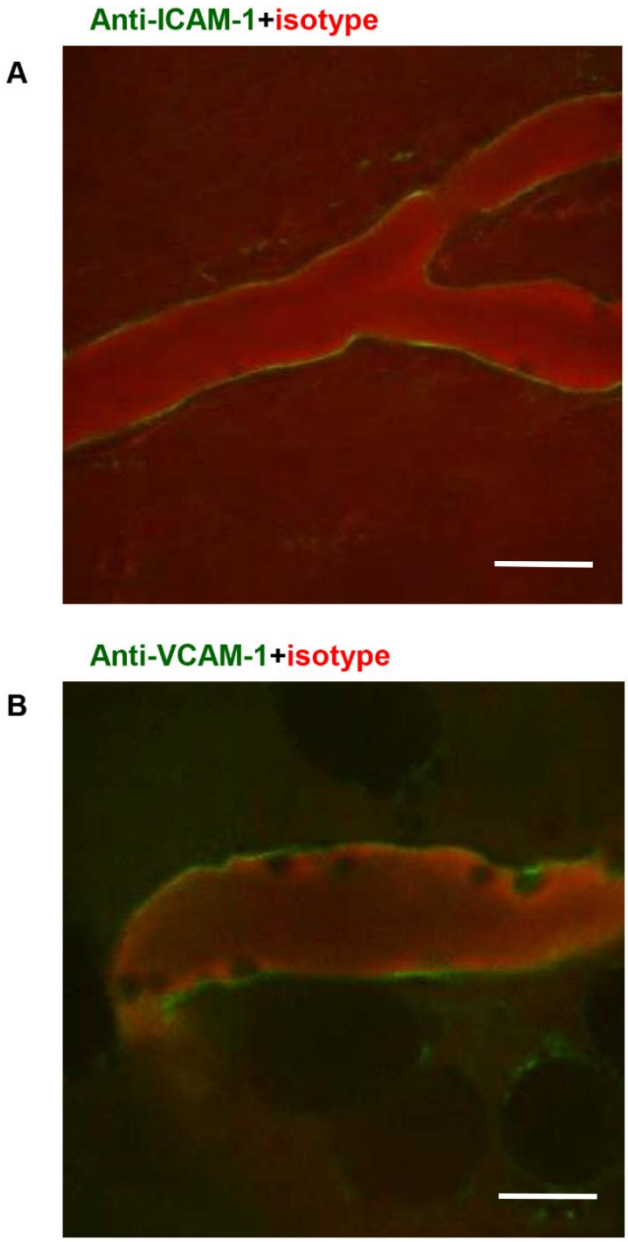

Figure 14. ICAM-1 and VCAM-1 in the parietal peritoneum venules. Expression of ICAM-1 and VCAM-1 in the peritoneal venules was observed with *in vivo* immunofluorescence confocal microscopy after IV injection of (A) Alexa Fluor® 488-labeled anti-ICAM-1 or (B) Alexa Fluor® 488-labeled anti-VCAM-1 with Alexa Fluor® 568-labeled isotype control antibodies 4 hours after IP injection of *S. aureus* LTA, scale bar = 20 μm, n = 3 mice. Antibody blockade of ICAM-1 and VCAM-1 does not decrease leukocyte adhesion even though both molecules are expressed on the endothelium of the parietal peritoneum microcirculation.

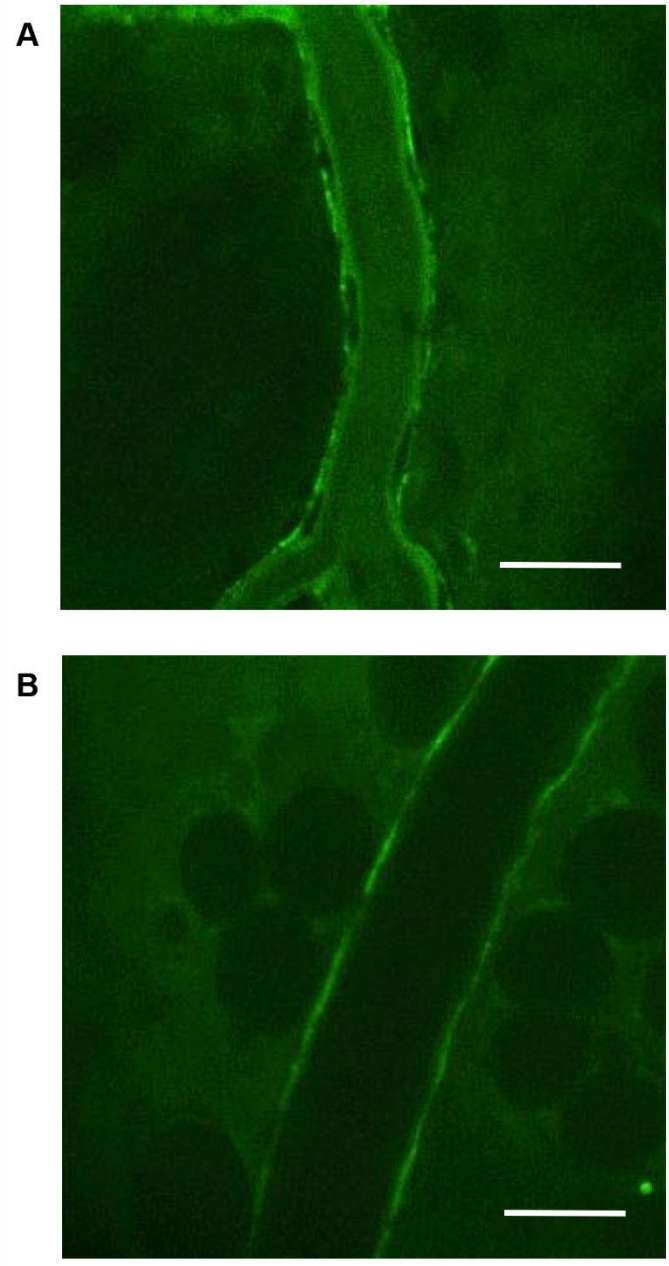

Figure 15. Intravenous versus intraperitoneal injection of fluorescent antibodies. ***In vivo*** **fluorescence confocal microscopy images of venules of the parietal peritoneum labeled with 40 μg of Alexa Fluor® 488-conjugated anti-syndecan-1 injected IV (A) or IP (B) into saline-injected wild-type mice. The two different routes of administration resulted in comparable fluorescent anti-syndecan-1 binding to the peritoneal venules. Representative images, *n* = 3 mice, scale bar = 20 μm.**

3.4 Chemokine presentation in the parietal peritoneum microcirculation

3.4.1 MIP-2 protein expression in the microcirculation of the parietal peritoneum does not depend on syndecan-1: To examine whether syndecan-1 co-localizes with chemokines *in vivo*, Alexa Fluor® 568-labeled anti-syndecan-1 was co-injected IV with either Alexa Fluor® 488-labeled anti-MIP-2, anti-KC or anti-MCP-1 antibodies 4 hours after LTA challenge. Anti-MIP-2 antibody labeled peritoneal venules (**Figure 16A**) in wild-type mice and appeared to partially overlap with the binding pattern of the anti-syndecan-1 antibody. To determine whether MIP-2 protein expression on the peritoneal venules is dependent on syndecan-1, *Sdc1*$^{-/-}$ animals were injected with fluorescent anti-MIP-2 antibodies. IVM imaging revealed that the *Sdc1*$^{-/-}$ mice have normal expression of this chemokine in the peritoneal venules (**Figure 16B**). Binding of anti-KC (**Figure 16C**) and anti-MCP-1 (**Figure 16D**) was not detected in the peritoneal microcirculation of wild-type animals 4 hours after LTA injection. Anti-MIP-2 and anti-syndecan-1 did not bind to peritoneal arterioles of wild-type animals (**Figure 16E**). These results suggest that at 4 hours after LTA injection, MIP-2 appears in the parietal peritoneum venules but KC and MCP-1 do not. This MIP-2 protein expression is not dependent on syndecan-1.

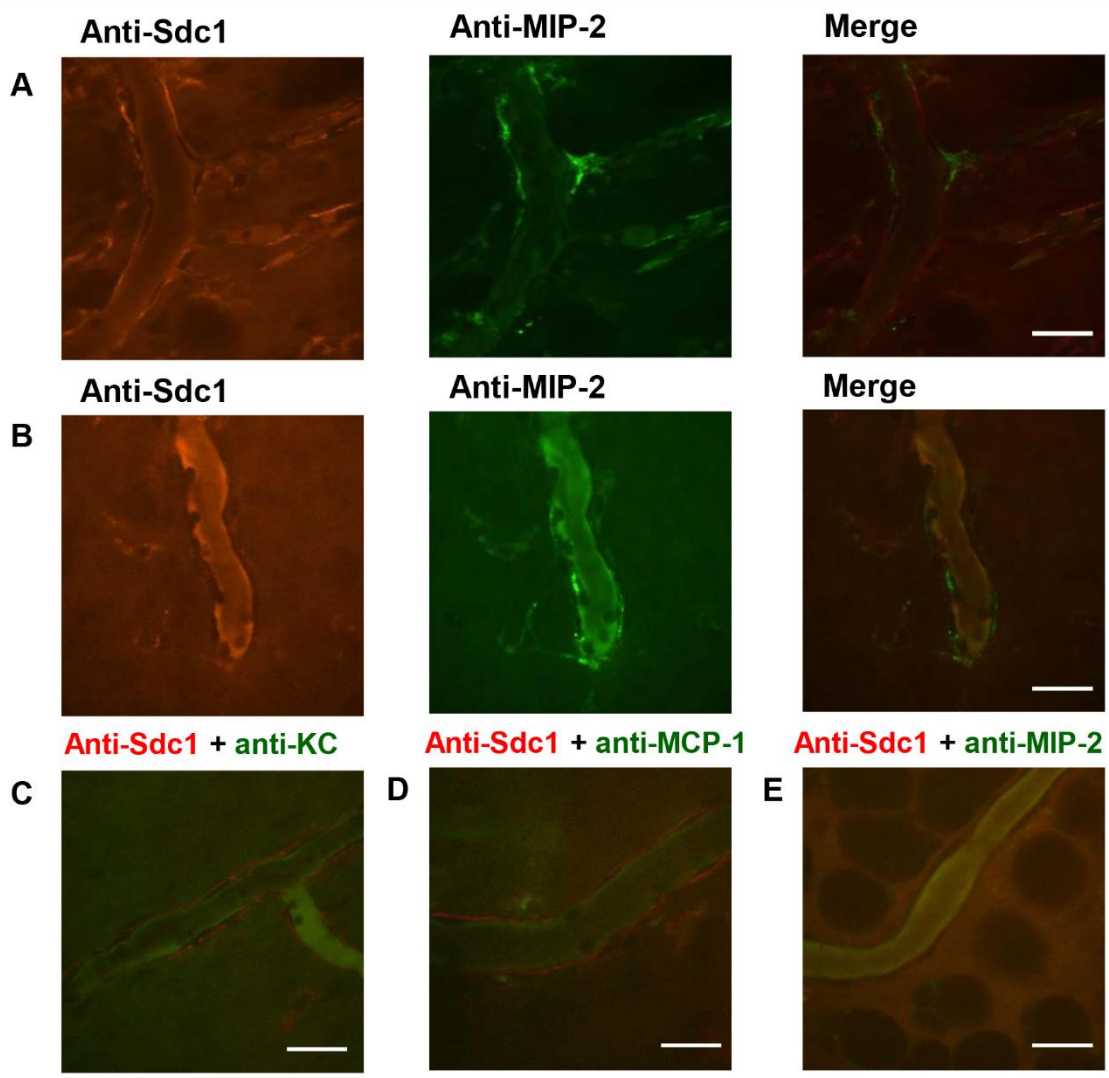

Figure 16. MIP-2 protein levels in the peritoneal microcirculation do not depend on syndecan-1. Four hours after IP injection of *S. aureus* LTA (125 μg), mice were prepared for fluorescence confocal IVM and injected IV with fluorescent antibodies. Microscopic images of MIP-2 expression on the venules of the parietal peritoneum were acquired after IV injection of Alexa Fluor® 568-conjugated anti-syndecan-1 along with Alexa Fluor® 488-conjugated anti-MIP-2 in (A) wild-type mice and (B) *Sdc1*$^{-/-}$ mice. No binding of (C) Alexa Fluor® 488-conjugated anti-KC nor (D) Alexa Fluor® 488-conjugated MCP-1 was detected on the peritoneal venules and (E) Alexa Fluor® 488-conjugated MIP-2 did not label arterioles, representative images, *n* = 3 mice, scale bar = 20 μm. MIP-2 is expressed on the peritoneal venules in both, wild-type and *Sdc1*$^{-/-}$ mice.

3.4.2 Syndecan-2, but not syndecan-3 nor syndecan-4, is present on the venules of the parietal peritoneum: To determine whether there are other heparan sulfate proteoglycans expressed on the peritoneal venules that may bind to chemokines such as MIP-2, wild-type animals were injected IV with Alexa Fluor® 488-conjugated anti-syndecan-2, Alexa Fluor® 488-conjugated anti-syndecan-3 or Alexa Fluor® 488-conjugated anti-syndecan-4 along with Alexa Fluor® 568-conjugated isotype control antibodies 4 hours after LTA-stimulation. Syndecan-2 protein expression was observed on the venules (**Figure 17A**) but no binding of anti-syndecan-3 (**Figure 17B**) nor anti-syndecan-4 antibodies (**Figure 17C**) was detected in the peritoneal microcirculation. However, the quality of the antibodies in this study was not assessed. This *in vivo* finding is in contrast to *in vitro* evidence where various mouse endothelial cell lines were found to highly express syndecan-3 and syndecan-4 in addition to syndecan-2 but not syndecan-1 (Kim *et al.*, 1994). There was some co-localization between Alexa Fluor® 488-conjugated anti-syndecan-2 and Alexa Fluor® 568-conjugated anti-MIP-2 in the peritoneal venules (**Figure 18**). These data suggest that syndecan-1 and syndecan-2 may be redundant proteoglycans in chemokine presentation.

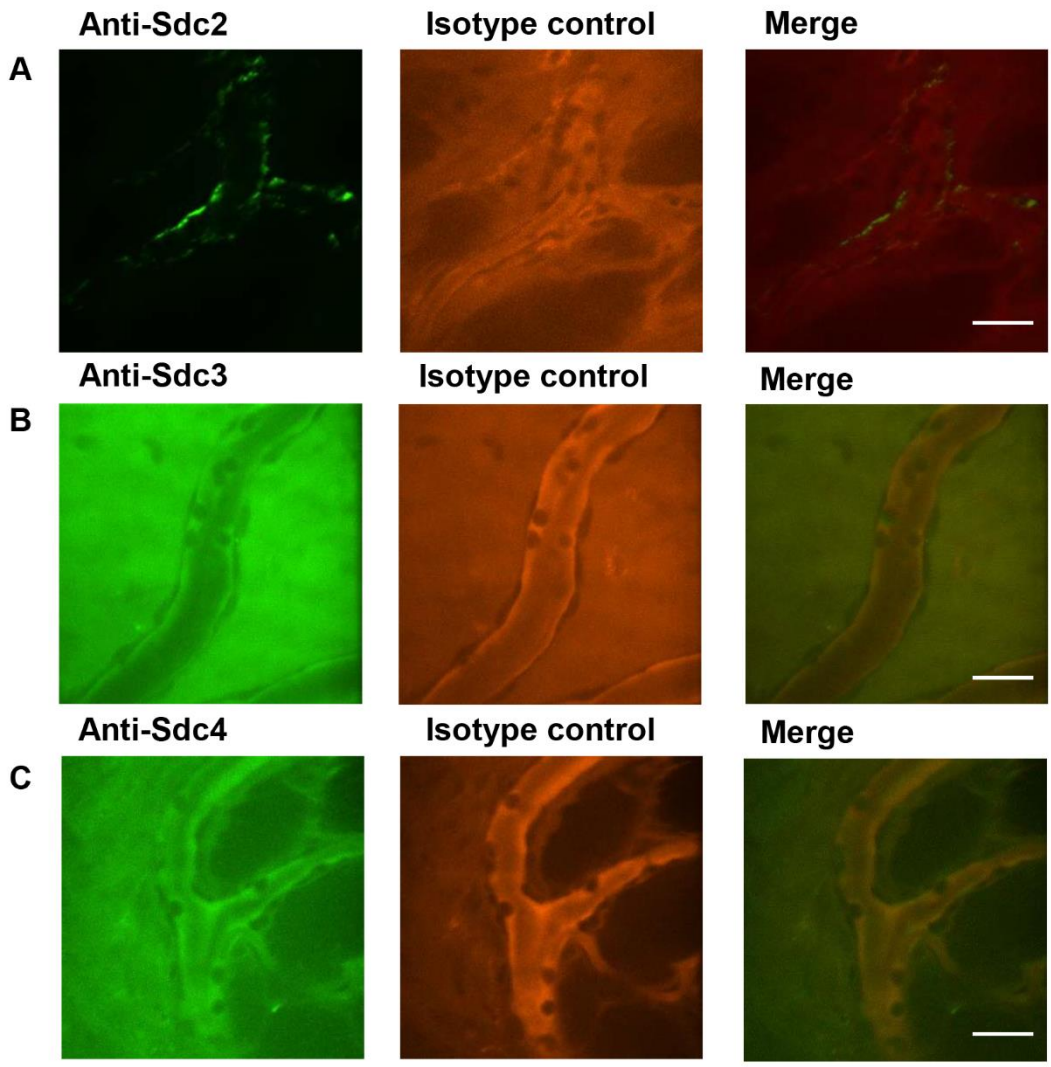

Figure 17. Syndecan-2 but not syndecan-3 nor syndecan-4 is present on the peritoneal venules. Wild-type mice were prepared for fluorescence confocal IVM 4 hours after IP injection of *S. aureus* LTA (125 μg). (A) Alexa Fluor® 488-conjugated anti-syndecan-2 appeared on the venular wall but no binding of (B) Alexa Fluor® 488-conjugated anti-syndecan-3 nor (C) Alexa Fluor® 488-conjugated anti-syndecan-4 was detected in the peritoneal microcirculation. Representative images, *n* = 3 mice, scale bar = 20 μm.

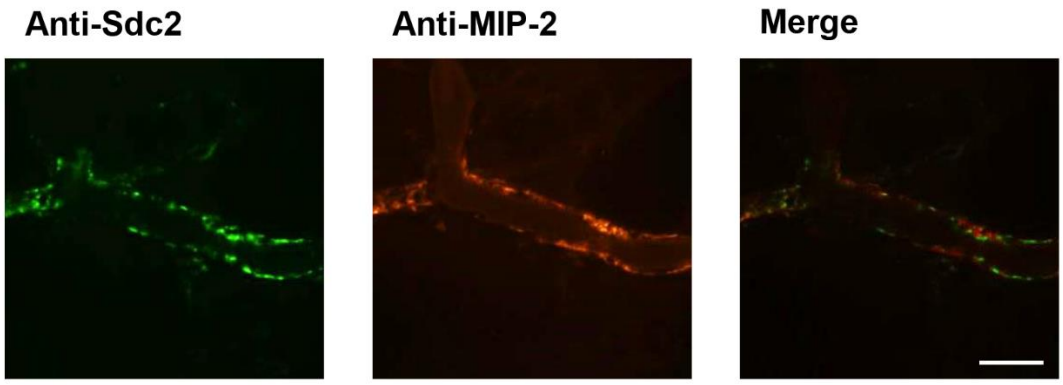

Figure 18. Syndecan-2 partially co-localizes with MIP-2 on peritoneal venules. Wild-type mice were prepared for fluorescence confocal IVM 4 hours after IP injection of *S. aureus* LTA (125 μg) and injected IV with fluorescent anti-syndecan-2 and anti-MIP-2. There was some co-localization between Alexa Fluor® 488-conjugated anti-syndecan-2 and Alexa Fluor® 568-conjugated anti-MIP-2 in the peritoneal venules. Representative images, *n* = 3 mice, scale bar = 20 μm.

3.4.3 Anti-duffy antigen/receptor for chemokines (DARC) does not label the parietal peritoneum microcirculation: Since we didn't observe strong co-localization between the syndecans and MIP-2, we wanted to determine if the promiscuous chemokine receptor DARC is expressed in the parietal peritoneum microcirculation and whether it plays a role in chemokine sequestration in this tissue. Confocal IVM of the peritoneal microcirculation showed no fluorescent anti-DARC antibody binding in the microcirculation or the extravascular space (**Figure 19**).

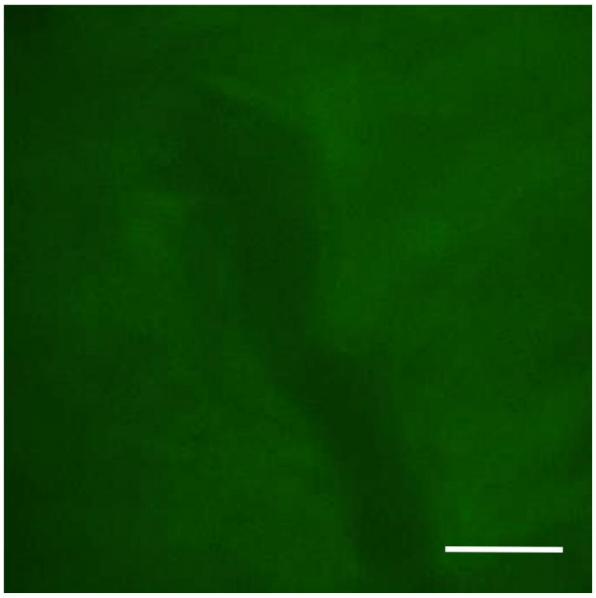

Figure 19. Anti-DARC does not label the peritoneal microcirculation. ***In vivo*** **fluorescence confocal microscopy image of a parietal peritoneum venule after intravenous administration of Alexa Fluor® 488-conjugated anti-DARC, *n* = 3 naïve mice, scale bar = 20 *μ*m.**

3.5 Effects of subacute exposure to peritoneal dialysis solution and the peritoneal catheter on leukocyte recruitment to the parietal peritoneum microcirculation

3.5.1 Animal characteristics: During the catheter acclimatization and the dialysis period, there were no significant changes in behaviour or appearance of the animals and skin incisions healed well with no signs of infection. There were no differences in the weights of the animals between the catheter control group and catheter with dialysis group at the start (25.75 ± 0.63g versus 25.75 ± 0.25g, respectively) and end (29.25 ± 0.75g versus 30.00 ± 0.91g, respectively) of the experiment. However, 3/4 animals in the catheter control group and 4/4 animals in the catheter with dialysis group exhibited some redness and scabbing on the skin over the port for approximately 3 weeks after surgical implantation, but this did not interfere with solution injections into the port.

3.5.2 Leukocyte-endothelial cell interactions in response to subacute exposure to peritoneal dialysis solution and catheter: The abdomen was opened via midline laparotomy and the parietal peritoneum was prepared for IVM. Some mice had adipose tissue wrapping around the catheter at the entry site on the abdominal wall, but this did not result in the occlusion of the catheter tip. Specifically, 1/4 mice had omental wrapping of the catheter and 2/4 mice had gonadal adipose tissue wrapping of the catheter in both groups. The mesothelial layer, submesothelial compact zone and underlying venules were visualized and the numbers of rolling, adherent and

extravascular leukocytes were determined (**Figure 20**). The region visualized included the area that came in contact with the intra-abdominal catheter tip protruding towards the left side. The peritoneal lining appeared damaged in the catheterized groups with disorganized and hypertrophied mesothelial cells and overall hypercellularity (**Figure 20, first column**). Although much heterogeneity was observed, the submesothelial connective tissue in the catheter control and dialysis groups appeared to have less organized collagen bundles and this was overall similar between the two groups (**Figure 20, second column**).

The number of rolling leukocytes was significantly increased in the catheterized animals compared with naive controls (**Figure 21A**) while the number of adherent leukocytes was not significantly higher compared with naive levels (**Figure 21B**). The number of extravascular leukocytes was significantly increased in the catheterized animals compared with naïve mice (**Figure 21C**). Leukocyte-endothelial cell interactions did not differ between catheterized controls and solution-treated animals with a catheter, however.

Figure 20. Mice with peritoneal catheter implants have disruption of the mesothelial layer and increased leukocyte infiltration. BALB/c male mice were dialyzed with PD fluids daily over 6 weeks through a catheter implant. Four hours after the last dialysis solution (2.5% glucose) injection, the mice were prepared for IVM and the parietal peritoneum and the underlying microcirculation were imaged with transillumination technique. The mesothelial layer (first column), submesothelial compact zone (second column) and underlying venules (third column) were visualized. (A) Naïve mice had an intact mesothelial layer and had minimal leukocyte infiltration in the venules. (B) The group of mice that had catheter implants without dialysis and (C) the group that received dialysis fluids through the catheter had rounded and hypertrophied mesothelial cells and increased leukocyte infiltration in the peritoneal tissue. Representative images, *n* = 4-6 mice, scale bar = 20 μm.

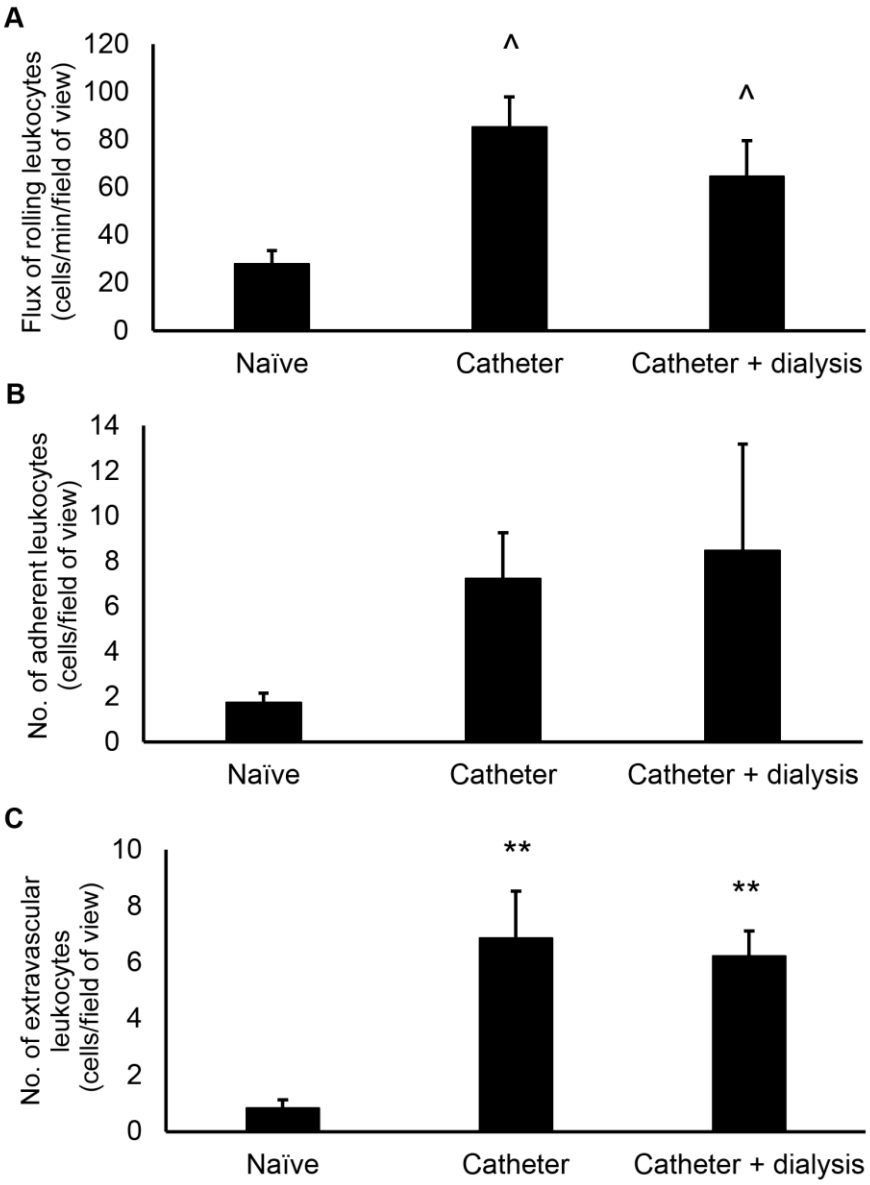

Figure 21. Catheterized mice have increased numbers of rolling and perivenular leukocytes in the parietal peritoneum microcirculation. The microcirculation of the parietal peritoneum was imaged with IVM after 6 weeks of PD. The number of (A) rolling and (B) adherent leukocytes in the peritoneal venules as well as the number of (C) extravascular leukocytes were quantified. Mice that had catheter implants, regardless of the presence of the dialysis solution, had significantly increased numbers of rolling and extravascular leukocytes. Data recorded as mean ± SEM and analyzed with ANOVA with Bonferroni correction, 4-6 venules averaged per count, n = 4-6 mice, ^$p < 0.05$ and **$p < 0.001$ compared with naïve controls.

Blood was collected following completion of IVM observations. Systemic leukocyte counts and differential leukocyte counts revealed monocytosis in the catheter control group (**Table 2**). Systemic leukocyte counts and differential counts did not differ between the naïve mice that underwent IVM compared with baseline controls that did not undergo intravital imaging. The number of peritoneal leukocytes was elevated in the spent dialysate from the dialyzed animals compared to baseline peritoneal lavage levels with 16.89 ± 4.31 versus 3.52 ± 0.43 total peritoneal leukocytes x 10^6, respectively, but were not significantly different as determined by a Student's *t* test, $p = 0.0526$. The spent dialysate was collected before laparotomy and tested negative for bacterial cultures grown over night at 37°C on TSA plates. These results indicate that the peritoneal catheter implant induced increased leukocyte rolling in the microvessels underlying the parietal peritoneum and resulted in increased accumulation of perivenular leukocytes independently from the dialysis solution treatment.

Table 2. Differential leukocyte counts after 6 weeks of PD.

Group	Total cells X 10^9/L	Neutrophils	Lymphocytes	Monocytes
Baseline	4.08±0.67	0.99±0.27	3.06±0.42	0.037±0.010
Naïve	5.74±0.83	1.43±0.37	4.17±0.56	0.10±0.02
Catheter	10.87±2.31^*	3.17±0.79	5.13±2.06	0.64±0.23^*
Catheter + dialysis	8.87±1.27^	2.47±1.14	6.01±0.90	0.37±0.09

After the completion of surgery and IVM observations, blood was collected via cardiac puncture and total systemic leukocyte counts and differential leukocyte counts were performed. Catheterized animals without dialysis had significantly increased numbers of systemic leukocytes and systemic monocytes compared with naïve controls. Data recorded as mean ± SEM and analyzed with ANOVA with

Bonferroni correction, n = 4 mice, ^p < 0.05 compared with baseline and *p < 0.05 compared with naïve controls.

3.5.3 Structural changes in the anterior abdominal wall after subacute exposure to peritoneal dialysis solution and catheter: After IVM, samples of the abdominal wall were excised from the left upper quadrant and the left lower quadrant for H&E staining. This corresponded to the area above and below the region in contact with the catheter. The sections showed similar structural changes of the peritoneal layer in mice that served as the catheterized controls and solution-treated animals (**Figure 22**). There were no differences in measurements of the submesothelial thickness (**Figure 23A**) and the vascular density (**Figure 23B**) between the two groups. Since these samples were not directly in contact with the catheter, the structural changes observed indicate the catheter induced local inflammatory responses in the peritoneum. There were no significant differences in these histologic changes between the sections taken from the upper and lower abdominal wall. These results indicate that in this subacute PD model, the catheter was responsible for the increased fibrosis and angiogenesis.

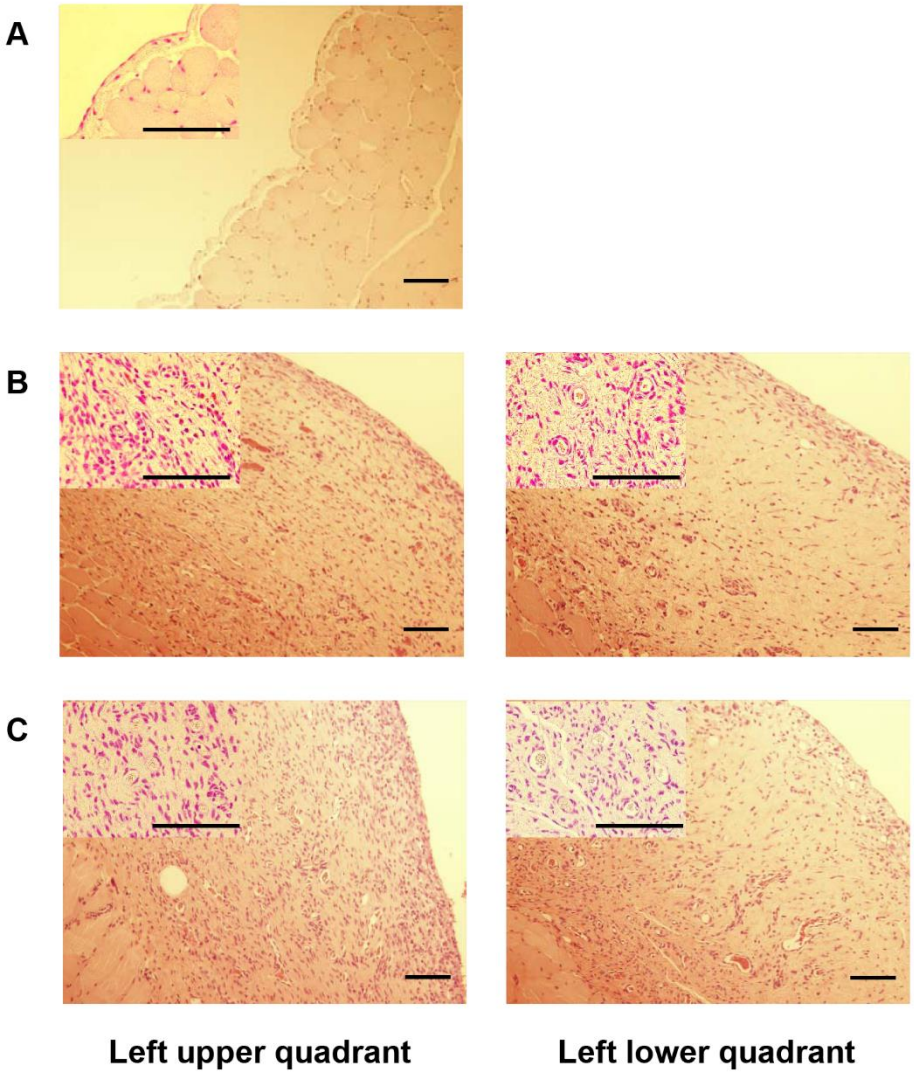

Figure 22. Catheter control mice and dialyzed mice exhibit similar histologic alterations in the parietal peritoneum. H&E-stained sections of the anterior abdominal wall, collected from the left side after completion of IVM. (A) A thin peritoneal layer was observed in the naïve mice while the (B) catheter control and (C) dialyzed groups both had submesothelial thickening, hypercellularity and increased vascularization after 8 week exposure to the catheter implant. The insets show increased vascular density in the submesothelial zone. Representative images, *n* = 4-6 mice, scale bar = 100 μm.

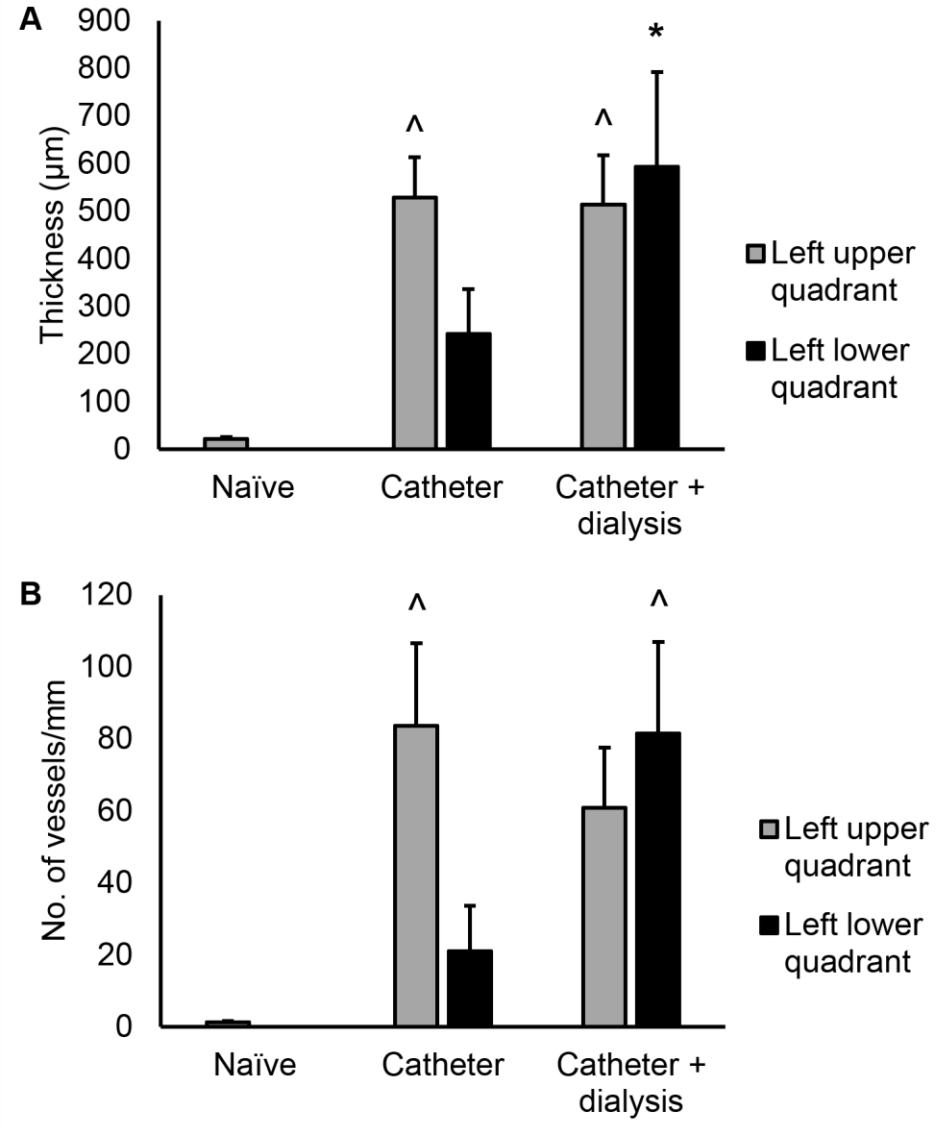

Figure 23. The peritoneal catheter induced severe fibrosis and angiogenesis in the peritoneal layer. The (A) thickness and (B) vascular density of the peritoneal layer were quantified from the H&E stained sections. Data recorded as mean ± SEM and analyzed with ANOVA with Bonferroni correction, *n* = 4-6 mice, ^*p* < 0.05 and **p* < 0.01 compared with naïve controls. The catheter control group exhibited similar levels of fibrosis and angiogenesis in the peritoneal layer of the upper and lower abdominal wall as the dialyzed mice.

3.6 Syndecan-1 in *S. aureus* infection during subacute peritoneal dialysis

3.6.1 Animal characteristics: Following catheter implantation surgery, there were no significant changes in behaviour or appearance of the animals and skin incisions healed well with no signs of infection. One mouse in the *Sdc1*$^{-/-}$ group was euthanized at the end of the catheter acclimatization period due to fighting injuries from the cage mate. There were no differences in the weights of the animals between the wild-type group and *Sdc1*$^{-/-}$ group at the start (26.93 ± 0.30g versus 25.88 ± 0.55g, respectively) and end (30.50 ± 0.42g versus 29.13 ± 0.44g, respectively) of the experiment. However, 8/14 animals in the wild-type group and 7/8 animals in the *Sdc1*$^{-/-}$ group exhibited redness and scabbing on the skin over the port for approximately 3 weeks after surgical implantation, but this did not interfere with solution injections into the port. Upon midline laparotomy, 1/14 wild-type mice had omental wrapping of the catheter at the entry site on the abdominal wall and 8/14 wild-type mice and 5/8 *Sdc1*$^{-/-}$ mice had gonadal adipose tissue wrapping at catheter entry site with no occlusion of the catheter tip.

3.6.2 Sdc1*$^{-/-}$ *mice have higher S. aureus loads in the abdominal wall after peritoneal dialysis: To determine whether subacute exposure to peritoneal dialysis and lack of syndecan-1 affects the progression of *S. aureus* IP infection, wild-type and *Sdc1*$^{-/-}$ mice were infected through the peritoneal catheter while control animals were injected IP on the right side. The catheterized animals were also injected with dialysis solution

immediately after the injection of *S. aureus* into the subcutaneous port. Four hours post-infection, peritoneal lavage was performed and blood was collected. Samples of the abdominal wall were extracted and homogenized. The lavage fluid and tissues were serially diluted and plated to enumerate CFU. There were no significant differences in the CFU counts from the peritoneal lavage between dialyzed animals and IP controls, as well as wild-type and *Sdc1*$^{-/-}$ mice (**Figure 24A**). There were also no differences in CFU counts from blood samples between any of the groups (**Figure 24B**). An outlier was excluded from the *Sdc1*$^{-/-}$ dialysis group because the value was far beyond the range of values calculated by subtraction and addition of 1.5 times the interquartile range to the first and third quartile. Contamination during cardiac puncture was strongly suspected. Nevertheless, ANOVA tests with Bonferroni correction did not show any significant difference between the groups with and without the inclusion of the outlier. The bacterial counts from the blood suggested sepsis in some animals, which was accompanied by diarrhea and slower movement. The CFU counts from the abdominal wall homogenate samples were significantly increased in the *Sdc1*$^{-/-}$ animals but only in the group that underwent peritoneal dialysis (**Figure 24C**). All of the infected animals had significantly increased numbers of peritoneal leukocytes compared with baseline levels (**Table 3**). Although the peritoneal leukocyte counts appeared to be reduced in the *Sdc1*$^{-/-}$ animals, the difference did not reach statistical significance with an ANOVA with Bonferroni correction (wild-type IP versus *Sdc1*$^{-/-}$ IP, $p = 0.0844$, and wild-type PD versus *Sdc1*$^{-/-}$ PD, $p = 0.124$). Systemic white blood cell counts did not significantly differ between the different groups, however, the number of systemic neutrophils was

significantly decreased in the dialyzed wild-type animals compared with IP controls. Also, the number of systemic monocytes was significantly elevated in wild-type animals with IP *S. aureus* injection compared with baseline levels (**Table 3**). The results indicate that the parietal peritoneum and the underlying tissue of *Sdc1*$^{-/-}$ mice are more susceptible to *S. aureus* invasion in the context of peritoneal dialysis-induced injury.

3.6.3 Host material deposition in the peritoneal dialysis catheters of Sdc1*$^{-/-}$ *and wild-type mice: Host material deposition, inflammatory cell recruitment and *S. aureus* attachment to the catheter surface do not appear to differ between catheters extracted from *Sdc1*$^{-/-}$ and wild-type mice that were injected with *S. aureus* through the catheter. Leukocytes and crenated red blood cells were recruited to the catheter lumen (**Figure 25A**). The inflammatory cells interacted with *S. aureus* microcolonies (**Figure 25B**). Some of the *S. aureus* cells that were injected in a suspension through the catheter port and flushed with dialysis solution were deposited on the catheter luminal surface (**Figure 25C**). In some areas of the catheters, there was host material deposition (**Figure 25D**). Leukocytes reacted to the foreign body by attachment to the surface within a fibrin network along with platelets and red blood cells (**Figure 25E-F**). This included macrophages and neutrophils that appeared to communicate through cell surface extensions (**Figure 25F**). These results indicate that syndecan-1 deficiency in the inflammatory cells does not alter their recruitment to the foreign body.

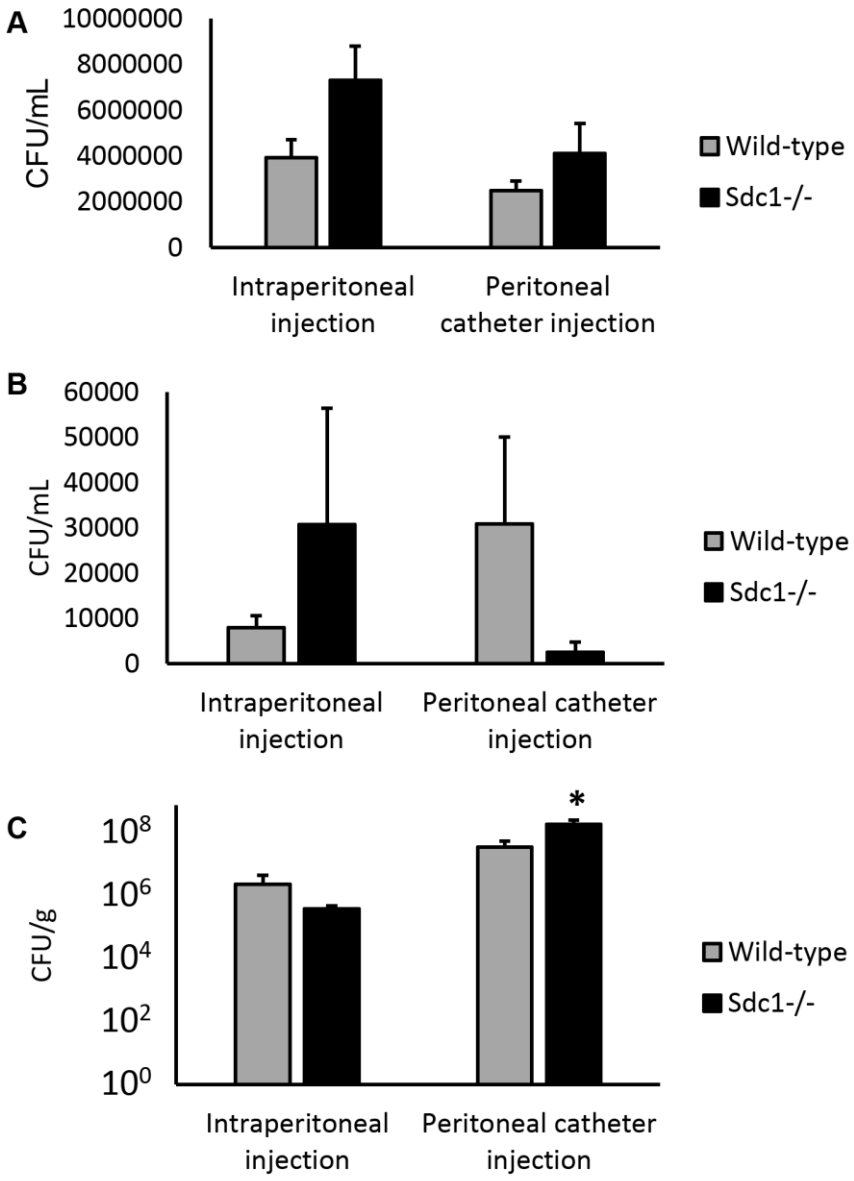

Figure 24. *Sdc1*$^{-/-}$ mice have higher *S. aureus* loads in the abdominal wall after peritoneal dialysis. Viable bacteria counts from lavage (A) samples, (B) blood and (C) abdominal wall homogenates from *Sdc1*$^{-/-}$ and wild-type mice that were injected with 1.8 x 10^8 CFU of *S. aureus* through the PD catheter or with an IP injection and sacrificed 4 hours later. Data recorded as mean ± SEM and analyzed with ANOVA with Bonferroni correction, n = 8-14 mice, *$p < 0.01$ compared with all other groups. *Sdc1*$^{-/-}$ mice that were dialyzed for 4 weeks had a significantly higher number of viable bacterial cells in the abdominal wall samples.

Table 3. Peritoneal lavage leukocyte counts and differential blood leukocyte counts.

Treatment/strain	Total peritoneal cells x 10^6	Total blood cells x 10^9/L	Blood neutrophils	Blood lymphocytes	Blood monocytes
Baseline Wild-type	3.52±0.43	4.08±0.67	0.99±0.27	3.06±0.42	0.037±0.010**
Baseline *Sdc1*$^{-/-}$	2.78±0.28	4.56±0.68	1.14±0.26	3.40±0.51	0.019±0.0076
S. aureus Intraperitoneal injection Wild-type	25.78±3.43***	4.98±0.65	1.80±0.20	3.14±0.53	0.34±0.072
S. aureus Intraperitoneal injection *Sdc1*$^{-/-}$	15.94±1.57***	3.62±0.49	1.58±0.31	2.01±0.25	0.033±0.016**
S. aureus Catheter injection Wild-type	31.65±1.90***	3.12±0.33	0.79±0.12*	2.14±0.27	0.19±0.041
S. aureus Catheter injection *Sdc1*$^{-/-}$	22.42±1.89***	3.29±0.52	1.05±0.16	2.11±0.41	0.13±0.031

Peritoneal lavage was done at subacute PD study end-point and blood was collected via cardiac puncture 4 hours after *S. aureus* infection. Data recorded as mean ± SEM and analyzed with ANOVA with Bonferroni correction, 6 counts averaged per mouse, n = 8-14 mice, *$p < 0.01$ and **$p < 0.001$ compared with wild-type IP injection control, ***$p < 0.0001$ compared with baseline values. Infected mice had significantly increased numbers of peritoneal leukocytes compared with baseline but the leukocyte counts did not differ significantly.

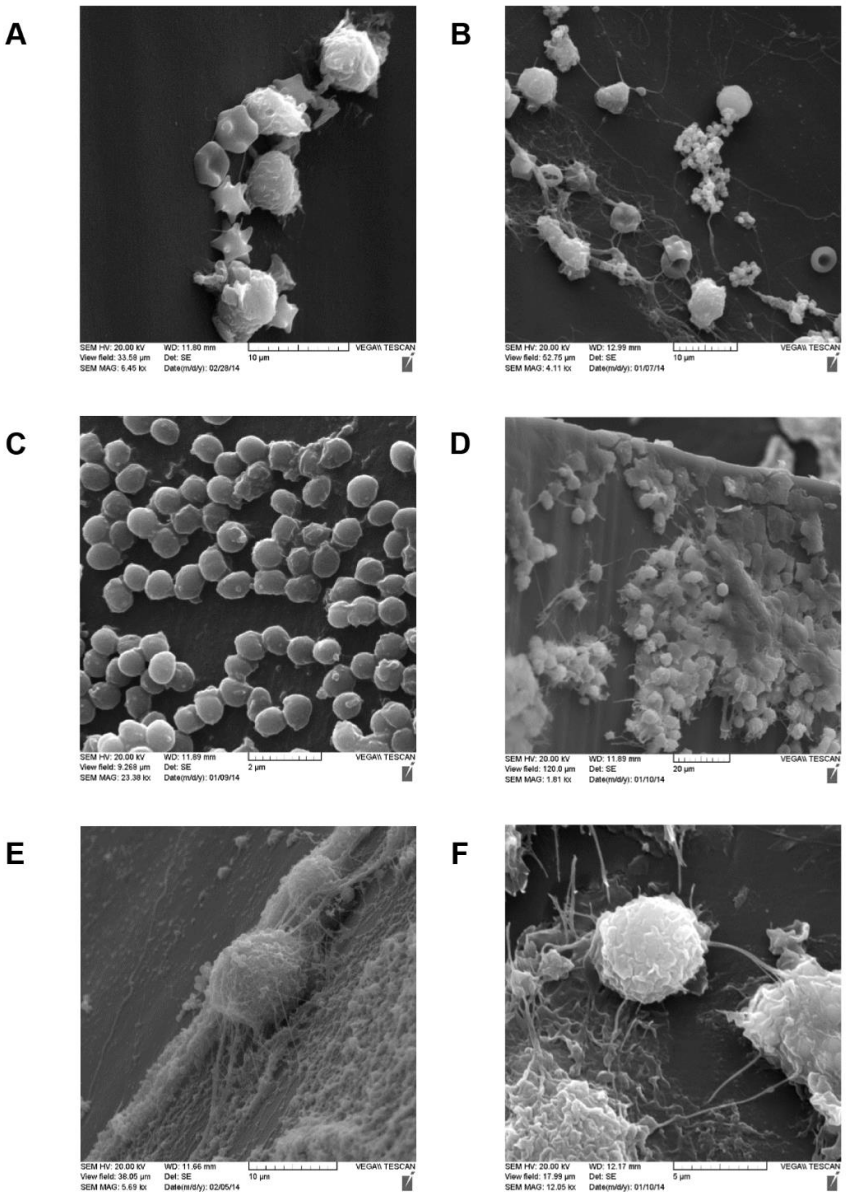

Figure 25. Host reaction to the peritoneal dialysis catheters. **After 4 weeks of PD, the intra-abdominal portion of the peritoneal catheter was collected from *Sdc1*$^{-/-}$ and wild-type mice that were injected with *S. aureus* through the catheter. The catheters were fixed and prepared for SEM imaging. (A-B) Leukocytes were recruited to the lumen of the catheter. (C) The *S. aureus* that was injected into the catheter port adhered to the catheter surface. (D) Host material was deposited on the catheter and (E-F) leukocytes were seen interacting. Note: images A, B and E are derived from catheters of *Sdc1*$^{-/-}$ mice and images C, D and F are derived from catheters of wild-type mice.**

3.6.4 Histopathologic analysis of structural changes of the peritoneum in subacute PD: The samples of the anterior abdominal wall from animals that received dialysis solution through the catheter were collected on the contralateral side to the catheter entry site and were above the area that came into contact with the intra-abdominal catheter tip. For the control animals that received a suspension of *S. aureus* through an IP injection, the section of the abdominal wall collected was contralateral and superior to the injection point. Animals that served as baseline controls had an intact mesothelial surface (**Figure 26A**) and no leukocyte infiltration. Mice that received an IP injection of *S. aureus* surprisingly did not exhibit much leukocyte infiltration and mesothelial disruption (**Figure 26B**). In many areas of the abdominal wall sample, mice that were treated with PD had thickening of the submesothelial compact zone, with increased vascularization, interstitial hypercellularity and severe leukocyte infiltration (**Figure 26C**). The average thickness of the peritoneal and submesothelial layer was significantly increased in the mice that received PD. However, there was no significant difference between *Sdc1*$^{-/-}$ mice and wild-type animals (**Figure 27A**). The number of peritoneum-associated vessels was significantly increased in dialyzed animals compared to controls but did not differ between the *Sdc1*$^{-/-}$ mice and wild-type animals (**Figure 27B**). This suggests that syndecan-1 is not a modulator of fibrosis and angiogenesis in PD-induced histopathology.

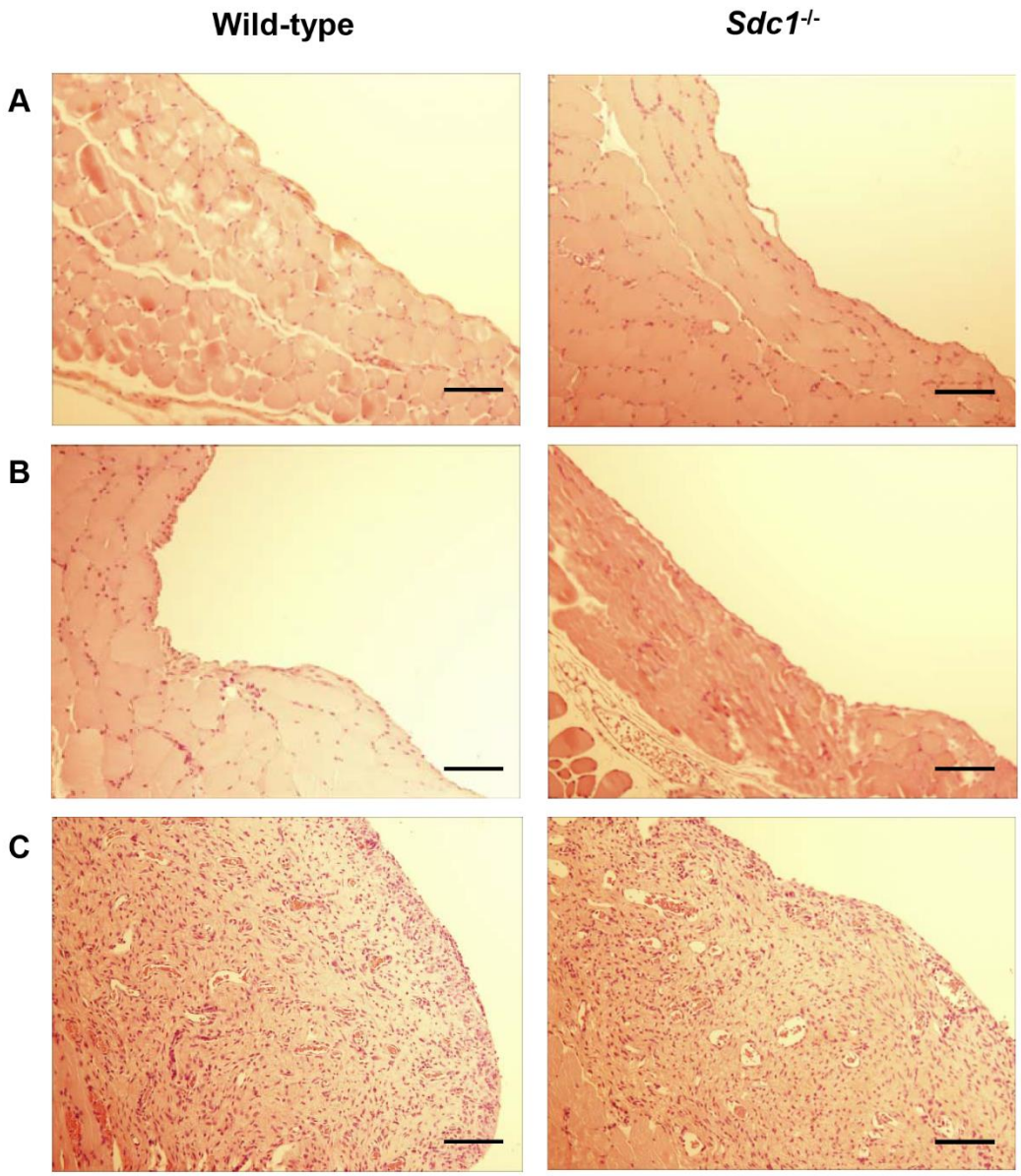

Figure 26. Severe peritoneal pathology in *Sdc1*$^{-/-}$ and wild-type mice with subacute PD. At the study endpoint, samples of the abdominal wall were collected from (A) *Sdc1*$^{-/-}$ and wild-type mice that served as baseline controls, (B) *Sdc1*$^{-/-}$ and wild-type mice that were injected with *S. aureus* IP and (C) mice that were treated with PD for 4 weeks. The samples were fixed, sectioned and stained with H&E for histopathologic analysis. The peritoneal layer of dialyzed mice was thickened and is seen spanning the entire field of view. Representative images, *n* = 8-14 mice, scale bar = 100 μm.

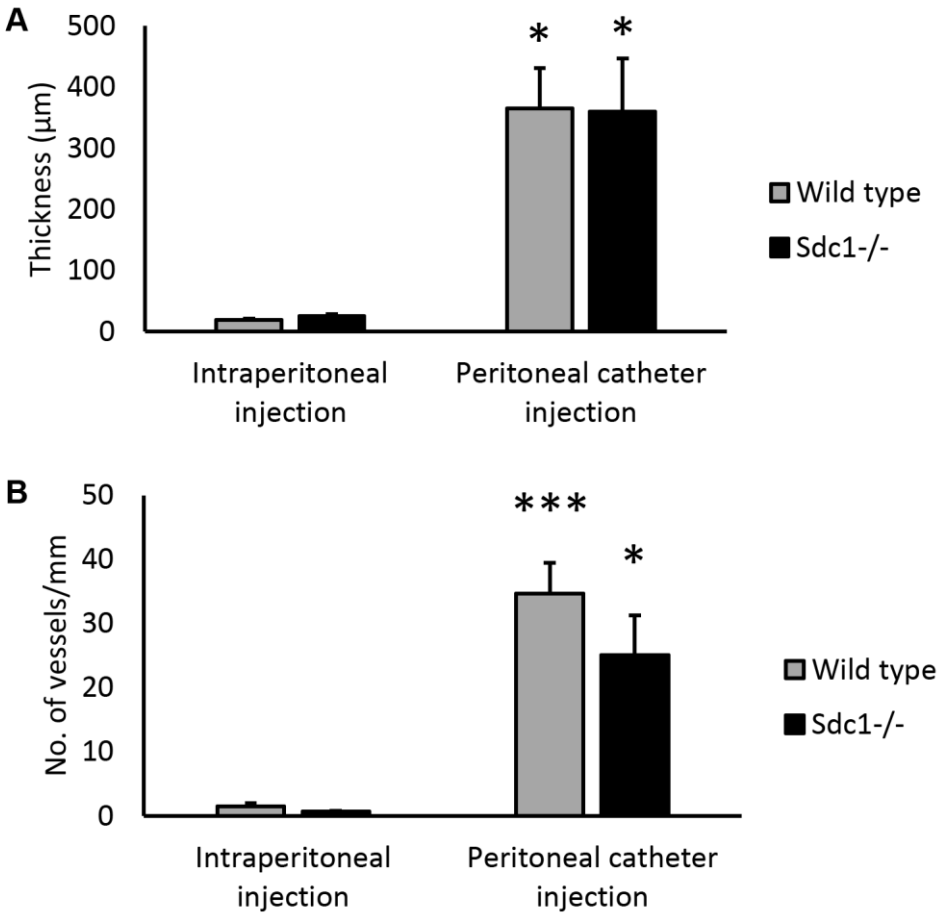

Figure 27. *Sdc1*$^{-/-}$ and wild-type mice exhibit similar degree of fibrosis and angiogenesis during subacute PD. The (A) thickness and (B) vascular density of the peritoneal layer were quantified from the H&E stained sections. Data recorded as mean ± SEM and analyzed with ANOVA with Bonferroni correction, *n* = 8-14 mice, **p* < 0.01 and ****p* < 0.0001 compared with controls that did not receive PD and were infected with *S. aureus* through an IP injection. There were no differences in the levels of fibrosis and angiogenesis in the peritoneum of *Sdc1*$^{-/-}$ and wild-type mice.

3.7 IVM of the parietal peritoneum microcirculation during *S. aureus* infection

3.7.1 S. aureus infection decreases subendothelial syndecan-1 protein expression in the peritoneal venules: During LTA-induced inflammation, syndecan-1 was highly expressed in the peritoneal venules on the subendothelial side (**Figure 28A**). To examine the effects of *S. aureus* infection on syndecan-1 levels in the peritoneal microcirculation, confocal fluorescence IVM was performed on wild-type mice that were injected IP with GFP-expressing *S. aureus* (**Figure 28B**) and 4 hours later, the mice were injected IV with Alexa Fluor® 568-labeled anti-syndecan-1. With *S. aureus* intra-abdominal infection, anti-syndecan-1 antibody did not label peritoneal venules (**Figure 28C**) and this was confirmed with quantification of fluorescence intensity from the anti-syndecan-1 antibodies on peritoneal venules in LTA-injected and *S. aureus*-infected mice (**Figure 29**). The GFP-expressing *S. aureus* cells were not visible against the tissue autofluorescence (**Figure 28C**). These findings indicate that *S. aureus* infection decreased syndecan-1 levels in the subendothelial region of peritoneal venules.

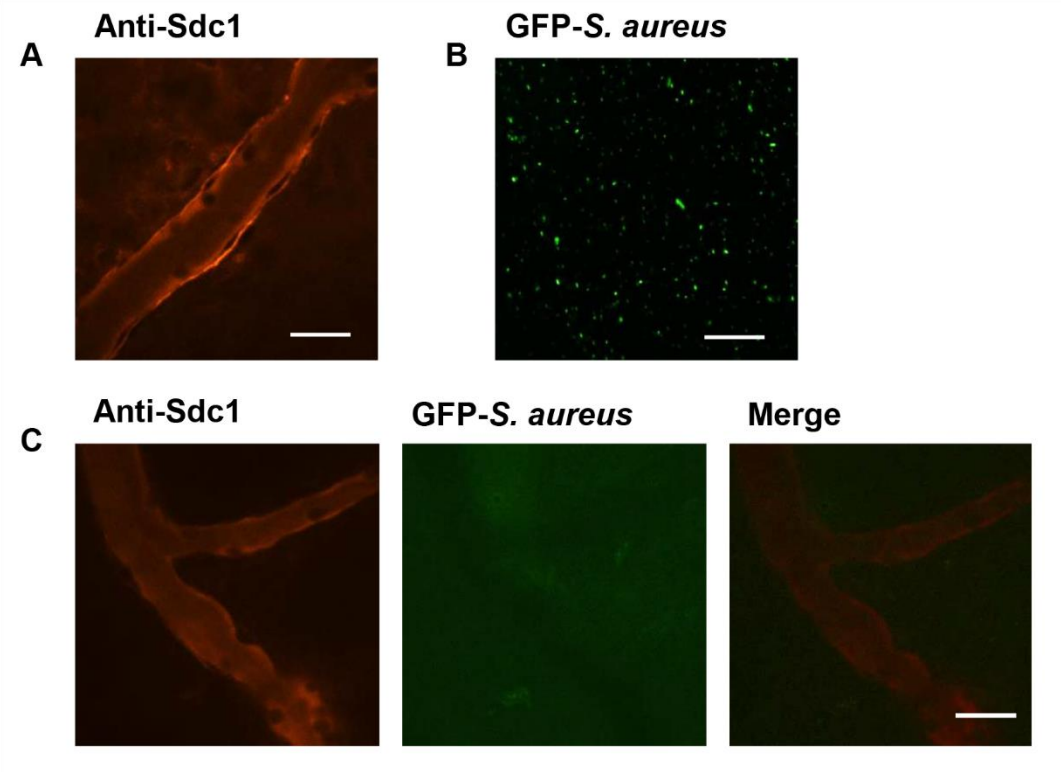

Figure 28. *S. aureus* infection decreases subendothelial syndecan-1 levels in the peritoneal venules. Wild-type mice were injected IP with (A) 125 μg of LTA from *S. aureus* or (B) 1.8 x 10^8 CFU of GFP-expressing *S. aureus*. Four hours later, the mice were prepared for immunofluorescence IVM and Alexa Fluor® 568-labeled anti-syndecan-1 antibodies were injected IV. The microcirculation of the parietal peritoneum was examined. Syndecan-1 was detected in the subendothelial compartment of venules in LTA-stimulated mice (A) but not with *S. aureus* infection (C). Representative images, *n* = 4 mice, scale bar = 20 μm.

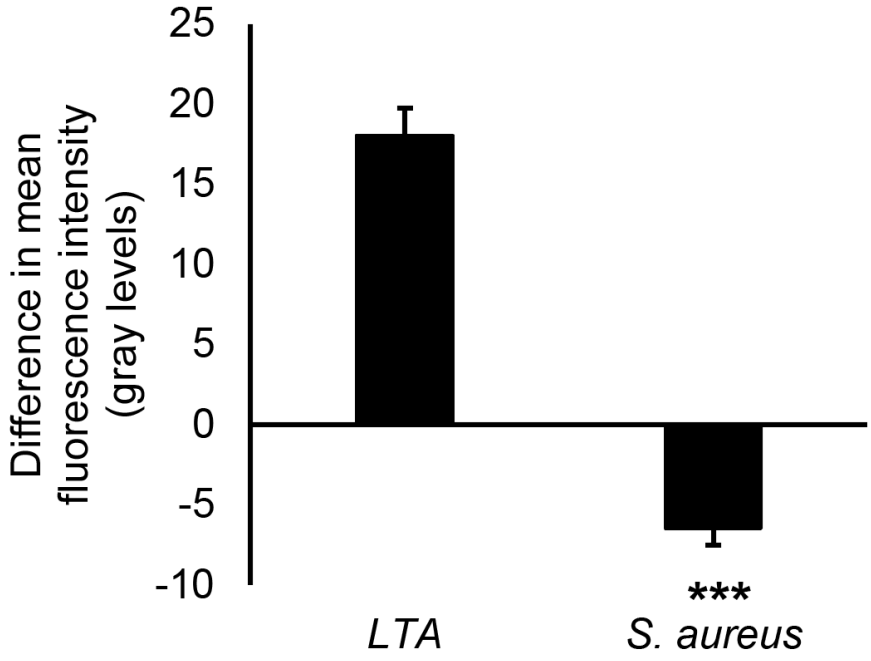

Figure 29. Decreased subendothelial anti-syndecan-1 fluorescence intensity in *S. aureus* IP infection (1.8 x 10^8 CFU). Quantification of the fluorescence intensity from the antibodies labeling the subendothelial surface showed that syndecan-1 protein expression during *S. aureus* infection was significantly decreased. Data recorded as mean ± SEM and analyzed with Student's *t* test, 4 venules averaged per mouse, *n* = 4 mice, ***$p < 0.0001$ compared with LTA.

3.7.2 Syndecan-1 does not modulate leukocyte recruitment to the parietal peritoneum microcirculation during S. aureus infection: To investigate whether syndecan-1 deficiency alters leukocyte recruitment during *S. aureus* infection, wild-type and *Sdc1*$^{-/-}$ mice were injected with a suspension of *S. aureus* IP and prepared for IVM 4 hours later. Control mice were injected IP with sterile saline. Mice infected with *S. aureus* did not have significantly different numbers of rolling leukocytes compared with saline controls (**Figure 30A**). The number of adherent (**Figure 30B**) and extravascular (**Figure 30C**) leukocytes was significantly increased in *S. aureus* infection. However, there were no significant differences in leukocyte rolling, adhesion and extravasation between the wild-type and *Sdc1*$^{-/-}$ mice. Thus, syndecan-1 does not modulate leukocyte recruitment in the parietal peritoneum microcirculation during *S. aureus* infection.

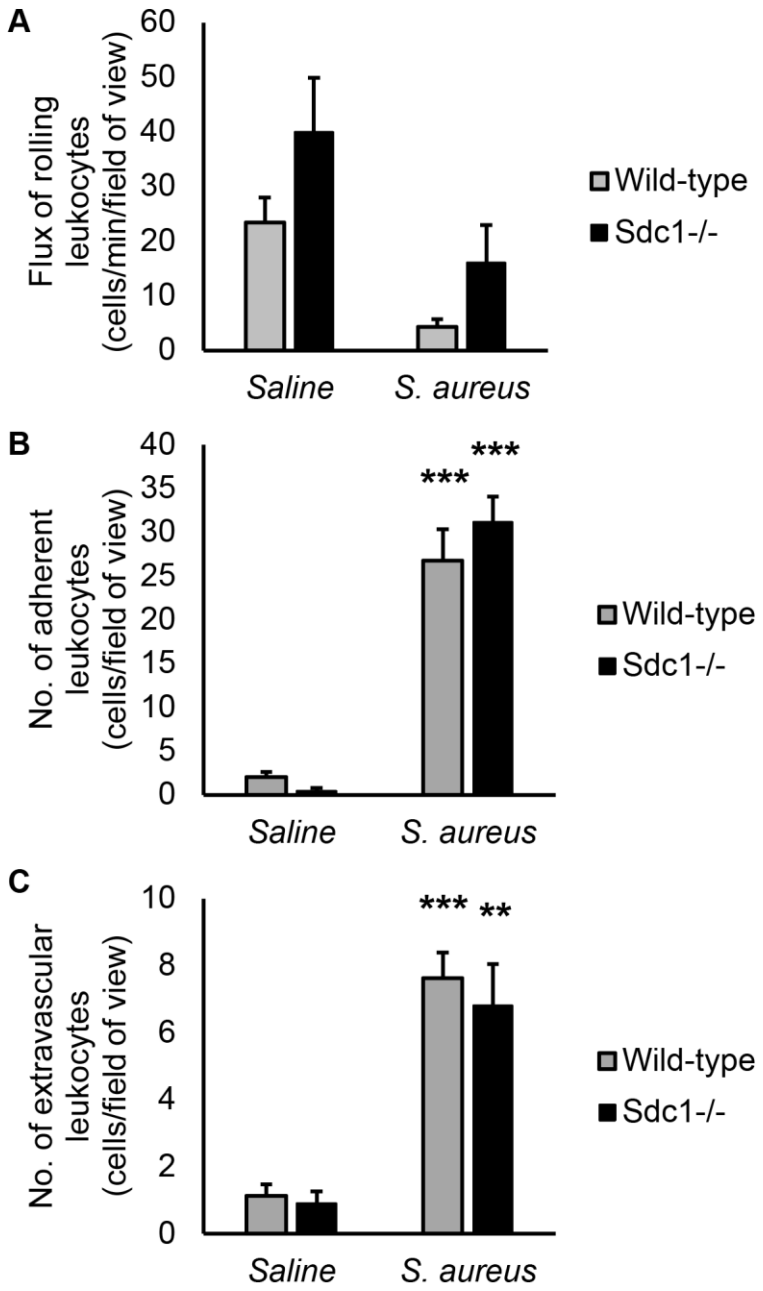

Figure 30. Syndecan-1 does not modulate leukocyte recruitment to the parietal peritoneum microcirculation during *S. aureus* infection. Wild-type and *Sdc1*$^{-/-}$ mice were injected IP with 1.8 x 10^{8} CFU of *S. aureus*. Four hours later, the mice were prepared for IVM and the microcirculation of the parietal peritoneum was imaged. The number of (A) rolling and (B) adherent leukocytes in the peritoneal venules as well as the number of (C) extravascular leukocytes were quantified. *S.*

aureus **infection significantly increased the number of adherent and extravascular leukocytes compared with saline controls. However, there were no significant differences in leukocyte recruitment between the** ***Sdc1*** $^{-/-}$ **and wild-type mice. Data recorded as mean ± SEM and analyzed with ANOVA with Bonferroni correction, 4-6 venules averaged per count,** ***n*** **= 4 mice, *****p* **< 0.001 and ******p* **< 0.0001 compared with saline.**

CHAPTER 4: DISCUSSION

Syndecan-1 is believed to be a constituent of the endothelial glycocalyx, a glycoprotein and proteoglycan-rich layer that coats the luminal surface of blood vessels (Pries *et al.*, 2000). Since increased plasma levels of syndecan-1 are associated with glycocalyx breakdown, syndecan-1 is used as a marker of glycocalyx degradation (Rehm *et al.*, 2007). The present study showed that syndecan-1 is expressed in the microcirculation underlying the parietal peritoneum. However, these *in vivo* results indicate that syndecan-1 is localized to the basolateral side of the endothelial cell layer of venules, challenging the idea that syndecan-1 is a major part of the glycocalyx lining the luminal surface of the vasculature. Venular endothelial cells are surrounded by a basement membrane with interspersed pericytes. Syndecan-1 is known to bind various extracellular matrix components, such as collagen type IV (San Antonio *et al.*, 1994), which is a major constituent of basement membranes. Thus, our findings are more consistent with the idea that syndecan-1 anchors the venular endothelial cells, and perhaps pericytes, to the underlying basement membrane. Since the present study is the first report of confocal fluorescence intravital imaging of syndecan-1 in the mouse microcirculation of the parietal peritoneum, it is possible that the different protein expression pattern observed is specific to this tissue.

Syndecan-1 is predominantly expressed on epithelial cells in a basolateral fashion. This basolateral restriction is dependent on the PDZ-binding motif of the cytoplasmic tail of syndecan-1 interacting with cytosolic PDZ domain-containing proteins (Maday *et al.*, 2008; Miettinen *et al.*, 1994). Since the mesothelial cells that form the parietal

peritoneum are structured as squamous epithelium, we hypothesized that syndecan-1 is also expressed on these cells. Indeed, the fluorescent *ex vivo* images of the transverse sections of the anterior abdominal wall showed that syndecan-1 is present on the mesothelial cells that form the parietal peritoneum.

Cell surface and plasma levels of syndecan-1 were reported to change in inflammation and other pathologic conditions. During skin wound healing in mice, syndecan-1 was induced at the basal surface of endothelial cells of capillaries in granulation tissue but was absent in normal skin (Elenius *et al.*, 1991). In hemorrhagic shock, plasma levels of shed syndecan-1 in severely injured patients were increased (Haywood-Watson *et al.*, 2011). Systemic shed syndecan-1 levels were also reported to be associated with inflammation, coagulopathy and increased mortality in trauma patients (Johansson *et al.*, 2011). The significance of syndecan-1 shedding is largely unclear, although it is postulated to mediate processes such as resolution of inflammation (Hayashida *et al.*, 2009b) and pathogen dissemination (Haynes *et al.*, 2005). By quantifying the intensity from the fluorescent antibodies bound to syndecan-1 along the subendothelial surface, we showed that there is no significant difference in the protein level of syndecan-1 between LTA-treated animals and saline controls. This suggests that syndecan-1 is constitutively expressed on the endothelium in the parietal peritoneum microcirculation and that no significant shedding occurs in inflammation. However, pro-inflammatory effects of the surgical preparation for IVM cannot be excluded. Therefore, syndecan-1 levels in the tissue homogenate of the parietal peritoneum with the attached abdominal wall, as well as blood plasma and peritoneal

lavage fluid were measured in response to IP injection of saline, LTA and TNFα by ELISA in a separate group of animals. In agreement with the fluorescence IVM results, the ELISA did not reveal any significant difference in syndecan-1 levels in the musculoperitoneal tissue, in the peritoneal effluent and in plasma between saline controls and LTA or TNFα-stimulated animals. These results suggest that "sterile" inflammation did not promote syndecan-1 shedding. However, it is important to note that syndecan-1 shedding was repeatedly shown to be induced by pathogens (Chen *et al.*, 2007; Park *et al.*, 2001), such as *S. aureus* (Hayashida *et al.*, 2011), and the microbial components that activate syndecan-1 shedding from cellular membranes were deduced to be *S. aureus* α- and β-toxins (Park *et al.*, 2004). Thus, perhaps we didn't observe significant syndecan-1 shedding in this model of LTA-induced peritonitis because of the absence of certain staphylococcal toxins. Indeed, 4 hours after IP injection of a suspension of viable *S. aureus* cells, syndecan-1 protein expression along the basolateral surface of venular endothelium was severely diminished. This result suggests that *S. aureus* LTA-induced inflammation differs from the inflammatory responses that occur during infection with viable *S. aureus* cells.

To study the role of syndecan-1 in leukocyte-endothelial cell interactions in the parietal peritoneum during inflammation, the microcirculatory responses to *S. aureus* LTA, *E. coli* LPS and TNFα as well as *S. aureus* were examined. While stimulation with LTA and TNFα significantly increased leukocyte adhesion in the vasculature of the musculoperitoneal wall, leukocyte adhesion did not significantly differ after injection of LPS compared with control and LPS treatment decreased the number of rolling

leukocytes. The decreased inflammatory response to LPS in the parietal peritoneum microcirculation was not due to an inability of this tissue to respond to LPS as murine peritoneal cells do express the molecules of the LPS signaling pathway—Toll-like receptor 4 (TLR4), CD14 and myeloid differentiation factor 2 (MD2) (Kato *et al.*, 2004). Moreover, this effect is likely due to leukocyte sequestration in the lungs and the liver after IP injection of LPS. It was previously reported that IP injection of LPS rapidly causes neutropenia and TLR4-dependent neutrophil accumulation in the lungs (Andonegui *et al.*, 2003). This neutrophil sequestration in the lungs was associated with reduced leukocyte trafficking to peripheral vascular beds. Specifically, leukocyte rolling in the cremaster post-capillary venules was significantly decreased (Andonegui *et al.*, 2003), similar to what we observed in the parietal peritoneum microcirculation.

Local and systemic microcirculatory responses to LPS and LTA differ substantially 4 hours after administration of these bacterial products (Yipp *et al.*, 2002). In the murine cremaster muscle, local administration of *E. coli* LPS with an intrascrotal injection resulted in significantly increased numbers of rolling, adherent and extravascular leukocytes whereas intrascrotal *S. aureus* LTA injection had no effect on leukocyte-endothelial cell interactions in this vascular bed. Systemic administration of LPS with an IP injection resulted in decreased leukocyte recruitment in the cremasteric microcirculation but IP injection of LTA, again, had no effect on leukocyte recruitment to the cremaster muscle (Yipp *et al.*, 2002). The IP injection of the bacterial products in the current report is a unique situation as this is both a systemic response and a local response and, unlike the cremaster muscle, LTA injection had pro-inflammatory effects

on the peritoneal microcirculation. Thus, even though the cremaster muscle is an extension of the abdominal musculature and its tunica vaginalis is a remnant of the peritoneum, there are significant differences in responses to LTA in the vascular beds of these tissues. However, an additional difference is that highly purified LTA was used in the cremaster muscle study.

In the current study, infection of mice with live *S. aureus* cells did not cause depletion of leukocytes in the peritoneal microcirculation that was observed with LPS injection. Also, *S. aureus* IP infection did not result in lowered systemic white blood cell counts that is seen in cecal ligation and puncture (CLP) model of sepsis (Ondiveeran & Fox-Robichaud, 2004). Thus, although some animals in this study did exhibit behavioral changes, dysentery and bacteremia, overall they did not reach the degree of sepsis observed in the CLP models. The *S. aureus* bacterial infection resulted in greater leukocyte recruitment compared to injection of LTA from *S. aureus*. However, there were no differences between wild-type animals and *Sdc1*$^{-/-}$ mice. Contrary to our findings in the peritoneal venules, IP injection of live *S. aureus* cells resulted in diminished leukocyte rolling and adhesion in the mouse cremaster microcirculation (Yipp *et al.*, 2002). However, this study used a higher dose of live *S. aureus* cells than the amount used in our study.

Our findings that *Sdc1*$^{-/-}$ mice have similar leukocyte recruitment to the wild-type controls during inflammation do not mirror observations in the retinal microcirculation as well as the mesenteric venules of *Sdc1*$^{-/-}$ mice (Gotte *et al.*, 2002). *Sdc1*$^{-/-}$ mice on a BALB/c background were found to have an elevated number of adherent leukocytes in

unstimulated retinal vasculature and bone marrow transplant studies indicated that the increased adhesion depended on *Sdc1*$^{-/-}$ leukocytes as opposed to the endothelial component in the retina (Gotte *et al.*, 2002). However, we did not observe syndecan-1 expression on leukocytes recruited to the peritoneal venules after IP injection of LTA. This implies that the *Sdc1*$^{-/-}$ leukocytes in this bone marrow transplant study were influenced by the syndecan-1 deficient environment during development. The same study showed that 3 hours after IP injection of murine recombinant TNFα, *Sdc1*$^{-/-}$ mice had a significantly decreased number of rolling leukocytes and reduced rolling velocity (Gotte *et al.*, 2002). This was accompanied by a significantly increased number of adherent leukocytes per mesenteric venule and extravascular leukocytes were noted in the *Sdc1*$^{-/-}$ mice but not the wild-type controls. A consistent phenotype was observed by others in inflammatory and normal conditions. In murine experimental autoimmune encephalomyelitis, *Sdc1*$^{-/-}$ mice had increased infiltration by disease-causing Th1 and Th17 cells in brain tissue and increased disease severity (Zhang *et al.*, 2013). Similarly, *Sdc1*$^{-/-}$ mice had increased and prolonged leukocyte infiltration in delayed-type hypersensitivity response (Masouleh *et al.*, 2009). In cremasteric venules of *Sdc1*$^{-/-}$ mice, there was increased leukocyte adhesion under normal conditions (Savery *et al.*, 2013). Also, syndecan-1 deficiency was marked by higher neutrophil and macrophage influx to the glomerulus in anti-glomerular basement membrane nephritis which was accompanied by increased injury and worse renal function (Rops *et al.*, 2007). Together, these studies propose that syndecan-1 is a negative regulator of leukocyte recruitment and in the absence of syndecan-1, leukocyte recruitment is exaggerated and

inflammatory reactions are dysregulated. The disparate findings between these studies and the current report may be due to differences in mechanisms that regulate inflammatory processes in the different tissues examined. Interestingly, *in vitro* work suggested that there is a greater increase in adhesion to endothelial culture cells with monocytes than neutrophils from *Sdc1*$^{-/-}$ mice (Gotte *et al.*, 2005). However, we did not observe any CX_3CR1^+ monocyte recruitment to peritoneal venules 4 hours after saline, LTA or TNFα injection and the leukocyte infiltrate was composed of $Ly6G^+$ neutrophils. The reason for this may be that higher numbers of monocytes are usually recruited only after 3 to 4 days following peritonitis (Hurst *et al.*, 2001). Our findings suggest syndecan-1 is not a regulator of neutrophil recruitment during LTA-induced inflammation in the parietal peritoneum microcirculation during early inflammation. This further highlights the uniqueness of the parietal peritoneum microcirculation.

Syndecan-1 was shown to mediate neutrophil transendothelial migration *in vitro* (Marshall *et al.*, 2003). To determine whether *Sdc1*$^{-/-}$ mice have altered transendothelial leukocyte migration, extravascular cells were counted. The number of extravascular leukocytes did not differ between the wild-type and *Sdc1*$^{-/-}$ treated animals after saline, LTA or LPS injection but was significantly increased in the *Sdc1*$^{-/-}$ mice with TNFα treatment, suggesting different mechanisms govern leukocyte extravasation with TNFα. In fact, leukocyte recruitment in the hepatic microcirculation is governed by different molecular mechanisms depending on the pro-inflammatory stimulus and microvessel type (Fox-Robichaud & Kubes, 2000; Patrick *et al.*, 2007).

Since we saw that syndecan-1 did not regulate leukocyte recruitment in the peritoneal venules, we examined the role of other adhesion molecules in leukocyte rolling and adhesion in the microcirculation underlying the parietal peritoneum. We showed that leukocyte rolling in this tissue is mostly mediated by P-selectin with some dependency on β_2 integrin. However, blockade of the adhesion molecules β_2 integrin, ICAM-1 and VCAM-1 did not decrease leukocyte adhesion in the peritoneal microcirculation even though we showed that these molecules are expressed in the peritoneal venules. This suggests that there are redundant mechanisms that mediate leukocyte adhesion in this tissue. Perhaps, these mechanisms may involve ICAM-2, which was not tested in the current report.

Work by Massena and colleagues suggested that rolling leukocytes along the endothelial wall are exposed to chemokines on the luminal side and this promotes directional intravascular crawling and firm adhesion of the leukocyte to the endothelial cell which is ultimately followed by extravasation through the vessel wall (Massena *et al.*, 2010). Numerous studies reported that syndecan-1 binds to and concentrates chemokines in tissues. Syndecan-1 was found to be complexed with several different chemokines, including IL-8 (Massena *et al.*, 2010), KC (Li *et al.*, 2002), RANTES and MCP-1 (Slimani *et al.*, 2003), as well as CCL7, CCL11 and CCL17 (Xu *et al.*, 2005). MIP-2-binding to the venular endothelium of the cremaster muscle was found to be dependent on the presence of heparan sulfate (Massena *et al.*, 2010) and the chemokine-binding domain of heparan sulfate that associates with IL-8 was deciphered (Spillmann *et al.*, 1998). MIP-2 binding to heparan sulfate chains was proposed to direct

intraluminal crawling of neutrophils *in vivo* (Massena *et al.*, 2010). Yet in other situations, syndecan-1-binding to chemokines aided resolution of inflammation by removing MIP-2 and KC with syndecan-1 shedding *in vivo* (Hayashida *et al.*, 2009b).

For leukocyte extravasation to occur, a chemokine gradient across the vessel wall with higher chemokine concentrations in the extravascular space is required (Massena *et al.*, 2010). There is a steep gradient with heparan sulfate deposited on venules between the luminal and basolateral endothelial compartments, with higher heparan sulfate densities in the basolateral region (Stoler-Barak *et al.*, 2014). This heparan sulfate distribution was suggested to support steep chemokine gradients between the luminal and subendothelial aspects of post-capillary venules. Given that syndecan-1 possesses heparan sulfate chains and is expressed along the subendothelial surface in the parietal peritoneum microcirculation, we hypothesized that it concentrates chemokines at the site of inflammation to direct extravasating leukocytes. Co-injection of fluorescent anti-syndecan-1 with anti-MIP-2 antibodies after LTA challenge revealed that syndecan-1 did partially co-localize with MIP-2 *in vivo.* However, *Sdc1*$^{-/-}$ mice had similar expression patterns of MIP-2 in the peritoneal venules, indicating that syndecan-1 is not necessary for MIP-2 deposition in the parietal peritoneum microcirculation. Interestingly, the anti-MIP-2 antibody binding pattern on the peritoneal venules was irregular, unlike the bladder (Kowalewska *et al.*, 2011) and liver microcirculation (unpublished observations), which exhibit a more uniform binding pattern of the antibodies to chemokines along the endothelial surface. Syndecan-1 may have a redundant role in chemokine deposition on venules with other heparan sulfate

proteoglycans. We observed that syndecan-2 is also expressed on peritoneal venules with some overlap with MIP-2. However, the necessity of syndecan-2 for chemokine presentation on venules would be difficult to test *in vivo* since syndecan-2 null mice are not viable, perhaps due to its role in the developmental process (Fukumoto & Levin, 2005).

Since we found no evidence that syndecan-1 is necessary for chemokine presentation in the peritoneal venules, we wondered if another receptor, called DARC, is expressed in the parietal peritoneum microcirculation and whether it plays a role in chemokine sequestration in this tissue. DARC is a promiscuous chemokine receptor that acts as a molecular mop for chemokines. It has been proposed to sequester chemokines and decrease inflammation (Dawson *et al.*, 2000), and on the other hand, it was also reported to promote inflammation by presenting chemokines on the endothelial surface (Middleton *et al.*, 1997). In fact, DARC was shown to cooperate with heparan sulfate proteoglycans and the IL-8 receptors, CXCR1 and CXCR2, in the formation of filopodial protrusions on cultured endothelial cells that were proposed to present IL-8 to leukocytes (Whittall *et al.*, 2013). However, using confocal IVM and fluorescent-anti-DARC antibodies, we found no evidence that DARC is expressed in the parietal peritoneum microcirculation or the extravascular space in uninflamed conditions.

Although the role of certain proteoglycans was examined in PD (Yung & Chan, 2007b), the role of syndecan-1 has not been investigated in dialysis even though it was found to modulate inflammation (Li *et al.*, 2002), wound repair (Stepp *et al.*, 2002), angiogenesis (Oh *et al.*, 2010), fibrosis (Schellings *et al.*, 2010) and EMT (Kato *et al.*,

1995; Masola *et al.*, 2012). Many pathogens subvert syndecan-1 and use it to increase dissemination and host defense evasion during infection. One of the best characterized pathogens that manipulates syndecan-1 in infection is *S. aureus* (Hayashida *et al.*, 2011). Given that syndecan-1 regulates inflammation, fibrosis, angiogenesis and EMT and syndecan-1-microbial interactions are important in the pathogenesis of *S. aureus*, we chose to examine the role of this proteoglycan in PD with *S. aureus* infection.

In our study, syndecan-1 deficiency did not result in altered levels of fibrosis and angiogenesis in dialyzed mice compared with wild-type. Also, the responses to the catheter biomaterial were similar between *Sdc1*$^{-/-}$ mice and wild-type animals, with host material deposition and leukocyte recruitment to the catheter lumens. However, we observed that syndecan-1 deficiency made mice more susceptible to *S. aureus* colonization of the abdominal wall after 4 weeks of peritoneal dialysis. This is in contrast to what was reported in the corneal tissue, where *Sdc1*$^{-/-}$ mice cleared *S. aureus* infection more effectively with *S. aureus*-induced syndecan-1 shedding from the corneal epithelium (Hayashida *et al.*, 2011). However, we did observe that in a 4 hour *S. aureus* IP infection model, syndecan-1 expression in the subendothelial region of peritoneal venules was significantly diminished. Other studies also found protective effects of syndecan-1 deficiency in different infections with reduced tissue pathology. Syndecan-1 deficiency protected mice in *P. aeruginosa* lung infection (Park *et al.*, 2001) and this pathogen was found to promote syndecan-1 shedding. *Sdc1*$^{-/-}$ mice also had decreased mortality, less systemic bacterial dissemination and decreased cytokine production compared with wild-type animals in a burn-wound model with *P. aeruginosa* infection

(Haynes *et al.*, 2005). These studies used injury models that are acute in nature, whereas our study involved 6 week exposure to a peritoneal catheter and 4 week exposure to dialysis solution. This suggests that the ability of pathogens such as *S. aureus* to manipulate syndecan-1 shedding to enhance pathogenesis may be decreased in subacute injury models. Since it was reported that *Sdc1*$^{-/-}$ animals have increased neutrophil killing capacity of *S. aureus* cells (Hayashida *et al.*, 2011), the lack of this effect in our model may be due to neutrophil impairment since peritoneal leukocytes from wild-type dialyzed animals have decreased capacity to kill *S. aureus* (Hekking *et al.*, 2001b).

The negative effects of dialysis on inflammatory responses in the peritoneum were also observed *in vivo* by IVM to examine acute microvascular responses to PD fluid exposure and to determine how this exposure may alter responses to pro-inflammatory stimuli. The predominant focus of these IVM studies was on the microvascular beds of the mesentery (Frajewicki *et al.*, 2009; Mortier *et al.*, 2003; Schilte *et al.*, 2010; Zareie *et al.*, 2002), with the intestinal (Campbell *et al.*, 2006) and liver microcirculations being the exceptions (Patrick & Fox-Robichaud, 2010). The microcirculation of the parietal peritoneum was chosen for examination in our study because of the major contributions of this membrane to mass transport in dialysis and the observation that the abdominal wall exhibits the greatest morphological changes in human biopsies (Williams *et al.*, 2002). In particular, we were interested in this surface because the catheter implant runs directly through this tissue.

In the parietal peritoneum microcirculation, we observed that the number of rolling and extravascular leukocytes was significantly increased in the catheterized

animals but did not significantly differ between catheter controls and solution-treated catheterized animals, indicating that 6 week exposure to dialysis solution does not alter leukocyte-endothelial cell interactions in an additive fashion to the effects of the peritoneal catheter. In contrast to our observations, two studies found that the venules of the visceral peritoneum microcirculation showed significantly increased numbers of rolling leukocytes after 5 week exposure to conventional PD fluids compared with buffered control solution where both fluids were administered through a tunneled catheter (Schilte *et al.*, 2010; Zareie *et al.*, 2002). In both studies, the catheter control groups did not have altered baseline rolling compared with the naïve animals (Schilte *et al.*, 2010). Together, these findings highlight an important difference in the inflammatory responses of the visceral and parietal peritoneum microvascular beds to the PD fluids versus the catheter implant.

Increased rolling in the catheterized animals indicates that there was a basal level of inflammation that was absent in the naïve controls. However, this can also mean that there was increased sensitivity to inflammatory stimuli, such as surgical preparation. Nevertheless, our study suggests that the presence of the catheter resulted in increased systemic leukocyte counts and increased endothelial activation that promoted increased leukocyte rolling in the parietal peritoneum microcirculation.

The total blood leukocyte counts were elevated in the catheterized groups but a significant increase was only observed in the catheter control group compared with naïve mice. Interestingly, this group also had a significant increase in systemic monocytes. Monocyte recruitment to implants as a host response to foreign bodies is

well described, where monocytes are recruited and macrophages adhere and fuse to form foreign body giant cells (Anderson *et al.*, 1999). No significant differences in the number of systemic neutrophils were observed between any of the groups. Although the surgical preparation and IVM imaging are expected to contribute to the inflammation, the systemic leukocyte counts and differential white blood cell counts were not significantly different in the naïve mice used for IVM compared with baseline controls that were not subjected to intravital imaging. This indicates that the effects of the procedure were minimal in our study.

In rat models of PD, the catheter implant appears to make a large contribution to the damage of the parietal peritoneum. Changes in peritoneal structure, histology and function were more profound when PD fluids were instilled through a catheter implant as opposed to intraperitoneal injections with a needle over the course of an 8 week study (Flessner *et al.*, 2007). Animals with intraperitoneal catheters that were not exposed to dialysis solutions exhibited more histologic changes in the peritoneum than catheterized mice that were dialyzed over 20 weeks, while animals that did not have a catheter implanted but received daily intraperitoneal injections of dialysis solution exhibited comparatively less alterations in the peritoneum (Flessner *et al.*, 2010a). It was suggested that the PD catheter as a foreign body is an important factor in the peritoneal responses during PD and further investigation into the interaction of local peritoneal immune defense mechanisms and the catheter are required. It was also shown that catheter-induced inflammatory changes of the abdominal wall are more profound with subacute exposure to the catheter implants and gradually decline with chronic exposure

(Flessner *et al.*, 2010b). In this study, we observed significantly increased levels of fibrosis, manifested by increased submesothelial thickening, and increased vascular density after 8 week exposure to the peritoneal catheter which was examined with H&E staining. This supports our IVM observations where the submesothelial connective tissue appeared to have less organized collagen bundles in the catheterized animals compared with naïve mice. These pathological changes were similar between catheterized animals with and without dialysis fluid, indicating that the catheter was mainly responsible for these changes. Furthermore, we observed a significant increase in the number of extravascular leukocytes in the parietal abdominal wall in both groups of catheterized mice compared with naïve animals. However, again, there was no difference with the addition of PD solution, indicating that the leukocyte extravasation was a response to the catheter rather than the solution. This is in contrast to what was observed in a 5 week dialysis mouse model with a conventional lactated PD solution with 4.25% glucose delivered through a catheter implant (Gonzalez-Mateo *et al.*, 2009). The presence of the catheter did not significantly affect the function of the peritoneal layer and induced only localized inflammation and fibrosis (Gonzalez-Mateo *et al.*, 2009).

PD promotes new vessel formation (Zareie *et al.*, 2002) and it is easier for neutrophils to transmigrate because there is less resistance in the maturing vessel wall with underdeveloped basal lamina that are less abundant in pericytes. Examination of the leukocyte-endothelial cell interactions with *in vivo* models of PD is important as shown by a double layer transwell model of the peritoneal membrane with an

endothelial and a mesothelial layer (Welten *et al.*, 2004). This model showed that the endothelial cells are the rate determinants of neutrophil transmigration across this double layer while the mesothelial barrier did not have an additive effect (Welten *et al.*, 2004). Thus, the ability of neutrophils to interact with and transmigrate across the endothelium impacts neutrophil accumulation in the tissue and peritoneal cavity, which is important in bacterial peritonitis, where clearance of bacteria is correlated with neutrophil influx in the peritoneal cavity (Welten *et al.*, 2004). We observed an approximately 5-fold increase in IP leukocytes in the dialyzed mice compared with baseline values, although the increase was not significant as determined by a Student's *t* test. This correlates with observations in PD patients, where leukocytosis is detected in spent dialysate of patients in the absence of infection in the first two weeks of catheter implantation (Fijen *et al.*, 1988).

The animal model in our study does not precisely simulate PD and so its clinical relevance has limitations. PD patients experience some degree of kidney failure and develop uremia while the mice in our study were nonuremic in an effort to avoid complications of surgery with nephrectomy and development of uremia. However, uremic animal models indicate that with uremia there are differences in peritoneal permeability to water and solutes (Pawlaczyk *et al.*, 1999) and uremia impacts inflammatory responses (Zager *et al.*, 2009). Furthermore, our model involved injections of solutions through silicone catheters which were not drained as is done in CAPD after 4-6 hour dwell periods. Also, in the animal model, one injection was made per day, unlike the 4-6 fluid exchanges performed in CAPD per day and therefore

cytokines and growth factors in our model were not removed from the abdominal cavity by the effluent. As well, the catheter and injection port used in this study were completely covered by skin, unlike the percutaneous catheters of PD patients. Lastly, the catheter to peritoneal cavity ratio was greater in our mouse model compared to PD patients, which can promote more local inflammatory responses in the peritoneum. Nevertheless, our model utilized a conventional dialysis solution and silicone catheter commonly used in PD patients and responses were assessed by cutting-edge *in vivo* imaging. Thus, these results still offer valuable insight into the inflammatory microvascular responses to the peritoneal catheter and stress the importance of distinction between the effects of the catheter and PD fluid with *in vivo* animal models. In addition, our report on the response to a foreign body in the parietal peritoneum microcirculation is a novel addition to IVM models of chronic inflammation.

Conclusion and future directions

This study has established a mouse model to directly observe leukocyte recruitment in the parietal peritoneum microcirculation and characterize molecular expression in this tissue. With this novel model, the expression of syndecan-1 in the peritoneal microcirculation during peritonitis was defined. These results present clear evidence that syndecan-1 is highly expressed in the subendothelial region of peritoneal venules, challenging the predominant belief that syndecan-1 is found in the glycocalyx lining the luminal surface of blood vessels (although low level syndecan-1 expression on the luminal surface cannot be excluded) (Johansson *et al.*, 2011). This study also

highlighted that chemokines are mainly expressed in the subendothelial region of venules, likely contributing to leukocyte transendothelial migration. These findings also indicate that syndecan-1 is not a significant contributor to leukocyte recruitment and is redundant in chemokine presentation in this tissue. Syndecan-1 is, however, important for limiting *S. aureus* invasion of the parietal peritoneum and the underlying tissues as syndecan-1 deficiency increased susceptibility of mice to *S. aureus* infection in subacute PD. This suggests that effects of syndecan-1 on *S. aureus* infection differ with a longer injury model in the peritoneum. In acute infection, *S. aureus* promoted syndecan-1 shedding from the peritoneal microcirculation but this does not alter leukocyte-endothelial cell interactions *in vivo*. This highlights the distinctiveness of the parietal peritoneum microvascular responses compared with other microvascular beds. Together, these results indicate that syndecan-1 is not a significant modulator of inflammatory responses in the parietal peritoneum microcirculation but is important for providing a barrier to infection in subacute injury models.

Furthermore, we described the *in vivo* effects of the peritoneal catheter on the parietal peritoneum. We showed that the number of rolling leukocytes in the parietal peritoneum venules is enhanced in the presence of the peritoneal catheter implant and this is associated with an increase in the number of perivenular leukocytes. This study confirms the *ex vivo* observations of the effects of the peritoneal catheters on the parietal peritoneum in animal models which may limit their clinical translation (Flessner *et al.*, 2007; Flessner *et al.*, 2010a; Flessner *et al.*, 2010b; Peters *et al.*, 2011).

Since our study showed that *Sdc1*$^{-/-}$ mice are more susceptible to *S. aureus* infection after subacute exposure to PD yet they do not have altered leukocyte recruitment in *S. aureus* infection, future directions for this research should be focused on delineating potential aberrations in microbicidal function of phagocytic cells from *Sdc1*$^{-/-}$ mice that are resident and recruited in the peritoneal tissues. The reports that exposure to PD interfered with the peritoneal immune cells (Betjes *et al.*, 1993) and that *S. aureus*-induced syndecan-1 shedding diminished neutrophil microbicidal capacity (Hayashida *et al.*, 2011) warrant further investigation of the functional status of the immune cells in our PD model. An *in vitro* assay can be used to assess *S. aureus* killing capacity and cytokine secretion by neutrophils and macrophages isolated from tissues of wild-type and *Sdc1*$^{-/-}$ animals exposed to subacute PD. Measurement of systemic and tissue specific cytokines in these animals would also reveal whether there is dysregulated inflammation in the absence of syndecan-1, as shown in Gram-positive toxic shock (Hayashida *et al.*, 2008).

Future studies should also focus on describing the host's ability to clear *S. aureus* infection with syndecan-1 deficiency by using a longer time point for the infection and monitoring survival over 24 hours, 48 hours and at least 1 week. This may explain the differences observed in this study where syndecan-1 deficiency made mice more susceptible to *S. aureus* infection while current literature indicates that syndecan-1 deficiency protects mice from *S. aureus* infection (Hayashida *et al.*, 2011). Perhaps, even though with syndecan-1 deficiency there is increased infection of the abdominal wall tissue by *S. aureus*, these mice may still be able to eventually clear the infection as

effectively as the wild-type animals. This research may have clinical implications since it is possible that the increased occurrence of peritonitis and infections in PD may be related to syndecan-1 polymorphisms in patients.

Several acute experiments could further characterize inflammatory responses in the parietal peritoneum microcirculation. For example, the redundancy in chemokine presentation by different heparan sulfate proteoglycans can be examined with a focus on removal of heparan sulfate stores from the subendothelial compartment and the resulting effects on chemokine expression. Also, the chemokine expression pattern could be further characterized in syndecan-1 deficient mice with siRNA silencing of syndecan-2 in endothelial cells *in vivo*. Lastly, the use of ICAM-1, ICAM-2, α_4 and β_2 knock-out animals to decipher the molecular mechanisms of leukocyte recruitment may reveal the adhesion molecules that promote enhanced leukocyte recruitment in catheterized mice in subacute PD and provide molecular targets to ameliorate chronic inflammation in PD.

Finally, the finding that the peritoneal catheter had significant effects on leukocyte recruitment, angiogenesis and fibrosis in the parietal peritoneum in this thesis could be explored in PD patients with a multicentre observational study. In this study, the control patients could be individuals undergoing laparoscopic abdominal surgery. The peritoneal catheter controls could be patients with ventriculoperitoneal shunts. Trans-abdominal ultrasonography can be used to assess peritoneal thickness and vasculature. The rates of peritonitis can be recorded and peritoneal tissues can be consensually

collected during abdominal surgeries and post-mortem. This study could delineate the pathologic effects of the catheter versus the PD fluid in humans.

REFERENCES

Abbal, C., Lambelet, M., Bertaggia, D., Gerbex, C., Martinez, M., Arcaro, A., Schapira, M., & Spertini, O. (2006). Lipid raft adhesion receptors and Syk regulate selectin-dependent rolling under flow conditions. *Blood, 108*(10), 3352-3359. doi: 10.1182/blood-2006-04-013912

Acloque, H., Adams, M.S., Fishwick, K., Bronner-Fraser, M., & Nieto, M.A. (2009). Epithelial-mesenchymal transitions: the importance of changing cell state in development and disease. *J Clin Invest, 119*(6), 1438-1449. doi: 10.1172/JCI38019

Albelda, S.M., Muller, W.A., Buck, C.A., & Newman, P.J. (1991). Molecular and cellular properties of PECAM-1 (endoCAM/CD31): a novel vascular cell-cell adhesion molecule. *J.Cell Biol., 114*(5), 1059-1068.

Alexander, C.M., Reichsman, F., Hinkes, M.T., Lincecum, J., Becker, K.A., Cumberledge, S., & Bernfield, M. (2000). Syndecan-1 is required for Wnt-1-induced mammary tumorigenesis in mice. *Nat Genet, 25*(3), 329-332. doi: 10.1038/77108

Alexopoulou, A.N., Multhaupt, H.A., & Couchman, J.R. (2007). Syndecans in wound healing, inflammation and vascular biology. *Int J Biochem Cell Biol, 39*(3), 505-528. doi: 10.1016/j.biocel.2006.10.014

Allen, B.L., Filla, M.S., & Rapraeger, A.C. (2001). Role of heparan sulfate as a tissue-specific regulator of FGF-4 and FGF receptor recognition. *J Cell Biol, 155*(5), 845-858. doi: 10.1083/jcb.200106075

Anderson, J.M., Defife, K., McNally, A., Collier, T., & Jenney, C. (1999). Monocyte, macrophage and foreign body giant cell interactions with molecularly engineered surfaces. *J Mater Sci Mater Med, 10*(10/11), 579-588.

Andonegui, G., Bonder, C.S., Green, F., Mullaly, S.C., Zbytnuik, L., Raharjo, E., & Kubes, P. (2003). Endothelium-derived Toll-like receptor-4 is the key molecule in LPS-induced neutrophil sequestration into lungs. *J.Clin.Invest, 111*(7), 1011-1020. doi: 10.1172/JCI16510 [doi]

Andreoli, S.P., Mallett, C., Williams, K., McAteer, J.A., Rothlein, R., & Doerschuk, C.M. (1994). Mechanisms of polymorphonuclear leukocyte mediated peritoneal mesothelial cell injury. *Kidney Int, 46*(4), 1100-1109.

Aref, S., Goda, T., & El-Sherbiny, M. (2003). Syndecan-1 in multiple myeloma: relationship to conventional prognostic factors. *Hematology, 8*(4), 221-228. doi: 10.1080/1024533031000153630

Arndt, H., Kubes, P., & Granger, D.N. (1991). Involvement of neutrophils in ischemia-reperfusion injury in the small intestine. *Klin Wochenschr, 69*(21-23), 1056-1060.

Asuthkar, S., Velpula, K.K., Nalla, A.K., Gogineni, V.R., Gondi, C.S., & Rao, J.S. (2014). Irradiation-induced angiogenesis is associated with an MMP-9-miR-494-syndecan-1 regulatory loop in medulloblastoma cells. *Oncogene, 33*(15), 1922-1933. doi: 10.1038/onc.2013.151

Augustine, T., Brown, P.W., Davies, S.D., Summers, A.M., & Wilkie, M.E. (2009). Encapsulating peritoneal sclerosis: clinical significance and implications.

Nephron Clin Pract, 111(2), c149-154; discussion c154. doi: 10.1159/000191214

Baez, S. (1973). An open cremaster muscle preparation for the study of blood vessels by *in vivo* microscopy. *Microvasc Res, 5*(3), 384-394.

Bajory, Z., Hutter, J., Krombach, F., & Messmer, K. (2002). New method: the intravital videomicroscopic characteristics of the microcirculation of the urinary bladder in rats. *Urol.Res., 30*(3), 148-152. doi: 10.1007/s00240-002-0251-8 [doi]

Baldwin, E.T., Weber, I.T., St Charles, R., Xuan, J.C., Appella, E., Yamada, M., Matsushima, K., Edwards, B.F., Clore, G.M., Gronenborn, A.M., & et al. (1991). Crystal structure of interleukin 8: symbiosis of NMR and crystallography. *Proc Natl Acad Sci U S A, 88*(2), 502-506.

Barone, R.J., Campora, M.I., Gimenez, N.S., Ramirez, L., Santopietro, M., Grbavac, D., Pattin, M., & Panese, S.A. (2009). Peritoneum: a noble membrane in long-term dialysis treatment. *Adv.Perit.Dial., 25*, 80-84.

Beauvais, D.M., Ell, B.J., McWhorter, A.R., & Rapraeger, A.C. (2009). Syndecan-1 regulates alphavbeta3 and alphavbeta5 integrin activation during angiogenesis and is blocked by synstatin, a novel peptide inhibitor. *J.Exp.Med., 206*(3), 691-705. doi: jem.20081278 [pii];10.1084/jem.20081278 [doi]

Bernfield, M., Gotte, M., Park, P.W., Reizes, O., Fitzgerald, M.L., Lincecum, J., & Zako, M. (1999). Functions of cell surface heparan sulfate proteoglycans. *Annu.Rev.Biochem., 68*, 729-777. doi: 10.1146/annurev.biochem.68.1.729 [doi]

Betjes, M.G., Tuk, C.W., Struijk, D.G., Krediet, R.T., Arisz, L., Hoefsmit, E.C., & Beelen, R.H. (1993). Immuno-effector characteristics of peritoneal cells during CAPD treatment: a longitudinal study. *Kidney Int*, *43*(3), 641-648.

Betjes, M.G., Tuk, C.W., Visser, C.E., Zemel, D., Krediet, R.T., Arisz, L., & Beelen, R.H. (1994). Analysis of the peritoneal cellular immune system during CAPD shortly before a clinical peritonitis. *Nephrol Dial Transplant*, *9*(6), 684-692.

Betjes, M.G., Visser, C.E., Zemel, D., Tuk, C.W., Struijk, D.G., Krediet, R.T., Arisz, L., & Beelen, R.H. (1996). Intraperitoneal interleukin-8 and neutrophil influx in the initial phase of a CAPD peritonitis. *Perit Dial Int*, *16*(4), 385-392.

Brauner, A., Hylander, B., & Wretlind, B. (1993). Interleukin-6 and interleukin-8 in dialysate and serum from patients on continuous ambulatory peritoneal dialysis. *Am J Kidney Dis*, *22*(3), 430-435.

Brule, S., Charnaux, N., Sutton, A., Ledoux, D., Chaigneau, T., Saffar, L., & Gattegno, L. (2006). The shedding of syndecan-4 and syndecan-1 from HeLa cells and human primary macrophages is accelerated by SDF-1/CXCL12 and mediated by the matrix metalloproteinase-9. *Glycobiology*, *16*(6), 488-501. doi: 10.1093/glycob/cwj098

Bryers, J.D. (2008). Medical biofilms. *Biotechnol.Bioeng.*, *100*(1), 1-18. doi: 10.1002/bit.21838 [doi]

Burns, A.R., Bowden, R.A., Abe, Y., Walker, D.C., Simon, S.I., Entman, M.L., & Smith, C.W. (1999). P-selectin mediates neutrophil adhesion to endothelial cell borders. *J Leukoc Biol*, *65*(3), 299-306.

Cabrales, P., & Carvalho, L.J. (2010). Intravital microscopy of the mouse brain microcirculation using a closed cranial window. *J Vis Exp*(45). doi: 10.3791/2184

Campbell, J.E., Garrison, R.N., & Zakaria el, R. (2006). Clinical peritoneal dialysis solutions modulate white blood cell-intestinal vascular endothelium interaction. *Am J Surg, 192*(5), 610-616. doi: 10.1016/j.amjsurg.2006.08.016

Cannistra, S.A., Ottensmeier, C., Tidy, J., & DeFranzo, B. (1994). Vascular cell adhesion molecule-1 expressed by peritoneal mesothelium partly mediates the binding of activated human T lymphocytes. *Exp Hematol, 22*(10), 996-1002.

Carulli, S., Beck, K., Dayan, G., Boulesteix, S., Lortat-Jacob, H., & Rousselle, P. (2012). Cell surface proteoglycans syndecan-1 and -4 bind overlapping but distinct sites in laminin alpha3 LG45 protein domain. *J.Biol.Chem., 287*(15), 12204-12216. doi: M111.300061 [pii];10.1074/jbc.M111.300061 [doi]

Chakravarti, R., & Adams, J.C. (2006). Comparative genomics of the syndecans defines an ancestral genomic context associated with matrilins in vertebrates. *BMC Genomics, 7*, 83. doi: 10.1186/1471-2164-7-83

Chakravarti, R., Sapountzi, V., & Adams, J.C. (2005). Functional role of syndecan-1 cytoplasmic V region in lamellipodial spreading, actin bundling, and cell migration. *Mol Biol Cell, 16*(8), 3678-3691. doi: 10.1091/mbc.E04-10-0907

Chakravarty, L., Rogers, L., Quach, T., Breckenridge, S., & Kolattukudy, P.E. (1998). Lysine 58 and histidine 66 at the C-terminal alpha-helix of monocyte

chemoattractant protein-1 are essential for glycosaminoglycan binding. *J Biol Chem, 273*(45), 29641-29647.

Champigny, M.J., Mitchell, M., Fox-Robichaud, A., Trigatti, B.L., & Igdoura, S.A. (2009). A point mutation in the neu1 promoter recruits an ectopic repressor, Nkx3.2 and results in a mouse model of sialidase deficiency. *Mol Genet Metab, 97*(1), 43-52. doi: 10.1016/j.ymgme.2009.01.004

Chaterji, S., Lam, C.H., Ho, D.S., Proske, D.C., & Baker, A.B. (2014). Syndecan-1 regulates vascular smooth muscle cell phenotype. *PLoS One, 9*(2), e89824. doi: 10.1371/journal.pone.0089824

Chaudhary, K., & Khanna, R. (2010). Biocompatible peritoneal dialysis solutions: do we have one? *Clin.J.Am.Soc.Nephrol., 5*(4), 723-732. doi: CJN.05720809 [pii];10.2215/CJN.05720809 [doi]

Chen, Y., Hayashida, A., Bennett, A.E., Hollingshead, S.K., & Park, P.W. (2007). *Streptococcus pneumoniae* sheds syndecan-1 ectodomains through ZmpC, a metalloproteinase virulence factor. *J Biol Chem, 282*(1), 159-167. doi: 10.1074/jbc.M608542200

Chiorean, R., Berindan-Neagoe, I., Braicu, C., Florian, I.S., Leucuta, D., Crisan, D., & Cernea, V. (2014). Quantitative expression of serum biomarkers involved in angiogenesis and inflammation, in patients with glioblastoma multiforme: Correlations with clinical data. *Cancer Biomark, 14*(2), 185-194. doi: 10.3233/CBM-130310

Cizmeci-Smith, G., & Carey, D.J. (1997). Thrombin stimulates syndecan-1 promotor activity and expression of a form of syndecan-1 that binds antithrombin III in vascular smooth muscle cells. *Arterioscler.Thromb.Vasc.Biol., 17*(11), 2609-2616.

Clore, G.M., Appella, E., Yamada, M., Matsushima, K., & Gronenborn, A.M. (1990). Three-dimensional structure of interleukin 8 in solution. *Biochemistry, 29*(7), 1689-1696.

Clore, G.M., & Gronenborn, A.M. (1991). Comparison of the solution nuclear magnetic resonance and X-ray crystal structures of human recombinant interleukin-1 beta. *J Mol Biol, 221*(1), 47-53.

Cohen, T., Gitay-Goren, H., Sharon, R., Shibuya, M., Halaban, R., Levi, B.Z., & Neufeld, G. (1995). VEGF121, a vascular endothelial growth factor (VEGF) isoform lacking heparin binding ability, requires cell-surface heparan sulfates for efficient binding to the VEGF receptors of human melanoma cells. *J Biol Chem, 270*(19), 11322-11326.

Cohnheim, J. (1889). Lectures on general pathology: a handbook for practitioners and students. *The New Sydenham Society, London*.

Collins, R.G., Jung, U., Ramirez, M., Bullard, D.C., Hicks, M.J., Smith, C.W., Ley, K., & Beaudet, A.L. (2001). Dermal and pulmonary inflammatory disease in E-selectin and P-selectin double-null mice is reduced in triple-selectin-null mice. *Blood, 98*(3), 727-735.

Cross, A.S., Sakarya, S., Rifat, S., Held, T.K., Drysdale, B.E., Grange, P.A., Cassels, F.J., Wang, L.X., Stamatos, N., Farese, A., Casey, D., Powell, J., Bhattacharjee, A.K., Kleinberg, M., & Goldblum, S.E. (2003). Recruitment of murine neutrophils *in vivo* through endogenous sialidase activity. *J Biol Chem, 278*(6), 4112-4120. doi: 10.1074/jbc.M207591200

Dasgupta, M.K. (2002). Biofilms and infection in dialysis patients. *Semin.Dial., 15*(5), 338-346. doi: 0084 [pii]

Dasgupta, M.K. (1997). Silver-coated catheters in peritoneal dialysis. *Perit.Dial.Int., 17 Suppl 2,* S142-S145.

Dasgupta, M.K. (1994). Silver peritoneal catheters reduce bacterial colonization. *Adv.Perit.Dial., 10*, 195-198.

Dasgupta, M.K., Fox, S., Gagnon, D., Bettcher, K., & Ulan, R.A. (1992). Significant reduction of peritonitis rate by the use of Twin-bag system in a Canadian regional CAPD program. *Adv.Perit.Dial., 8*, 223-226.

Dasgupta, M.K., Kowalewaska-Grochowska, K., & Costerton, J.W. (1993). Biofilm and peritonitis in peritoneal dialysis. *Perit.Dial.Int., 13 Suppl 2,* S322-S325.

Dasgupta, M.K., Kowalewska-Grochowska, K., Larabie, M., & Costerton, J.W. (1991). Catheter biofilms and recurrent CAPD peritonitis. *Adv.Perit.Dial., 7*, 165-168.

Dasgupta, M.K., Ward, K., Noble, P.A., Larabie, M., & Costerton, J.W. (1994). Development of bacterial biofilms on silastic catheter materials in peritoneal dialysis fluid. *Am.J.Kidney Dis., 23*(5), 709-716. doi: S0272638694000934 [pii]

Davies, S.J., Bryan, J., Phillips, L., & Russell, G.I. (1996). Longitudinal changes in peritoneal kinetics: the effects of peritoneal dialysis and peritonitis. *Nephrol Dial Transplant, 11*(3), 498-506.

Davies, S.J., Phillips, L., Griffiths, A.M., Russell, L.H., Naish, P.F., & Russell, G.I. (1998). What really happens to people on long-term peritoneal dialysis? *Kidney Int, 54*(6), 2207-2217. doi: 10.1046/j.1523-1755.1998.00180.x

Dawson, T.C., Lentsch, A.B., Wang, Z., Cowhig, J.E., Rot, A., Maeda, N., & Peiper, S.C. (2000). Exaggerated response to endotoxin in mice lacking the Duffy antigen/receptor for chemokines (DARC). *Blood, 96*(5), 1681-1684.

Day, R.M., Mitchell, T.J., Knight, S.C., & Forbes, A. (2003). Regulation of epithelial syndecan-1 expression by inflammatory cytokines. *Cytokine, 21*(5), 224-233. doi: S1043466603000917 [pii]

Del Maschio, A., Zanetti, A., Corada, M., Rival, Y., Ruco, L., Lampugnani, M.G., & Dejana, E. (1996). Polymorphonuclear leukocyte adhesion triggers the disorganization of endothelial cell-to-cell adherens junctions. *J Cell Biol, 135*(2), 497-510.

Diamond, M.S., Alon, R., Parkos, C.A., Quinn, M.T., & Springer, T.A. (1995). Heparin is an adhesive ligand for the leukocyte integrin Mac-1 (CD11b/CD1). *J.Cell Biol., 130*(6), 1473-1482.

Dobra, K., Andang, M., Syrokou, A., Karamanos, N.K., & Hjerpe, A. (2000). Differentiation of mesothelioma cells is influenced by the expression of proteoglycans. *Exp Cell Res, 258*(1), 12-22. doi: 10.1006/excr.2000.4915

Donlan, R.M. (2001). Biofilms and device-associated infections. *Emerg.Infect.Dis., 7*(2), 277-281.

Donovan, K.L., Pacholok, S., Humes, J.L., Coles, G.A., & Williams, J.D. (1993). Intra-peritoneal free elastase in CAPD peritonitis. *Kidney Int, 44*(1), 87-90.

Elenius, K., Vainio, S., Laato, M., Salmivirta, M., Thesleff, I., & Jalkanen, M. (1991). Induced expression of syndecan in healing wounds. *J Cell Biol, 114*(3), 585-595.

Elenius, V., Gotte, M., Reizes, O., Elenius, K., & Bernfield, M. (2004). Inhibition by the soluble syndecan-1 ectodomains delays wound repair in mice overexpressing syndecan-1. *J Biol Chem, 279*(40), 41928-41935. doi: 10.1074/jbc.M404506200

Endo, K., Takino, T., Miyamori, H., Kinsen, H., Yoshizaki, T., Furukawa, M., & Sato, H. (2003). Cleavage of syndecan-1 by membrane type matrix metalloproteinase-1 stimulates cell migration. *J Biol Chem, 278*(42), 40764-40770. doi: 10.1074/jbc.M306736200

Esko, J.D., & Selleck, S.B. (2002). Order out of chaos: assembly of ligand binding sites in heparan sulfate. *Annu Rev Biochem, 71*, 435-471. doi: 10.1146/annurev.biochem.71.110601.135458

Feng, D., Nagy, J.A., Pyne, K., Dvorak, H.F., & Dvorak, A.M. (1998). Neutrophils emigrate from venules by a transendothelial cell pathway in response to FMLP. *J Exp Med, 187*(6), 903-915.

Fenton, S.S., Schaubel, D.E., Desmeules, M., Morrison, H.I., Mao, Y., Copleston, P., Jeffery, J.R., & Kjellstrand, C.M. (1997). Hemodialysis versus peritoneal

dialysis: a comparison of adjusted mortality rates. *Am J Kidney Dis, 30*(3), 334-342.

Feyzi, E., Lustig, F., Fager, G., Spillmann, D., Lindahl, U., & Salmivirta, M. (1997). Characterization of heparin and heparan sulfate domains binding to the long splice variant of platelet-derived growth factor A chain. *J Biol Chem, 272*(9), 5518-5524.

Fijen, J.W., Struijk, D.G., Krediet, R.T., Boeschoten, E.W., de Vries, J.P., & Arisz, L. (1988). Dialysate leucocytosis in CAPD patients without clinical infection. *Neth J Med, 33*(5-6), 270-280.

Finelli, A., Burrows, L.L., DiCosmo, F.A., DiTizio, V., Sinnadurai, S., Oreopoulos, D.G., & Khoury, A.E. (2002). Colonization-resistant antimicrobial-coated peritoneal dialysis catheters: evaluation in a newly developed rat model of persistent *Pseudomonas aeruginosa* peritonitis. *Perit.Dial.Int., 22*(1), 27-31.

Flessner, M.F., Credit, K., Henderson, K., Vanpelt, H.M., Potter, R., He, Z., Henegar, J., & Robert, B. (2007). Peritoneal changes after exposure to sterile solutions by catheter. *J.Am.Soc.Nephrol., 18*(8), 2294-2302. doi: ASN.2006121417 [pii];10.1681/ASN.2006121417 [doi]

Flessner, M.F., Credit, K., Richardson, K., Potter, R., Li, X., He, Z., Hoskins, G., & Henegar, J. (2010a). Peritoneal inflammation after twenty-week exposure to dialysis solution: effect of solution versus catheter-foreign body reaction. *Perit.Dial.Int., 30*(3), 284-293. doi: pdi.2009.00100 [pii];10.3747/pdi.2009.00100 [doi]

Flessner, M.F., Li, X., Potter, R., & He, Z. (2010b). Foreign-body response to sterile catheters is variable over 20 weeks. *Adv Perit Dial, 26*, 101-104.

Fox-Robichaud, A., & Kubes, P. (2000). Molecular mechanisms of tumor necrosis factor alpha-stimulated leukocyte recruitment into the murine hepatic circulation. *Hepatology, 31*(5), 1123-1127. doi: S0270913900124735 [pii];10.1053/he.2000.6961 [doi]

Frajewicki, V., Brod, V., Kushnir, D., Kohan, R., & Bitterman, H. (2009). Acute effects of peritoneal dialysis solutions in the mesenteric microcirculation. *Transl Res, 153*(5), 249-256. doi: 10.1016/j.trsl.2009.01.006

Fresenius Medical Care. (2008). Fresenius Medical Care Annual Report 2008 Dialysis Market. Retrieved September 17, 2013, from http://reports.fmc-ag.com/reports/fmc/annual/2008/gb/English/401040/dialysis-market.html

Fukumoto, T., & Levin, M. (2005). Asymmetric expression of Syndecan-2 in early chick embryogenesis. *Gene Expr Patterns, 5*(4), 525-528. doi: 10.1016/j.modgep.2004.12.001

Garrood, T., Lee, L., & Pitzalis, C. (2006). Molecular mechanisms of cell recruitment to inflammatory sites: general and tissue-specific pathways. *Rheumatology.(Oxford), 45*(3), 250-260. doi: kei207 [pii];10.1093/rheumatology/kei207 [doi]

Gattei, V., Godeas, C., Degan, M., Rossi, F.M., Aldinucci, D., & Pinto, A. (1999). Characterization of anti-CD138 monoclonal antibodies as tools for investigating

the molecular polymorphism of syndecan-1 in human lymphoma cells. *Br J Haematol, 104*(1), 152-162.

Gitay-Goren, H., Soker, S., Vlodavsky, I., & Neufeld, G. (1992). The binding of vascular endothelial growth factor to its receptors is dependent on cell surface-associated heparin-like molecules. *J Biol Chem, 267*(9), 6093-6098.

Gokal, R. (2002). Peritoneal dialysis in the 21st century: an analysis of current problems and future developments. *J.Am.Soc.Nephrol., 13 Suppl 1*, S104-S116.

Gokal, R., & Mallick, N.P. (1999). Peritoneal dialysis. *Lancet, 353*(9155), 823-828.

Gonzalez-Mateo, G.T., Loureiro, J., Jimenez-Hefferman, J.A., Bajo, M.A., Selgas, R., Lopez-Cabrera, M., & Aroeira, L.S. (2009). Chronic exposure of mouse peritoneum to peritoneal dialysis fluid: structural and functional alterations of the peritoneal membrane. *Perit Dial Int, 29*(2), 227-230.

Gotsch, U., Borges, E., Bosse, R., Boggemeyer, E., Simon, M., Mossmann, H., & Vestweber, D. (1997). VE-cadherin antibody accelerates neutrophil recruitment *in vivo. J Cell Sci, 110 (Pt 5)*, 583-588.

Gotte, M. (2003). Syndecans in inflammation. *FASEB J., 17*(6), 575-591. doi: 10.1096/fj.02-0739rev [doi];17/6/575 [pii]

Gotte, M., Bernfield, M., & Joussen, A.M. (2005). Increased leukocyte-endothelial interactions in syndecan-1-deficient mice involve heparan sulfate-dependent and -independent steps. *Curr.Eye Res., 30*(6), 417-422. doi: JTL031JG2851L3M8 [pii];10.1080/02713680590956289 [doi]

Gotte, M., Joussen, A.M., Klein, C., Andre, P., Wagner, D.D., Hinkes, M.T., Kirchhof, B., Adamis, A.P., & Bernfield, M. (2002). Role of syndecan-1 in leukocyte-endothelial interactions in the ocular vasculature. *Invest Ophthalmol.Vis.Sci., 43*(4), 1135-1141.

Gotte, M., Kersting, C., Radke, I., Kiesel, L., & Wulfing, P. (2007). An expression signature of syndecan-1 (CD138), E-cadherin and c-met is associated with factors of angiogenesis and lymphangiogenesis in ductal breast carcinoma in situ. *Breast Cancer Res, 9*(1), R8. doi: 10.1186/bcr1641

Grootjans, J.J., Reekmans, G., Ceulemans, H., & David, G. (2000). Syntenin-syndecan binding requires syndecan-synteny and the co-operation of both PDZ domains of syntenin. *J Biol Chem, 275*(26), 19933-19941. doi: 10.1074/jbc.M002459200

Halden, Y., Rek, A., Atzenhofer, W., Szilak, L., Wabnig, A., & Kungl, A.J. (2004). Interleukin-8 binds to syndecan-2 on human endothelial cells. *Biochem J, 377*(Pt 2), 533-538. doi: 10.1042/BJ20030729

Haldenby, K.A., Chappell, D.C., Winlove, C.P., Parker, K.H., & Firth, J.A. (1994). Focal and regional variations in the composition of the glycocalyx of large vessel endothelium. *J Vasc Res, 31*(1), 2-9.

Hayashida, A., Amano, S., & Park, P.W. (2011). Syndecan-1 promotes *Staphylococcus aureus* corneal infection by counteracting neutrophil-mediated host defense. *J.Biol.Chem., 286*(5), 3288-3297. doi: M110.185165 [pii];10.1074/jbc.M110.185165 [doi]

Hayashida, A., Bartlett, A.H., Foster, T.J., & Park, P.W. (2009a). *Staphylococcus aureus* beta-toxin induces lung injury through syndecan-1. *Am J Pathol, 174*(2), 509-518. doi: 10.2353/ajpath.2009.080394

Hayashida, K., Chen, Y., Bartlett, A.H., & Park, P.W. (2008). Syndecan-1 is an *in vivo* suppressor of Gram-positive toxic shock. *J.Biol.Chem., 283*(29), 19895-19903. doi: M801614200 [pii];10.1074/jbc.M801614200 [doi]

Hayashida, K., Parks, W.C., & Park, P.W. (2009b). Syndecan-1 shedding facilitates the resolution of neutrophilic inflammation by removing sequestered CXC chemokines. *Blood, 114*(14), 3033-3043. doi: blood-2009-02-204966 [pii];10.1182/blood-2009-02-204966 [doi]

Haynes, A., III, Ruda, F., Oliver, J., Hamood, A.N., Griswold, J.A., Park, P.W., & Rumbaugh, K.P. (2005). Syndecan 1 shedding contributes to *Pseudomonas aeruginosa* sepsis. *Infect.Immun., 73*(12), 7914-7921. doi: 73/12/7914 [pii];10.1128/IAI.73.12.7914-7921.2005 [doi]

Haywood-Watson, R.J., Holcomb, J.B., Gonzalez, E.A., Peng, Z., Pati, S., Park, P.W., Wang, W., Zaske, A.M., Menge, T., & Kozar, R.A. (2011). Modulation of syndecan-1 shedding after hemorrhagic shock and resuscitation. *PLoS.One., 6*(8), e23530. doi: 10.1371/journal.pone.0023530 [doi];PONE-D-11-07811 [pii]

Hekking, L.H., Huijsmans, A., Van Gelderop, E., Wieslander, A.P., Havenith, C.E., van den Born, J., & Beelen, R.H. (2001a). Effect of PD fluid instillation on the peritonitis-induced influx and bacterial clearing capacity of peritoneal cells. *Nephrol Dial Transplant, 16*(3), 679-685.

Hekking, L.H., Zareie, M., Driesprong, B.A., Faict, D., Welten, A.G., de Greeuw, I., Schadee-Eestermans, I.L., Havenith, C.E., van den Born, J., ter Wee, P.M., & Beelen, R.H. (2001b). Better preservation of peritoneal morphologic features and defense in rats after long-term exposure to a bicarbonate/lactate-buffered solution. *J Am Soc Nephrol, 12*(12), 2775-2786.

Henry-Stanley, M.J., Hess, D.J., Erlandsen, S.L., & Wells, C.L. (2005). Ability of the heparan sulfate proteoglycan syndecan-1 to participate in bacterial translocation across the intestinal epithelial barrier. *Shock, 24*(6), 571-576. doi: 00024382-200512000-00013 [pii]

Hess, D.J., Henry-Stanley, M.J., Erlandsen, S.L., & Wells, C.L. (2006). Heparan sulfate proteoglycans mediate *Staphylococcus aureus* interactions with intestinal epithelium. *Med.Microbiol.Immunol., 195*(3), 133-141. doi: 10.1007/s00430-005-0007-5 [doi]

Huang, M.T., Larbi, K.Y., Scheiermann, C., Woodfin, A., Gerwin, N., Haskard, D.O., & Nourshargh, S. (2006). ICAM-2 mediates neutrophil transmigration *in vivo*: evidence for stimulus specificity and a role in PECAM-1-independent transmigration. *Blood, 107*(12), 4721-4727. doi: 10.1182/blood-2005-11-4683

Hurst, S.M., Wilkinson, T.S., McLoughlin, R.M., Jones, S., Horiuchi, S., Yamamoto, N., Rose-John, S., Fuller, G.M., Topley, N., & Jones, S.A. (2001). Il-6 and its soluble receptor orchestrate a temporal switch in the pattern of leukocyte recruitment seen during acute inflammation. *Immunity, 14*(6), 705-714.

Hwang, J.M., Yamanouchi, J., Santamaria, P., & Kubes, P. (2004). A critical temporal window for selectin-dependent CD4+ lymphocyte homing and initiation of late-phase inflammation in contact sensitivity. *J Exp Med, 199*(9), 1223-1234. doi: 10.1084/jem.20032016

Ihrcke, N.S., Wrenshall, L.E., Lindman, B.J., & Platt, J.L. (1993). Role of heparan sulfate in immune system-blood vessel interactions. *Immunol Today, 14*(10), 500-505. doi: 10.1016/0167-5699(93)90265-M

Iozzo, R.V., & San Antonio, J.D. (2001). Heparan sulfate proteoglycans: heavy hitters in the angiogenesis arena. *J Clin Invest, 108*(3), 349-355. doi: 10.1172/JCI13738

Iwakiri, Y., Shah, V., & Rockey, D.C. (2014). Vascular Pathobiology in Chronic Liver Disease and Cirrhosis - Current Status and Future Directions. *J Hepatol*. doi: 10.1016/j.jhep.2014.05.047

Jackson, R.L., Busch, S.J., & Cardin, A.D. (1991). Glycosaminoglycans: molecular properties, protein interactions, and role in physiological processes. *Physiol Rev, 71*(2), 481-539.

Johansson, P.I., Stensballe, J., Rasmussen, L.S., & Ostrowski, S.R. (2011). A high admission syndecan-1 level, a marker of endothelial glycocalyx degradation, is associated with inflammation, protein C depletion, fibrinolysis, and increased mortality in trauma patients. *Ann.Surg., 254*(2), 194-200. doi: 10.1097/SLA.0b013e318226113d [doi];00000658-201108000-00003 [pii]

Jung, U., Bullard, D.C., Tedder, T.F., & Ley, K. (1996). Velocity differences between L- and P-selectin-dependent neutrophil rolling in venules of mouse cremaster muscle *in vivo*. *Am.J.Physiol, 271*(6 Pt 2), H2740-H2747.

Jung, U., Norman, K.E., Scharffetter-Kochanek, K., Beaudet, A.L., & Ley, K. (1998). Transit time of leukocytes rolling through venules controls cytokine-induced inflammatory cell recruitment *in vivo*. *J Clin Invest, 102*(8), 1526-1533. doi: 10.1172/JCI119893

Kainulainen, V., Nelimarkka, L., Jarvelainen, H., Laato, M., Jalkanen, M., & Elenius, K. (1996). Suppression of syndecan-1 expression in endothelial cells by tumor necrosis factor-alpha. *J.Biol.Chem., 271*(31), 18759-18766.

Kainulainen, V., Wang, H., Schick, C., & Bernfield, M. (1998). Syndecans, heparan sulfate proteoglycans, maintain the proteolytic balance of acute wound fluids. *J Biol Chem, 273*(19), 11563-11569.

Kalluri, R. (2009). EMT: when epithelial cells decide to become mesenchymal-like cells. *J Clin Invest, 119*(6), 1417-1419. doi: 10.1172/JCI39675

Kalluri, R., & Weinberg, R.A. (2009). The basics of epithelial-mesenchymal transition. *J Clin Invest, 119*(6), 1420-1428. doi: 10.1172/JCI39104

Kamler, M., Lehr, H.A., Barker, J.H., Saetzler, R.K., Galla, T.J., & Messmer, K. (1993). Impact of ischemia on tissue oxygenation and wound healing: intravital microscopic studies on the hairless mouse ear model. *Eur Surg Res, 25*(1), 30-37.

Kansas, G.S. (1996). Selectins and their ligands: current concepts and controversies. *Blood, 88*(9), 3259-3287.

Kato, M., Saunders, S., Nguyen, H., & Bernfield, M. (1995). Loss of cell surface syndecan-1 causes epithelia to transform into anchorage-independent mesenchyme-like cells. *Mol.Biol.Cell, 6*(5), 559-576.

Kato, S., Yuzawa, Y., Tsuboi, N., Maruyama, S., Morita, Y., Matsuguchi, T., & Matsuo, S. (2004). Endotoxin-induced chemokine expression in murine peritoneal mesothelial cells: the role of toll-like receptor 4. *J.Am.Soc.Nephrol., 15*(5), 1289-1299.

Kavanagh, D., Prescott, G.J., & Mactier, R.A. (2004). Peritoneal dialysis-associated peritonitis in Scotland (1999-2002). *Nephrol.Dial.Transplant., 19*(10), 2584-2591. doi: 10.1093/ndt/gfh386 [doi];gfh386 [pii]

Kelly, M., Hwang, J.M., & Kubes, P. (2007). Modulating leukocyte recruitment in inflammation. *J.Allergy Clin.Immunol., 120*(1), 3-10. doi: S0091-6749(07)00986-4 [pii];10.1016/j.jaci.2007.05.017 [doi]

Kendrick, J., & Teitelbaum, I. (2010). Strategies for improving long-term survival in peritoneal dialysis patients. *Clin.J.Am.Soc.Nephrol., 5*(6), 1123-1131. doi: CJN.04300709 [pii];10.2215/CJN.04300709 [doi]

Kilarski, W.W., Guc, E., Teo, J.C., Oliver, S.R., Lund, A.W., & Swartz, M.A. (2013). Intravital immunofluorescence for visualizing the microcirculatory and immune microenvironments in the mouse ear dermis. *PLoS One, 8*(2), e57135. doi: 10.1371/journal.pone.0057135

Kim, C.W., Goldberger, O.A., Gallo, R.L., & Bernfield, M. (1994). Members of the syndecan family of heparan sulfate proteoglycans are expressed in distinct cell-, tissue-, and development-specific patterns. *Mol Biol Cell, 5*(7), 797-805.

Kliment, C.R., Englert, J.M., Gochuico, B.R., Yu, G., Kaminski, N., Rosas, I., & Oury, T.D. (2009). Oxidative stress alters syndecan-1 distribution in lungs with pulmonary fibrosis. *J Biol Chem, 284*(6), 3537-3545. doi: 10.1074/jbc.M807001200

Kolaczkowska, E., & Kubes, P. (2013). Neutrophil recruitment and function in health and inflammation. *Nat Rev Immunol, 13*(3), 159-175. doi: 10.1038/nri3399

Kolb, M., & Collard, H.R. (2014). Staging of idiopathic pulmonary fibrosis: past, present and future. *Eur Respir Rev, 23*(132), 220-224. doi: 10.1183/09059180.00002114

Kolesnyk, I., Dekker, F.W., Boeschoten, E.W., & Krediet, R.T. (2010). Time-dependent reasons for peritoneal dialysis technique failure and mortality. *Perit.Dial.Int., 30*(2), 170-177. doi: pdi.2008.00277 [pii];10.3747/pdi.2008.00277 [doi]

Kowalewska, P.M., Burrows, L.L., & Fox-Robichaud, A.E. (2011). Intravital Microscopy of the Murine Urinary Bladder Microcirculation. *Microcirculation., 18*(8), 6607-6614. doi: 10.1111/j.1549-8719.2011.00123.x [doi]

Kuebler, W.M., Borges, J., Sckell, A., Kuhnle, G.E., Bergh, K., Messmer, K., & Goetz, A.E. (2000). Role of L-selectin in leukocyte sequestration in lung capillaries in a rabbit model of endotoxemia. *Am J Respir Crit Care Med, 161*(1), 36-43.

Kunkel, E.J., & Ley, K. (1996). Distinct phenotype of E-selectin-deficient mice. E-selectin is required for slow leukocyte rolling *in vivo*. *Circ.Res., 79*(6), 1196-1204.

Kuschert, G.S., Coulin, F., Power, C.A., Proudfoot, A.E., Hubbard, R.E., Hoogewerf, A.J., & Wells, T.N. (1999). Glycosaminoglycans interact selectively with chemokines and modulate receptor binding and cellular responses. *Biochemistry, 38*(39), 12959-12968. doi: bi990711d [pii]

Kuschert, G.S., Hoogewerf, A.J., Proudfoot, A.E., Chung, C.W., Cooke, R.M., Hubbard, R.E., Wells, T.N., & Sanderson, P.N. (1998). Identification of a glycosaminoglycan binding surface on human interleukin-8. *Biochemistry, 37*(32), 11193-11201. doi: 10.1021/bi972867o

Lai, K.N., Lai, K.B., Szeto, C.C., Lam, C.W., & Leung, J.C. (1999). Growth factors in continuous ambulatory peritoneal dialysis effluent. Their relation with peritoneal transport of small solutes. *Am J Nephrol, 19*(3), 416-422. doi: 13488

Lai, K.N., Tang, S.C., & Leung, J.C. (2007). Mediators of inflammation and fibrosis. *Perit.Dial.Int., 27 Suppl 2,* S65-S71. doi: 27/Supplement_2/S65 [pii]

Lamorte, S., Ferrero, S., Aschero, S., Monitillo, L., Bussolati, B., Omede, P., Ladetto, M., & Camussi, G. (2012). Syndecan-1 promotes the angiogenic phenotype of multiple myeloma endothelial cells. *Leukemia, 26*(5), 1081-1090. doi: 10.1038/leu.2011.290

Laudanna, C., Kim, J.Y., Constantin, G., & Butcher, E. (2002). Rapid leukocyte integrin activation by chemokines. *Immunol.Rev., 186,* 37-46. doi: imr18604 [pii]

Leabu, M., Ghinea, N., Muresan, V., Colceag, J., Hasu, M., & Simionescu, N. (1987). Cell surface chemistry of arterial endothelium and blood monocytes in the normolipidemic rabbit. *J Submicrosc Cytol, 19*(2), 193-208.

Lee, W.Y., Moriarty, T.J., Wong, C.H., Zhou, H., Strieter, R.M., van, R.N., Chaconas, G., & Kubes, P. (2010). An intravascular immune response to *Borrelia burgdorferi* involves Kupffer cells and iNKT cells. *Nat.Immunol., 11*(4), 295-302. doi: ni.1855 [pii];10.1038/ni.1855 [doi]

Ley, K., & Gaehtgens, P. (1991). Endothelial, not hemodynamic, differences are responsible for preferential leukocyte rolling in rat mesenteric venules. *Circ Res, 69*(4), 1034-1041.

Li, F.K., Davenport, A., Robson, R.L., Loetscher, P., Rothlein, R., Williams, J.D., & Topley, N. (1998). Leukocyte migration across human peritoneal mesothelial cells is dependent on directed chemokine secretion and ICAM-1 expression. *Kidney Int, 54*(6), 2170-2183. doi: 10.1046/j.1523-1755.1998.00174.x

Li, Q., Park, P.W., Wilson, C.L., & Parks, W.C. (2002). Matrilysin shedding of syndecan-1 regulates chemokine mobilization and transepithelial efflux of neutrophils in acute lung injury. *Cell, 111*(5), 635-646. doi: S0092867402010796 [pii]

Liang, O.D., Ascencio, F., Fransson, L.A., & Wadstrom, T. (1992). Binding of heparan sulfate to *Staphylococcus aureus*. *Infect.Immun., 60*(3), 899-906.

Liberek, T., Topley, N., Jorres, A., Coles, G.A., Gahl, G.M., & Williams, J.D. (1993). Peritoneal dialysis fluid inhibition of phagocyte function: effects of osmolality and glucose concentration. *J Am Soc Nephrol, 3*(8), 1508-1515.

Liberek, T., Topley, N., Luttmann, W., & Williams, J.D. (1996). Adherence of neutrophils to human peritoneal mesothelial cells: role of intercellular adhesion molecule-1. *J Am Soc Nephrol, 7*(2), 208-217.

Lo, W.K., Brendolan, A., Prowant, B.F., Moore, H.L., Khanna, R., Twardowski, Z.J., & Nolph, K.D. (1994). Changes in the peritoneal equilibration test in selected chronic peritoneal dialysis patients. *J Am Soc Nephrol, 4*(7), 1466-1474.

Lortat-Jacob, H. (2009). The molecular basis and functional implications of chemokine interactions with heparan sulphate. *Curr Opin Struct Biol, 19*(5), 543-548. doi: 10.1016/j.sbi.2009.09.003

Luo, J., Kato, M., Wang, H., Bernfield, M., & Bischoff, J. (2001). Heparan sulfate and chondroitin sulfate proteoglycans inhibit E-selectin binding to endothelial cells. *J Cell Biochem, 80*(4), 522-531.

Luo, J., Luo, Z., Zhou, N., Hall, J.W., & Huang, Z. (1999). Attachment of C-terminus of SDF-1 enhances the biological activity of its N-terminal peptide. *Biochem Biophys Res Commun, 264*(1), 42-47. doi: 10.1006/bbrc.1999.1476

Mactier, R. (2009). Peritonitis is still the achilles' heel of peritoneal dialysis. *Perit.Dial.Int., 29*(3), 262-266. doi: 29/3/262 [pii]

Maday, S., Anderson, E., Chang, H.C., Shorter, J., Satoh, A., Sfakianos, J., Folsch, H., Anderson, J.M., Walther, Z., & Mellman, I. (2008). A PDZ-binding motif

controls basolateral targeting of syndecan-1 along the biosynthetic pathway in polarized epithelial cells. *Traffic., 9*(11), 1915-1924. doi: TRA805 [pii];10.1111/j.1600-0854.2008.00805.x [doi]

Maiorca, R., Cancarini, G.C., Zubani, R., Camerini, C., Manili, L., Brunori, G., & Movilli, E. (1996). CAPD viability: a long-term comparison with hemodialysis. *Perit Dial Int, 16*(3), 276-287.

Margetts, P. (2009). Heparin and the peritoneal membrane. *Perit Dial Int, 29*(1), 16-19.

Margetts, P.J., & Bonniaud, P. (2003). Basic mechanisms and clinical implications of peritoneal fibrosis. *Perit Dial Int, 23*(6), 530-541.

Margetts, P.J., Bonniaud, P., Liu, L., Hoff, C.M., Holmes, C.J., West-Mays, J.A., & Kelly, M.M. (2005). Transient overexpression of TGF-{beta}1 induces epithelial mesenchymal transition in the rodent peritoneum. *J Am Soc Nephrol, 16*(2), 425-436. doi: 10.1681/ASN.2004060436

Margetts, P.J., Gyorffy, S., Kolb, M., Yu, L., Hoff, C.M., Holmes, C.J., & Gauldie, J. (2002a). Antiangiogenic and antifibrotic gene therapy in a chronic infusion model of peritoneal dialysis in rats. *J Am Soc Nephrol, 13*(3), 721-728.

Margetts, P.J., Kolb, M., Galt, T., Hoff, C.M., Shockley, T.R., & Gauldie, J. (2001). Gene transfer of transforming growth factor-beta1 to the rat peritoneum: effects on membrane function. *J.Am.Soc.Nephrol., 12*(10), 2029-2039.

Margetts, P.J., Kolb, M., Yu, L., Hoff, C.M., Holmes, C.J., Anthony, D.C., & Gauldie, J. (2002b). Inflammatory cytokines, angiogenesis, and fibrosis in the rat peritoneum. *Am.J.Pathol., 160*(6), 2285-2294.

Mariano, F., Tetta, C., Montrucchio, G., Cavalli, P.L., & Camussi, G. (1992). Role of alpha 1-proteinase inhibitor in restraining peritoneal inflammation in CAPD patients. *Kidney Int, 42*(3), 735-742.

Marshall, L.J., Ramdin, L.S., Brooks, T., DPhil, P.C., & Shute, J.K. (2003). Plasminogen activator inhibitor-1 supports IL-8-mediated neutrophil transendothelial migration by inhibition of the constitutive shedding of endothelial IL-8/heparan sulfate/syndecan-1 complexes. *J.Immunol., 171*(4), 2057-2065.

Masola, V., Gambaro, G., Tibaldi, E., Brunati, A.M., Gastaldello, A., D'Angelo, A., Onisto, M., & Lupo, A. (2012). Heparanase and syndecan-1 interplay orchestrates fibroblast growth factor-2-induced epithelial-mesenchymal transition in renal tubular cells. *J.Biol.Chem., 287*(2), 1478-1488. doi: M111.279836 [pii];10.1074/jbc.M111.279836 [doi]

Masouleh, B.K., Ten Dam, G.B., Wild, M.K., Seelige, R., van, d., V, Rops, A.L., Echtermeyer, F.G., Vestweber, D., van Kuppevelt, T.H., Kiesel, L., & Gotte, M. (2009). Role of the heparan sulfate proteoglycan syndecan-1 (CD138) in delayed-type hypersensitivity. *J.Immunol., 182*(8), 4985-4993. doi: 182/8/4985 [pii];10.4049/jimmunol.0800574 [doi]

Massena, S., Christoffersson, G., Hjertstrom, E., Zcharia, E., Vlodavsky, I., Ausmees, N., Rolny, C., Li, J.P., & Phillipson, M. (2010). A chemotactic gradient sequestered on endothelial heparan sulfate induces directional intraluminal

crawling of neutrophils. *Blood, 116*(11), 1924-1931. doi: blood-2010-01-266072 [pii];10.1182/blood-2010-01-266072 [doi]

Mendelssohn, D.C., & Wish, J.B. (2009). Dialysis delivery in Canada and the United States: a view from the trenches. *Am.J.Kidney Dis., 54*(5), 954-964. doi: S0272-6386(09)00936-6 [pii];10.1053/j.ajkd.2009.05.023 [doi]

Middleton, J., Neil, S., Wintle, J., Clark-Lewis, I., Moore, H., Lam, C., Auer, M., Hub, E., & Rot, A. (1997). Transcytosis and surface presentation of IL-8 by venular endothelial cells. *Cell, 91*(3), 385-395. doi: S0092-8674(00)80422-5 [pii]

Middleton, J., Patterson, A.M., Gardner, L., Schmutz, C., & Ashton, B.A. (2002). Leukocyte extravasation: chemokine transport and presentation by the endothelium. *Blood, 100*(12), 3853-3860. doi: 10.1182/blood.V100.12.3853

Miettinen, H.M., Edwards, S.N., & Jalkanen, M. (1994). Analysis of transport and targeting of syndecan-1: effect of cytoplasmic tail deletions. *Mol.Biol.Cell, 5*(12), 1325-1339.

Milstone, D.S., Fukumura, D., Padgett, R.C., O'Donnell, P.E., Davis, V.M., Benavidez, O.J., Monsky, W.L., Melder, R.J., Jain, R.K., & Gimbrone, M.A., Jr. (1998). Mice lacking E-selectin show normal numbers of rolling leukocytes but reduced leukocyte stable arrest on cytokine-activated microvascular endothelium. *Microcirculation, 5*(2-3), 153-171.

Mortier, S., De Vriese, A.S., McLoughlin, R.M., Topley, N., Schaub, T.P., Passlick-Deetjen, J., & Lameire, N.H. (2003). Effects of conventional and new peritoneal

dialysis fluids on leukocyte recruitment in the rat peritoneal membrane. *J.Am.Soc.Nephrol., 14*(5), 1296-1306.

Mortier, S., De Vriese, A.S., Van de Voorde, J., Schaub, T.P., Passlick-Deetjen, J., & Lameire, N.H. (2002). Hemodynamic effects of peritoneal dialysis solutions on the rat peritoneal membrane: role of acidity, buffer choice, glucose concentration, and glucose degradation products. *J Am Soc Nephrol, 13*(2), 480-489.

Mueller, K.A., Tavlaki, E., Schneider, M., Jorbenadze, R., Geisler, T., Kandolf, R., Gawaz, M., Mueller, II, & Zuern, C.S. (2013). Gremlin-1 identifies fibrosis and predicts adverse outcome in patients with heart failure undergoing endomyocardial biopsy. *J Card Fail, 19*(10), 678-684. doi: 10.1016/j.cardfail.2013.09.001

Mulivor, A.W., & Lipowsky, H.H. (2004). Inflammation- and ischemia-induced shedding of venular glycocalyx. *Am J Physiol Heart Circ Physiol, 286*(5), H1672-1680. doi: 10.1152/ajpheart.00832.2003

Mulivor, A.W., & Lipowsky, H.H. (2002). Role of glycocalyx in leukocyte-endothelial cell adhesion. *Am J Physiol Heart Circ Physiol, 283*(4), H1282-1291. doi: 10.1152/ajpheart.00117.2002

Murphy, J.W., Cho, Y., Sachpatzidis, A., Fan, C., Hodsdon, M.E., & Lolis, E. (2007). Structural and functional basis of CXCL12 (stromal cell-derived factor-1 alpha) binding to heparin. *J Biol Chem, 282*(13), 10018-10027. doi: 10.1074/jbc.M608796200

Murray, J.H. (2005). *Live Cell Imaging, a Laboratory Manual: Confocal Microscopy, Deconvolution, and Structured Illumination Methods* (Goldman, R.D. & Spector, D.L. Eds.). New York, USA: Cold Springs Harbour Laboratories Press.

Nakayama, M., Kawaguchi, Y., Yamada, K., Hasegawa, T., Takazoe, K., Katoh, N., Hayakawa, H., Osaka, N., Yamamoto, H., Ogawa, A., Kubo, H., Shigematsu, T., Sakai, O., & Horiuchi, S. (1997). Immunohistochemical detection of advanced glycosylation end-products in the peritoneum and its possible pathophysiological role in CAPD. *Kidney Int, 51*(1), 182-186.

Nelson, R.M., Cecconi, O., Roberts, W.G., Aruffo, A., Linhardt, R.J., & Bevilacqua, M.P. (1993). Heparin oligosaccharides bind L- and P-selectin and inhibit acute inflammation. *Blood, 82*(11), 3253-3258.

Ni, J., Moulin, P., Gianello, P., Feron, O., Balligand, J.L., & Devuyst, O. (2003). Mice that lack endothelial nitric oxide synthase are protected against functional and structural modifications induced by acute peritonitis. *J.Am.Soc.Nephrol., 14*(12), 3205-3216.

Norman, M.U., Van De Velde, N.C., Timoshanko, J.R., Issekutz, A., & Hickey, M.J. (2003). Overlapping roles of endothelial selectins and vascular cell adhesion molecule-1 in immune complex-induced leukocyte recruitment in the cremasteric microvasculature. *Am J Pathol, 163*(4), 1491-1503. doi: 10.1016/S0002-9440(10)63506-7

Nourshargh, S., Krombach, F., & Dejana, E. (2006). The role of JAM-A and PECAM-1 in modulating leukocyte infiltration in inflamed and ischemic tissues. *J Leukoc Biol, 80*(4), 714-718. doi: 10.1189/jlb.1105645

Oh, J.H., Lee, H.S., Park, S.H., Ryu, H.S., & Min, C.K. (2010). Syndecan-1 overexpression promotes tumor growth and angiogenesis in an endometrial cancer xenograft model. *Int.J.Gynecol.Cancer, 20*(5), 751-756.

Ojeh, N., Hiilesvuo, K., Warri, A., Salmivirta, M., Henttinen, T., & Maatta, A. (2008). Ectopic expression of syndecan-1 in basal epidermis affects keratinocyte proliferation and wound re-epithelialization. *J Invest Dermatol, 128*(1), 26-34. doi: 10.1038/sj.jid.5700967

Oliver, M.G., Specian, R.D., Perry, M.A., & Granger, D.N. (1991). Morphologic assessment of leukocyte-endothelial cell interactions in mesenteric venules subjected to ischemia and reperfusion. *Inflammation, 15*(5), 331-346.

Ondiveeran, H.K., & Fox-Robichaud, A.E. (2004). Pentastarch in a balanced solution reduces hepatic leukocyte recruitment in early sepsis. *Microcirculation, 11*(8), 679-687.

Oohira, A., Wight, T.N., & Bornstein, P. (1983). Sulfated proteoglycans synthesized by vascular endothelial cells in culture. *J Biol Chem, 258*(3), 2014-2021.

Pahakis, M.Y., Kosky, J.R., Dull, R.O., & Tarbell, J.M. (2007). The role of endothelial glycocalyx components in mechanotransduction of fluid shear stress. *Biochem Biophys Res Commun, 355*(1), 228-233. doi: 10.1016/j.bbrc.2007.01.137

Pajek, J., Kveder, R., Bren, A., Gucek, A., Ihan, A., Osredkar, J., & Lindholm, B. (2008). Short-term effects of a new bicarbonate/lactate-buffered and conventional peritoneal dialysis fluid on peritoneal and systemic inflammation in CAPD patients: a randomized controlled study. *Perit Dial Int, 28*(1), 44-52.

Panasco, M.S., Pelajo-Machado, M., & Lenzi, H.L. (2010). Omental and pleural milky spots: different reactivity patterns in mice infected with *Schistosoma mansoni* reveals coelomic compartmentalisation. *Mem Inst Oswaldo Cruz, 105*(4), 440-444.

Park, P.W., Foster, T.J., Nishi, E., Duncan, S.J., Klagsbrun, M., & Chen, Y. (2004). Activation of syndecan-1 ectodomain shedding by *Staphylococcus aureus* alpha-toxin and beta-toxin. *J.Biol.Chem., 279*(1), 251-258. doi: 10.1074/jbc.M308537200 [doi];M308537200 [pii]

Park, P.W., Pier, G.B., Hinkes, M.T., & Bernfield, M. (2001). Exploitation of syndecan-1 shedding by *Pseudomonas aeruginosa* enhances virulence. *Nature*, *411*(6833), 98-102. doi: 10.1038/35075100

Park, P.W., Pier, G.B., Preston, M.J., Goldberger, O., Fitzgerald, M.L., & Bernfield, M. (2000a). Syndecan-1 shedding is enhanced by LasA, a secreted virulence factor of *Pseudomonas aeruginosa*. *J Biol Chem*, *275*(5), 3057-3064.

Park, P.W., Reizes, O., & Bernfield, M. (2000b). Cell surface heparan sulfate proteoglycans: selective regulators of ligand-receptor encounters. *J Biol Chem, 275*(39), 29923-29926. doi: 10.1074/jbc.R000008200

Passlick-Deetjen, J., Pischetsrieder, M., Witowski, J., Bender, T.O., Jorres, A., & Lage, C. (2001). *In vitro* superiority of dual-chambered peritoneal dialysis solution with possible clinical benefits. *Perit Dial Int, 21 Suppl 3*, S96-101.

Patrick, A.L., & Fox-Robichaud, A. (2010). Effects of a 4 hour exposure to conventional peritoneal dialysis fluids on the murine hepatic microcirculation. *FASEB J, 24*, 590.519.

Patrick, A.L., Rullo, J., Beaudin, S., Liaw, P., & Fox-Robichaud, A.E. (2007). Hepatic leukocyte recruitment in response to time-limited expression of TNF-alpha and IL-1beta. *Am.J.Physiol Gastrointest.Liver Physiol, 293*(4), G663-G672. doi: 00070.2007 [pii];10.1152/ajpgi.00070.2007 [doi]

Pawlaczyk, K., Kuzlan-Pawlaczyk, M., Wieczorowska-Tobis, K., Polubinska, A., Breborowicz, A., & Oreopoulos, D. (1999). Evaluation of the effect of uremia on peritoneal permeability in an experimental model of continuous ambulatory peritoneal dialysis in anephric rats. *Adv Perit Dial, 15*, 32-35.

Peters, T., Potter, R., Li, X., He, Z., Hoskins, G., & Flessner, M.F. (2011). Mouse model of foreign body reaction that alters the submesothelium and transperitoneal transport. *Am J Physiol Renal Physiol, 300*(1), F283-289. doi: 10.1152/ajprenal.00328.2010

Petri, B., & Bixel, M.G. (2006). Molecular events during leukocyte diapedesis. *FEBS J, 273*(19), 4399-4407. doi: 10.1111/j.1742-4658.2006.05439.x

Phillipson, M., Heit, B., Colarusso, P., Liu, L., Ballantyne, C.M., & Kubes, P. (2006). Intraluminal crawling of neutrophils to emigration sites: a molecularly distinct

process from adhesion in the recruitment cascade. *J Exp Med, 203*(12), 2569-2575. doi: 10.1084/jem.20060925

Popova, T.G., Millis, B., Bailey, C., & Popov, S.G. (2012). Platelets, inflammatory cells, von Willebrand factor, syndecan-1, fibrin, fibronectin, and bacteria co-localize in the liver thrombi of *Bacillus anthracis*-infected mice. *Microb Pathog, 52*(1), 1-9. doi: 10.1016/j.micpath.2011.08.004

Popova, T.G., Millis, B., Bradburne, C., Nazarenko, S., Bailey, C., Chandhoke, V., & Popov, S.G. (2006). Acceleration of epithelial cell syndecan-1 shedding by anthrax hemolytic virulence factors. *BMC Microbiol, 6*, 8. doi: 10.1186/1471-2180-6-8

Posthuma, N., ter Wee, P., Donker, A.J., Dekker, H.A., Oe, P.L., & Verbrugh, H.A. (1999). Peritoneal defense using icodextrin or glucose for daytime dwell in CCPD patients. *Perit Dial Int, 19*(4), 334-342.

Pries, A.R., Secomb, T.W., & Gaehtgens, P. (2000). The endothelial surface layer. *Pflugers Arch., 440*(5), 653-666.

Proudfoot, A.E., Handel, T.M., Johnson, Z., Lau, E.K., LiWang, P., Clark-Lewis, I., Borlat, F., Wells, T.N., & Kosco-Vilbois, M.H. (2003). Glycosaminoglycan binding and oligomerization are essential for the *in vivo* activity of certain chemokines. *Proc Natl Acad Sci U S A, 100*(4), 1885-1890. doi: 10.1073/pnas.0334864100

Purushothaman, A., & Sanderson, R. (2009). SDC1 (Syndecan-1). *Atlas of genetics and cytogenetics in oncology and haematology, 13*(1), 57-61.

Purushothaman, A., Uyama, T., Kobayashi, F., Yamada, S., Sugahara, K., Rapraeger, A.C., & Sanderson, R.D. (2010). Heparanase-enhanced shedding of syndecan-1 by myeloma cells promotes endothelial invasion and angiogenesis. *Blood, 115*(12), 2449-2457. doi: 10.1182/blood-2009-07-234757

Quinn, Q., & Fox-Robichaud, A. (2009). Effects of peritoneal dialysis solutions on the murine peritoneal microcirculation. *FASEB J, 23*, 762.761.

Rapraeger, A.C. (2001). Molecular interactions of syndecans during development. *Semin Cell Dev Biol, 12*(2), 107-116. doi: 10.1006/scdb.2000.0239

Rapraeger, A.C., Ell, B.J., Roy, M., Li, X., Morrison, O.R., Thomas, G.M., & Beauvais, D.M. (2013). Vascular endothelial-cadherin stimulates syndecan-1-coupled insulin-like growth factor-1 receptor and cross-talk between alphaVbeta3 integrin and vascular endothelial growth factor receptor 2 at the onset of endothelial cell dissemination during angiogenesis. *FEBS J, 280*(10), 2194-2206. doi: 10.1111/febs.12134

Read, R.R., Eberwein, P., Dasgupta, M.K., Grant, S.K., Lam, K., Nickel, J.C., & Costerton, J.W. (1989). Peritonitis in peritoneal dialysis: bacterial colonization by biofilm spread along the catheter surface. *Kidney Int., 35*(2), 614-621.

Rehm, M., Bruegger, D., Christ, F., Conzen, P., Thiel, M., Jacob, M., Chappell, D., Stoeckelhuber, M., Welsch, U., Reichart, B., Peter, K., & Becker, B.F. (2007). Shedding of the endothelial glycocalyx in patients undergoing major vascular surgery with global and regional ischemia. *Circulation, 116*(17), 1896-1906.

doi: CIRCULATIONAHA.106.684852

[pii];10.1161/CIRCULATIONAHA.106.684852 [doi]

Rogachev, B., Hausmann, M.J., Yulzari, R., Weiler, M., Holmes, C., Faict, D., Chaimovitz, C., & Douvdevani, A. (1997). Effect of bicarbonate-based dialysis solutions on intracellular pH (pHi) and TNFalpha production by peritoneal macrophages. *Perit Dial Int, 17*(6), 546-553.

Rollins, B.J., Walz, A., & Baggiolini, M. (1991). Recombinant human MCP-1/JE induces chemotaxis, calcium flux, and the respiratory burst in human monocytes. *Blood, 78*(4), 1112-1116.

Rops, A.L., Gotte, M., Baselmans, M.H., van den Hoven, M.J., Steenbergen, E.J., Lensen, J.F., Wijnhoven, T.J., Cevikbas, F., van den Heuvel, L.P., van Kuppevelt, T.H., Berden, J.H., & van der Vlag, J. (2007). Syndecan-1 deficiency aggravates anti-glomerular basement membrane nephritis. *Kidney Int, 72*(10), 1204-1215. doi: 10.1038/sj.ki.5002514

Rosenberg, R.D., Shworak, N.W., Liu, J., Schwartz, J.J., & Zhang, L. (1997). Heparan sulfate proteoglycans of the cardiovascular system. Specific structures emerge but how is synthesis regulated? *J Clin Invest, 100*(11 Suppl), S67-75.

Rubin, J., Clawson, M., Planch, A., & Jones, Q. (1988a). Measurements of peritoneal surface area in man and rat. *Am J Med Sci, 295*(5), 453-458.

Rubin, J., Herrera, G.A., & Collins, D. (1991). An autopsy study of the peritoneal cavity from patients on continuous ambulatory peritoneal dialysis. *Am.J.Kidney Dis., 18*(1), 97-102. doi: S0272638691001415 [pii]

Rubin, J., Jones, Q., & Andrew, M. (1989). An analysis of ultrafiltration during acute peritoneal dialysis in rats. *Am.J.Med.Sci., 298*(6), 383-389.

Rubin, J., Jones, Q., Planch, A., & Bower, J.D. (1988b). The minimal importance of the hollow viscera to peritoneal transport during peritoneal dialysis in the rat. *ASAIO Trans., 34*(4), 912-915.

Rubin, J., Jones, Q., Planch, A., Rushton, F., & Bower, J. (1986). The importance of the abdominal viscera to peritoneal transport during peritoneal dialysis in the dog. *Am.J.Med.Sci., 292*(4), 203-208.

Rubin, J., Jones, Q., Planch, A., & Stanek, K. (1987). Systems of membranes involved in peritoneal dialysis. *J.Lab Clin.Med., 110*(4), 448-453. doi: 0022-2143(87)90386-6 [pii]

Ruhrberg, C., Gerhardt, H., Golding, M., Watson, R., Ioannidou, S., Fujisawa, H., Betsholtz, C., & Shima, D.T. (2002). Spatially restricted patterning cues provided by heparin-binding VEGF-A control blood vessel branching morphogenesis. *Genes Dev, 16*(20), 2684-2698. doi: 10.1101/gad.242002

Sakarya, S., Rifat, S., Zhou, J., Bannerman, D.D., Stamatos, N.M., Cross, A.S., & Goldblum, S.E. (2004). Mobilization of neutrophil sialidase activity desialylates the pulmonary vascular endothelial surface and increases resting neutrophil adhesion to and migration across the endothelium. *Glycobiology, 14*(6), 481-494. doi: 10.1093/glycob/cwh065

Salmivirta, M., Heino, J., & Jalkanen, M. (1992). Basic fibroblast growth factor-syndecan complex at cell surface or immobilized to matrix promotes cell growth. *J.Biol.Chem., 267*(25), 17606-17610.

San Antonio, J.D., Karnovsky, M.J., Gay, S., Sanderson, R.D., & Lander, A.D. (1994). Interactions of syndecan-1 and heparin with human collagens. *Glycobiology, 4*(3), 327-332.

Sanderson, R.D., & Bernfield, M. (1988). Molecular polymorphism of a cell surface proteoglycan: distinct structures on simple and stratified epithelia. *Proc Natl Acad Sci U S A, 85*(24), 9562-9566.

Sanderson, R.D., Hinkes, M.T., & Bernfield, M. (1992). Syndecan-1, a cell-surface proteoglycan, changes in size and abundance when keratinocytes stratify. *J Invest Dermatol, 99*(4), 390-396.

Sanderson, R.D., Lalor, P., & Bernfield, M. (1989). B lymphocytes express and lose syndecan at specific stages of differentiation. *Cell Regul, 1*(1), 27-35.

Savery, M.D., Jiang, J.X., Park, P.W., & Damiano, E.R. (2013). The endothelial glycocalyx in syndecan-1 deficient mice. *Microvasc Res, 87*, 83-91. doi: 10.1016/j.mvr.2013.02.001

Schall, T.J., Bacon, K., Toy, K.J., & Goeddel, D.V. (1990). Selective attraction of monocytes and T lymphocytes of the memory phenotype by cytokine RANTES. *Nature, 347*(6294), 669-671. doi: 10.1038/347669a0

Schellings, M.W., Vanhoutte, D., van Almen, G.C., Swinnen, M., Leenders, J.J., Kubben, N., van Leeuwen, R.E., Hofstra, L., Heymans, S., & Pinto, Y.M.

(2010). Syndecan-1 amplifies angiotensin II-induced cardiac fibrosis. *Hypertension, 55*(2), 249-256. doi: HYPERTENSIONAHA.109.137885 [pii];10.1161/HYPERTENSIONAHA.109.137885 [doi]

Schilte, M.N., Fabbrini, P., Wee, P.M., Keuning, E.D., Zareie, M., Tangelder, G.J., van Lambalgen, A.A., Beelen, R.H., & van den Born, J. (2010). Peritoneal dialysis fluid bioincompatibility and new vessel formation promote leukocyte-endothelium interactions in a chronic rat model for peritoneal dialysis. *Microcirculation., 17*(4), 271-280. doi: MICC24 [pii];10.1111/j.1549-8719.2010.00024.x [doi]

Schlessinger, J., Lax, I., & Lemmon, M. (1995). Regulation of growth factor activation by proteoglycans: what is the role of the low affinity receptors? *Cell, 83*(3), 357-360.

Schmid-Schonbein, G.W., Usami, S., Skalak, R., & Chien, S. (1980). The interaction of leukocytes and erythrocytes in capillary and postcapillary vessels. *Microvasc Res, 19*(1), 45-70.

Schubert, C., Christophers, E., Swensson, O., & Isei, T. (1989). Transendothelial cell diapedesis of neutrophils in inflamed human skin. *Arch.Dermatol.Res., 281*(7), 475-481.

Schuenke, M., Schulte, E., Schumacher, U., Voll, M., & Wesker, K. (2006). *Thieme Atlas of Anatomy: General Anatomy and Musculoskeletal System* (Ross, L.M. & Lamperti, E.D. Eds.). Stuttgart, New York, USA: Thieme.

Shaw, J.P., Johnson, Z., Borlat, F., Zwahlen, C., Kungl, A., Roulin, K., Harrenga, A., Wells, T.N., & Proudfoot, A.E. (2004). The X-ray structure of RANTES: heparin-derived disaccharides allows the rational design of chemokine inhibitors. *Structure, 12*(11), 2081-2093. doi: 10.1016/j.str.2004.08.014

Silvestro, L., Ruikun, C., Sommer, F., Duc, T.M., Biancone, L., Montrucchio, G., & Camussi, G. (1994). Platelet-activating factor-induced endothelial cell expression of adhesion molecules and modulation of surface glycocalyx, evaluated by electron spectroscopy chemical analysis. *Semin Thromb Hemost, 20*(2), 214-222. doi: 10.1055/s-2007-1001905

Simionescu, M., & Simionescu, N. (1986). Functions of the endothelial cell surface. *Annu Rev Physiol, 48*, 279-293. doi: 10.1146/annurev.ph.48.030186.001431

Slimani, H., Charnaux, N., Mbemba, E., Saffar, L., Vassy, R., Vita, C., & Gattegno, L. (2003). Binding of the CC-chemokine RANTES to syndecan-1 and syndecan-4 expressed on HeLa cells. *Glycobiology, 13*(9), 623-634. doi: 10.1093/glycob/cwg083 [doi];cwg083 [pii]

Spillmann, D., Witt, D., & Lindahl, U. (1998). Defining the interleukin-8-binding domain of heparan sulfate. *J.Biol.Chem., 273*(25), 15487-15493.

Stepp, M.A., Gibson, H.E., Gala, P.H., Iglesia, D.D., Pajoohesh-Ganji, A., Pal-Ghosh, S., Brown, M., Aquino, C., Schwartz, A.M., Goldberger, O., Hinkes, M.T., & Bernfield, M. (2002). Defects in keratinocyte activation during wound healing in the syndecan-1-deficient mouse. *J.Cell Sci., 115*(Pt 23), 4517-4531.

Stojimirovic, B., Trpinac, D., Obradovic, M., Milutinovic, D., Obradovic, D., & Nesic, V. (2001). [Changes in peritoneal mesothelial cells in patients on peritoneal dialysis]. *Med.Pregl., 54*(5-6), 219-223.

Stoler-Barak, L., Moussion, C., Shezen, E., Hatzav, M., Sixt, M., & Alon, R. (2014). Blood Vessels Pattern Heparan Sulfate Gradients between Their Apical and Basolateral Aspects. *PLoS One, 9*(1), e85699. doi: 10.1371/journal.pone.0085699

Swartz, R., Messana, J., Holmes, C., & Williams, J. (1991). Biofilm formation on peritoneal catheters does not require the presence of infection. *ASAIO Trans, 37*(4), 626-634.

Szatmari, T., Mundt, F., Heidari-Hamedani, G., Zong, F., Ferolla, E., Alexeyenko, A., Hjerpe, A., & Dobra, K. (2012). Novel genes and pathways modulated by syndecan-1: implications for the proliferation and cell-cycle regulation of malignant mesothelioma cells. *PLoS One, 7*(10), e48091. doi: 10.1371/journal.pone.0048091

Tekstra, J., Visser, C.E., Tuk, C.W., Brouwer-Steenbergen, J.J., Burger, C.W., Krediet, R.T., & Beelen, R.H. (1996). Identification of the major chemokines that regulate cell influxes in peritoneal dialysis patients. *J Am Soc Nephrol, 7*(11), 2379-2384.

Thurlow, L.R., Hanke, M.L., Fritz, T., Angle, A., Aldrich, A., Williams, S.H., Engebretsen, I.L., Bayles, K.W., Horswill, A.R., & Kielian, T. (2011). *Staphylococcus aureus* biofilms prevent macrophage phagocytosis and attenuate

inflammation *in vivo*. *J.Immunol., 186*(11), 6585-6596. doi: jimmunol.1002794 [pii];10.4049/jimmunol.1002794 [doi]

Tonelli, M., Hemmelgarn, B., Culleton, B., Klarenbach, S., Gill, J.S., Wiebe, N., & Manns, B. (2007). Mortality of Canadians treated by peritoneal dialysis in remote locations. *Kidney Int., 72*(8), 1023-1028. doi: 5002443 [pii];10.1038/sj.ki.5002443 [doi]

Tortora, G.J., & Derrickson, B. (2006). *Principles of Anatomy and Physiology* (Roesch, B. Ed. 11 ed.). USA: John Wiley and Sons, Inc.

Turin, T.C., Tonelli, M., Manns, B.J., Ahmed, S.B., Ravani, P., James, M., & Hemmelgarn, B.R. (2012). Lifetime risk of ESRD. *J.Am.Soc.Nephrol., 23*(9), 1569-1578. doi: ASN.2012020164 [pii];10.1681/ASN.2012020164 [doi]

van Diepen, A.T., van Esch, S., Struijk, D.G., & Krediet, R.T. (2014). The First Peritonitis Episode Alters the Natural Course of Peritoneal Membrane Characteristics in Peritoneal Dialysis Patients. *Perit Dial Int*. doi: 10.3747/pdi.2014.00277

Vanhoutte, D., Schellings, M.W., Gotte, M., Swinnen, M., Herias, V., Wild, M.K., Vestweber, D., Chorianopoulos, E., Cortes, V., Rigotti, A., Stepp, M.A., Van de Werf, F., Carmeliet, P., Pinto, Y.M., & Heymans, S. (2007). Increased expression of syndecan-1 protects against cardiac dilatation and dysfunction after myocardial infarction. *Circulation, 115*(4), 475-482. doi: 10.1161/CIRCULATIONAHA.106.644609

Varki, A., Cummings, R., Esko, J., Freeze, H., Hart, G., & Marth, J. (1999). *Essentials of Glycobiology*. Cold Spring Harbor, New York: Cold Spring Harbor Laboratory Press.

Vriese, A.S.D., White, R., Granger, D.N., & Lameire, N.H. (2009). *Nolph and Gokal's Textbook of Peritoneal Dialysis: The Peritoneal Microcirculation IN Peritoneal Dialysis* (Science, S. Ed.).

Wang, H., Xu, C., Kong, X., Li, X., Kong, X., Wang, Y., Ding, X., & Yang, Q. (2014). Trail Resistance Induces Epithelial-Mesenchymal Transition and Enhances Invasiveness by Suppressing PTEN via miR-221 in Breast Cancer. *PLoS One, 9*(6), e99067. doi: 10.1371/journal.pone.0099067

Wang, I.K., Chang, Y.C., Liang, C.C., Chuang, F.R., Chang, C.T., Lin, H.H., Lin, C.C., Yen, T.H., Lin, P.C., Chou, C.Y., Huang, C.C., Tsai, W.C., & Chen, J.H. (2012). Bacteremia in hemodialysis and peritoneal dialysis patients. *Intern Med, 51*(9), 1015-1021.

Wang, L., Brown, J.R., Varki, A., & Esko, J.D. (2002). Heparin's anti-inflammatory effects require glucosamine 6-O-sulfation and are mediated by blockade of L- and P-selectins. *J Clin Invest, 110*(1), 127-136. doi: 10.1172/JCI14996

Webb, L.M., Ehrengruber, M.U., Clark-Lewis, I., Baggiolini, M., & Rot, A. (1993). Binding to heparan sulfate or heparin enhances neutrophil responses to interleukin 8. *Proc Natl Acad Sci U S A, 90*(15), 7158-7162.

Wegmann, F., Petri, B., Khandoga, A.G., Moser, C., Khandoga, A., Volkery, S., Li, H., Nasdala, I., Brandau, O., Fassler, R., Butz, S., Krombach, F., & Vestweber, D.

(2006). ESAM supports neutrophil extravasation, activation of Rho, and VEGF-induced vascular permeability. *J Exp Med, 203*(7), 1671-1677. doi: 10.1084/jem.20060565

Welten, A.G., Zareie, M., van den Born, J., ter Wee, P.M., Schalkwijk, C.G., Driesprong, B.A., Mul, F.P., Hordijk, P.L., Beelen, R.H., & Hekking, L.H. (2004). *In vitro* and *in vivo* models for peritonitis demonstrate unchanged neutrophil migration after exposure to dialysis fluids. *Nephrol Dial Transplant, 19*(4), 831-839. doi: 10.1093/ndt/gfh024

Whittall, C., Kehoe, O., King, S., Rot, A., Patterson, A., & Middleton, J. (2013). A chemokine self-presentation mechanism involving formation of endothelial surface microstructures. *J.Immunol., 190*(4), 1725-1736. doi: jimmunol.1200867 [pii];10.4049/jimmunol.1200867 [doi]

Williams, J.D., Craig, K.J., Topley, N., Von, R.C., Fallon, M., Newman, G.R., Mackenzie, R.K., & Williams, G.T. (2002). Morphologic changes in the peritoneal membrane of patients with renal disease. *J.Am.Soc.Nephrol., 13*(2), 470-479.

Williams, J.D., Craig, K.J., von Ruhland, C., Topley, N., Williams, G.T., & Biopsy Registry Study, G. (2003). The natural course of peritoneal membrane biology during peritoneal dialysis. *Kidney Int Suppl, Dec*(88), S43-49.

Wong, J., Johnston, B., Lee, S.S., Bullard, D.C., Smith, C.W., Beaudet, A.L., & Kubes, P. (1997). A minimal role for selectins in the recruitment of leukocytes into the

inflamed liver microvasculature. *J.Clin.Invest, 99*(11), 2782-2790. doi: 10.1172/JCI119468 [doi]

Worapamorn, W., Xiao, Y., Li, H., Young, W.G., & Bartold, P.M. (2002). Differential expression and distribution of syndecan-1 and -2 in periodontal wound healing of the rat. *J Periodontal Res, 37*(4), 293-299.

Xu, J., Park, P.W., Kheradmand, F., & Corry, D.B. (2005). Endogenous attenuation of allergic lung inflammation by syndecan-1. *J.Immunol., 174*(9), 5758-5765. doi: 174/9/5758 [pii]

Yanez-Mo, M., Lara-Pezzi, E., Selgas, R., Ramirez-Huesca, M., Dominguez-Jimenez, C., Jimenez-Heffernan, J.A., Aguilera, A., Sanchez-Tomero, J.A., Bajo, M.A., Alvarez, V., Castro, M.A., del Peso, G., Cirujeda, A., Gamallo, C., Sanchez-Madrid, F., & Lopez-Cabrera, M. (2003). Peritoneal dialysis and epithelial-to-mesenchymal transition of mesothelial cells. *N Engl J Med, 348*(5), 403-413. doi: 10.1056/NEJMoa020809

Yang, L., Froio, R.M., Sciuto, T.E., Dvorak, A.M., Alon, R., & Luscinskas, F.W. (2005). ICAM-1 regulates neutrophil adhesion and transcellular migration of TNF-alpha-activated vascular endothelium under flow. *Blood, 106*(2), 584-592. doi: 10.1182/blood-2004-12-4942

Yeates, K., Zhu, N., Vonesh, E., Trpeski, L., Blake, P., & Fenton, S. (2012). Hemodialysis and peritoneal dialysis are associated with similar outcomes for end-stage renal disease treatment in Canada. *Nephrol Dial Transplant, 27*(9), 3568-3575. doi: 10.1093/ndt/gfr674

Yipp, B.G., Andonegui, G., Howlett, C.J., Robbins, S.M., Hartung, T., Ho, M., & Kubes, P. (2002). Profound differences in leukocyte-endothelial cell responses to lipopolysaccharide versus lipoteichoic acid. *J.Immunol., 168*(9), 4650-4658.

Yung, S., & Chan, T.M. (2007a). Mesothelial cells. *Perit.Dial.Int., 27 Suppl 2*, S110-S115. doi: 27/Supplement_2/S110 [pii]

Yung, S., & Chan, T.M. (2007b). Peritoneal proteoglycans: much more than ground substance. *Perit.Dial.Int., 27*(4), 375-390. doi: 27/4/375 [pii]

Zager, R.A., Johnson, A.C., & Lund, S. (2009). Uremia impacts renal inflammatory cytokine gene expression in the setting of experimental acute kidney injury. *Am J Physiol Renal Physiol, 297*(4), F961-970. doi: 10.1152/ajprenal.00381.2009

Zarbock, A., & Ley, K. (2009). New insights into leukocyte recruitment by intravital microscopy. *Curr.Top.Microbiol.Immunol., 334*, 129-152. doi: 10.1007/978-3-540-93864-4_6 [doi]

Zarbock, A., Lowell, C.A., & Ley, K. (2007). Spleen tyrosine kinase Syk is necessary for E-selectin-induced alpha(L)beta(2) integrin-mediated rolling on intercellular adhesion molecule-1. *Immunity, 26*(6), 773-783. doi: 10.1016/j.immuni.2007.04.011

Zareie, M., van Lambalgen, A.A., De Vriese, A.S., van, G.E., Lameire, N., ter Wee, P.M., Beelen, R.H., van den Born, J., & Tangelder, G.J. (2002). Increased leukocyte rolling in newly formed mesenteric vessels in the rat during peritoneal dialysis. *Perit.Dial.Int., 22*(6), 655-662.

Zelmer, J.L. (2007). The economic burden of end-stage renal disease in Canada. *Kidney Int., 72*(9), 1122-1129. doi: 5002459 [pii];10.1038/sj.ki.5002459 [doi]

Zemel, D., Krediet, R.T., Koomen, G.C., Kortekaas, W.M., Geertzen, H.G., & ten Berge, R.J. (1994). Interleukin-8 during peritonitis in patients treated with CAPD; an *in-vivo* model of acute inflammation. *Nephrol Dial Transplant, 9*(2), 169-174.

Zhang, J., Oh, K.H., Xu, H., & Margetts, P.J. (2008). Vascular endothelial growth factor expression in peritoneal mesothelial cells undergoing transdifferentiation. *Perit Dial Int, 28*(5), 497-504.

Zhang, X., Wu, C., Song, J., Gotte, M., & Sorokin, L. (2013). Syndecan-1, a cell surface proteoglycan, negatively regulates initial leukocyte recruitment to the brain across the choroid plexus in murine experimental autoimmune encephalomyelitis. *J Immunol, 191*(9), 4551-4561. doi: 10.4049/jimmunol.1300931

Zlotnik, A., & Yoshie, O. (2000). Chemokines: a new classification system and their role in immunity. *Immunity, 12*(2), 121-127.

Zweers, M.M., de Waart, D.R., Smit, W., Struijk, D.G., & Krediet, R.T. (1999). Growth factors VEGF and TGF-beta1 in peritoneal dialysis. *J Lab Clin Med, 134*(2), 124-132.